12-17-2011

International Conference on Advances in Civil Engineering

Prof.Srikanta Patnaik Mentor
IRNet India, patnaik_srikanta@yahoo.co.in

Proceedings of International Conference on

ADVANCES IN CIVIL ENGINEERING

(ICACE-2011)
17th –18th DECEMBER, 2011
BHUBANESWAR, India

Interscience Research Network (IRNet)
Bhubaneswar, India

Editorial

With an increasing sophistication and increasing luxury on the face of materialism, the human race is striving for state of the art infrastructure for its every social institution. The role of civil engineering is prominent in this context. Civil engineering is the oldest engineering discipline after military engineering,[4] and it was defined to distinguish non-military engineering from military engineering. It is traditionally broken into several sub-disciplines including environmental engineering, geotechnical engineering, structural engineering, transportation engineering, municipal or urban engineering, water resources engineering, materials engineering, coastal engineering,[4] surveying, and construction engineering.[6] Civil engineering takes place on all levels: in the public sector from municipal through to national governments, and in the private sector from individual homeowners through to international companies. Civil engineering comprises many disciplines and in the recent years many sub disciplines have been emerging. Civil engineering is concerned with the overall interface of human created fixed projects with the greater world. General civil engineers work closely with surveyors and specialized civil engineers to fit and serve fixed projects within their given site, community and terrain by designing grading, drainage, pavement, water supply, sewer service, electric and communications supply, and land divisions. General engineers spend much of their time visiting project sites, developing community consensus, and preparing construction plans. General civil engineering is also referred to as site engineering, a branch of civil engineering that primarily focuses on converting a tract of land from one usage to another. Civil engineers typically apply the principles of geotechnical engineering, structural engineering, environmental engineering, transportation engineering and construction engineering to residential, commercial, and industrial and public works projects of all sizes and levels of construction. Structural engineering is concerned with the structural design and structural analysis of buildings, bridges, towers, flyovers, tunnels, off shore structures like oil and gas fields in the sea, and other structures. This involves identifying the loads which act upon a structure and the forces and stresses which arise within that structure due to those loads, and then designing the structure to successfully support and resist those loads. The loads can be self weight of the structures, other dead load, live loads, moving (wheel) load, wind load, earthquake load, load from temperature change etc. Another aspect of Civil engineering is materials science. Material engineering deals with ceramics such as concrete, mix asphalt concrete, metals Focus around increased strength, metals such as aluminum and steel, and polymers such as polymethylmethacrylate (PMMA) and carbon fibers. Geo technical and environmental engineering also plays an important role in it. In dealing with the rise scarcity of the natural resources like water Civil Engineering steer it in a different form called Water Resource Engineering.

As the area is broad and requires cross functionally expert reviewers for technical scrutiny of the papers, we have tried to impart justice to all the paper in its publication in the proceeding. In all sense we have been transcendental in this field in developing the fauna of the conference.. In meeting the professional commitments we maintained the sanctity by adhering to ethics, ontology and semiotics. I beg apology for any inconveniency caused to the participants and delegates in the journey of this conference. I have regards for the IRNet family members, reviewers, and support staffs for their generous gifts of time, energy and effort. Specifically I owe indebtedness to the authors for their intellectual contributions in this conference.

I wish this conference to become a grand success.

Thanks and Regards

Prof. R. K. Panigrahi
Professor & Head
Department of Civil Engineering
Synergy Institute of Engineering and Technology
Dhenkanal-759001, India

An Experimental Approach to Free Vibration Response of Woven Fiber Composite Plates under Free-Free Boundary Condition

Itishree Mishra & Shishir Kumar Sahu

Department of Civil Engineering, NIT, Rourkela, 769008, India

Abstract **-** The present study involves extensive experimental works to investigate the free vibration of woven fiber Glass/Epoxy composite plates in free-free boundary conditions. The specimens of woven glass fiber and epoxy matrix composite plates are manufactured by the hand-layup technique. Elastic parameters of the plate are also determined experimentally by tensile testing of specimens using Instron 1195. An experimental investigation is carried out using modal analysis technique with Fast Fourier Transform Analyzer, PULSE lab shop, impact hammer and contact accelerometer to obtain the Frequency Response Functions. Also, this experiment is used to validate the results obtained from the FEM numerical analysis based on a first order shear deformation theory. The effects of different geometrical parameters including number of layers, aspect ratio, and fiber orientation of woven fiber composite plates are studied in free-free boundary conditions in details. This study may provide valuable information for researchers and engineers in design applications.

Key words **-** *Woven composite, Frequency Response function, Modal Analysis, Finite element Method.*

I. INTRODUCTION

Woven fabrics as an attractive reinforcement provide excellent integrity and conformability for advanced structural composite applications. The reinforcement of composites with industry driven woven fiber materials lead to improved properties of composite structures in terms of acoustical, elastical and thermal properties. Glass fibers are the most commonly used ones in low to medium performance composites because of their high tensile strength and low cost. In woven fiber composites, fibers are woven in both principal directions at right angles to each other (warp and fill directions). To better understand any structural vibration problem, the resonant frequencies of a structure need to be identified and quantified. Today due to the advancement in computer aided data acquisition systems and instrumentation, experimental modal Analysis has become an extremely important tool in the hands of an experimentalist. A number of researchers have been developed numerous solution methods to analysis the dynamic behavior of laminated composite laminates. However experimental investigations on woven fabric composite laminated Structures are still limited. There have been few experimental investigations of the free vibration of free-free anisotropic plates. Clary [1] investigated theoretically and experimentally the effect of the effect of fiber orientation on the first five flexural modes of rectangular, unidirectional, boron-epoxy panels. The agreement between theoretical and experimental frequencies was generally good, though there were large errors in some of the predictions of thinner panels. Cawley and Adams [2] used finite element method which included transverse shear deformation to predict the natural modes of free-free CFRP plates. This method produced improved accuracy for the theoretical results for anisotropic plates. Dutt and Shivanand [3] studied the free vibration response of C-F-F-F and C-F-C-F woven carbon composite laminates using a FFT analyzer and compared with FEM tool ANSYS. This work presents an experimental study of modal testing of woven fiber Glass/Epoxy laminated composite plates using FFT analyzer. The main objective of this work is to contribute for a better understanding of the dynamic behavior of components made from industry driven woven fiber composite materials, specifically for the case of plates. The effects of different geometrical parameters including number of layers, aspect ratio and fiber orientation of industry driven woven fiber composite plates in free-free boundary condition are studied in details.

II. FINITE ELEMENT FORMULATIONS

The first order shear deformation theory is used to develop a finite element approach for the prediction of natural frequencies and modes of laminated composite pates. The formulation is essentially similar to that of chakraborty *et al.* [4]. Consider a laminate composite plate of length ‘a’ and width ‘b’ consisting of N number of thin homogenous arbitrarily oriented orthotropic layers having a total thickness ‘h’ is considered as shown in fig.1.T In the present investigation, an eight noded two dimensional quadratic isoparametric element

having five degrees of freedom (u, v, w,θ_x, θ_y) per node is used for analysis. A program for vibration analysis of Laminated Composite plate is developed using the formulation based on finite element method (FEM) for free-free boundary conditions. Reduced integration technique is adopted to avoid possible shear locking. The overall stiffness and mass matrices are obtained by assembling the corresponding element matrices, using skyline technique.

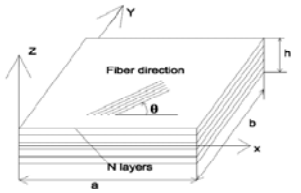

Fig. 1 : Laminated Composite Plate

The displacement field is in the form of

$$u(x, y, z) = u_0(x, y) + z\theta_Y(x, y)$$

$$v(x, y, z) = v_0(x, y) + z\theta_X(x, y)$$

$$w(x, y, z, t) = w_0(x, y)$$

Where u, v, w and u_0, v_0 and w_0 are displacement components in the x, y and z directions anywhere in the plate and at mid-plane respectively. θ_x and θ_y represent rotations of the mid-plane normal about x and y axes respectively. The associated strain components are:

$$\begin{Bmatrix} \varepsilon_{xx} \\ \varepsilon_{yy} \\ \gamma_{xy} \\ \gamma_{xz} \\ \gamma_{yz} \end{Bmatrix} = \begin{Bmatrix} \varepsilon^0_{xx} \\ \varepsilon^0_{yy} \\ \varepsilon^0_{xy} \\ \varepsilon^0_{xz} \\ \varepsilon^0_{yz} \end{Bmatrix} + z \begin{Bmatrix} k_{xx} \\ k_{yy} \\ k_{xy} \\ k_{xz} \\ k_{yz} \end{Bmatrix}$$

Where ε^0_x, ε^0_y and ε^0_z are the midplane strains and k_{xx}, k_{yy} and k_{xy} are the curvatures of the laminated plate

A. *Stress –Strain Relations:*

$$\begin{Bmatrix} N_{xx} \\ N_{yy} \\ N_{xy} \\ M_{xx} \\ M_{yy} \\ M_{xy} \\ Q_{xz} \\ Q_{xz} \end{Bmatrix} = \begin{bmatrix} A_{11} & A_{12} & A_{16} & B_{11} & B_{12} & B_{16} & 0 & 0 \\ A_{12} & A_{22} & A_{26} & B_{12} & B_{22} & B_{26} & 0 & 0 \\ A_{16} & A_{26} & A_{66} & B_{16} & B_{26} & B_{66} & 0 & 0 \\ B_{11} & B_{12} & B_{16} & D_{11} & D_{12} & D_{16} & 0 & 0 \\ B_{12} & B_{22} & B_{26} & D_{12} & D_{22} & D_{26} & 0 & 0 \\ B_{16} & B_{26} & B_{66} & D_{16} & D_{26} & D_{66} & 0 & 0 \\ 0 & 0 & 0 & 0 & 0 & 0 & S_{44} & S_{45} \\ 0 & 0 & 0 & 0 & 0 & 0 & S_{45} & S_{55} \end{bmatrix} \begin{Bmatrix} \varepsilon^0_{xx} \\ \varepsilon^0_{yy} \\ \gamma^0_{xy} \\ K_{xx} \\ K_{yy} \\ K_{xy} \\ \gamma^0_{xz} \\ \gamma^0_{yz} \end{Bmatrix}$$

A_{ij}, B_{ij}, D_{ij}, and S_{ij} are the extensional, bending-stretching coupling, bending and transverse stiffnesses. They may be defind as

$$A_{ij} = \sum_{k=1}^{n} \left(\overline{Q_{ij}}\right)_k (z_k - z_{k-1})$$

$$B_{ij} = \frac{1}{2} \sum_{k=1}^{n} \left(\overline{Q_{ij}}\right)_k (z_k^2 - z_{k-1}^2)$$

$$D_{ij} = \frac{1}{3} \sum_{k=1}^{n} \left(\overline{Q_{ij}}\right)_k (z_k^3 - z_{k-1}^3) \quad \text{For } i, j = 1, 2, 6$$

$$S_{ij} = \alpha \sum_{k=1}^{n} \left(\overline{Q_{ij}}\right)_k (z_k - z_{k-1}) \text{ For } i, j = 4, 5$$

α = shear correction factor =5/6 (Assumed for the numerical solutions)

z_k, z_{k-1}= top and bottom distance of lamina from mid-plane.

B. Finite Element Matrices:

The element matrices are derived as given below

1) *Element stiffness matrix:*

$$[K]_e = \int_{-1}^{+1}\int_{-1}^{+1} [B]^T [D][B] |J| \, d\xi \, d\eta$$

2) Element mass matrix or consistent mass matrix:-

$$[M]_e = \int_{-1}^{+1}\int_{-1}^{+1} [N]^T [P][N] |J| \, d\xi \, d\eta$$

C. Governing Equations

The equations of equilibrium of a discretised elastic structure undergoing small deformations can be expressed as

$$[\boldsymbol{M}]]\{\ddot{\boldsymbol{u}}\} + [\boldsymbol{c}]\,]\{\dot{\boldsymbol{u}}\} + [\boldsymbol{k}]\{\boldsymbol{u}\} = \{\boldsymbol{F}(\boldsymbol{t})\}$$

For free undamped vibration, the equation reduces to

$$[\boldsymbol{M}]]\{\ddot{\boldsymbol{u}}\} + [\boldsymbol{k}]\{\boldsymbol{u}\} = \{\boldsymbol{0}\}$$

If modal co-ordinates are employed the equation becomes

$$\left[[\boldsymbol{K}] - \boldsymbol{\omega^2}[\boldsymbol{M}]\{\boldsymbol{\phi}\}\right] = \{\boldsymbol{0}\}$$

Where ω and {φ} represents the natural frequencies and the corresponding Eigen vectors of the generalized Eigen value problem.

III. EXPERIMENTAL PROGRAMME:

A. Materials Required for Fabrication of Plates:

The constituent materials used for fabricating the epoxy/glass fiber plates are: E-glass woven roving as reinforcement (from Owens corning), Epoxy as resin, Hardener as catalyst (10% of the weight of epoxy), Polyvinyl alcohol as a releasing agent.

B. Fabrication Procedure:

The composite plate specimens used in this research were made from 0/90 woven glass fiber with epoxy matrix. Specimens were fabricated by hand layup technique**.** The percentage of fiber and matrix has taken as 50:50 in weight for fabrication of the plates. A flat plywood rigid platform is selected. A plastic sheet i.e. a mould releasing sheet was kept on the plywood platform and a thin film of polyvinyl alcohol is applied as a releasing agent by use of spray gun. Laminating Starts with the application of a gel coat (epoxy and hardener) deposited on the mould by brush, whose main purpose was to provide a smooth external surface and to protect the fibers from direct exposure to the environment. Ply was cut from roll of woven roving. Layers of reinforcement were placed on the mould at top of the gel coat and gel coat was applied again by brush. Any air which may be entrapped was removed using steel rollers. The process of hand lay-up was the continuation of the above process before the gel coat had fully hardened. After completion of all layer, again a plastic sheet was covered the top of last ply by applying polyvinyl alcohol inside the sheet as releasing agent. Again one flat ply board and a heavy flat metal rigid platform were kept top of the plate for compressing purpose. The plates were left for a minimum of 48 hours in room temperature before being transported and cut to exact shape for testing.

Fig. 2 : Plate Casting

C. Determination of Material constants:

The material constants (i.e. of: E_1, E_2, E_{45}) of woven fiber Glass/Epoxy composite plate were determined experimentally by performing tensile tests on specimens cut in longitudinal and transverse directions, and at 45° to the longitudinal direction using INSTRON 1195 machine as per ASTM standard : D 3039/D 3039M-2008[5]. The shear modulus was determined using the formula from Jones [6].

Table1. Material properties of composite plates:

Layer	E_1 GPa	E_2 GPa	E_{45} GPa	G_{12} GPa	ν_{12}
8	7.4	7.4	5.81	2.15	0.17

D. Experimental Setup and Test Procedure for Free Vibration Test:

To simulate free boundary conditions, all the four edges of the plate are hanged in an iron frame using a flexible string as shown in Figure 1. The connections of FFT analyzer, laptop, transducers, modal hammer, and cables to the system were done as per the guidance manual shown in fig.2. The pulse lab shop software key was inserted to the port of laptop. The plate was excited in a selected point by means of Impact hammer (Model 2302-5), fixed on the hammer. The resulting vibrations of the specimens on the selected point were measured by an accelerometer (B&K, Type 4507) mounted on the specimen by means of bees wax.

Fig. 3 : Iron Frame for making Free-Free B.C

Fig. 4 : Vibration test set up

For FRF, at each singular point the modal hammer was struck five times and the average value of the response was displayed on the screen of the display unit At the time of striking with modal hammer to the points

on the specimen precaution were taken for making the stroke to be perpendicular to the surface of the plates. Then By moving the cursor to the peaks of the FRF the frequencies are measured.

IV. RESULTS AND DISCUSSIONS:

Numerical results are carried out to determine the capability of the present formulation to predict the natural frequency of woven fiber composite plates.

A. Comparison with Previous Studies:

The present formulation is validated for vibration analysis of composites panels in free-free boundary conditions as shown in Table 2. The four lowest non-dimensional frequencies obtained by the present finite element are compared with numerical solution published by Ju *et al*. [7].

Table. 2: Comparison of natural frequencies (Hz) of vibration of 8 layer laminated composite plate $[0°/90°/45°/90°]_s$ at free-free boundary conditions.

a=b=0.25m, t=0.00212, E_1 = 132 Gpa, E_2 = 5.35 Gpa

G_{12} = 2.79 Gpa, ν_{12}=0.3, $\boldsymbol{\rho}$=1446.20 kg/m ^{3}

Reference	Natural frequencies at free-free boundary conditions			
	1	2	3	4
Ju *et* al.[6]	73.30	202.59	243.37	264.90
Present FEM	72.53	201.39	243.54	263.26

B. Experimental and Numerical Results:

Results:

After validating the formulation with the existing literature, both the experimental and numerical results for vibration study of laminated composite plates are presented. Here for free vibration analysis, the study is aimed upon the following parameters:

1) Effect of number of layers of a laminate
2) Effect of fiber orientations
3) Effect of aspect ratio

1) Effect of Number of layers of laminate:

To examine the effects of no. of layers of laminate, three different types of laminate are fabricated, which are made up of 8, 12 and 16 layers. The natural frequencies for free vibration are obtained both experimentally and numerically for free-free boundary condition. The variation of natural frequencies with increasing layer of laminate for both experimental results and numerical results are shown graphically in figure-5. All the geometrical dimensions of the composite plates are same as described in table-3. From figure 5 it is observed that as the number of layers increases, the natural frequency also increases as excepted. There is a considerable variation in the natural frequency made up of 12 and 16 layers whereas for 8 layers of composite plates it is less.

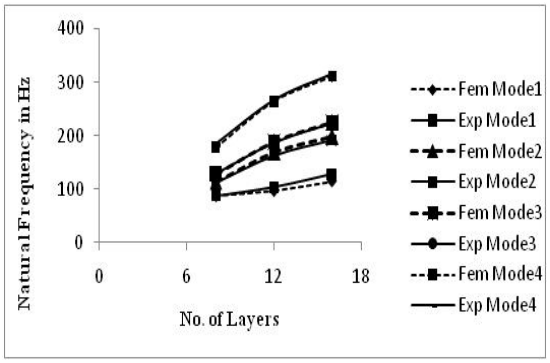

Fig. 5 : Variation of natural frequency of Experimental and numerical results with different no. of layers

2) *Effect of fiber orientation:*

In order to know the effect of fiber orientations on natural frequencies of laminated plate, (8-layers) three types of plates with fiber orientations i.e. $[0]_8$, $[30/-30]_4$, $[45/-45]_4$ are considered having thickness 0.0032m and $\boldsymbol{\rho}$ is taken as 1580 kg/m^3. The variations of natural frequency with fiber orientation are presented in fig.6 for free-free boundary condition. The results obtained from free vibration of the plates of both experiment and present FEM are in good agreement. As observed from fig.6 the experimental results show a good agreement with the FEM proving that the fiber angle has influence on the dynamic behavior of the laminated plates. As the fiber angle increases, the natural frequencies decrease. It is observed that the maximum frequency occurs at $\theta = 0^0$ and the minimum occurs at $\theta = 30^0$.

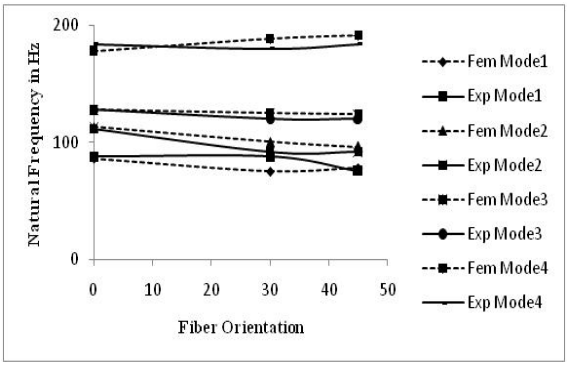

Fig. 6 : Variation of natural frequency of experimental and numerical results with different fiber orientation

From the experimental results, it is observed that increasing the angle of the fibers from 0^0 to 30^0 reduces the natural frequency by about 13% (i.e. from 86 to 75 Hz) for the 1st mode and by about 11.5% (i.e. from 113 to 100 Hz) for the 2nd mode.

3) *Effect of Aspect ratio:*

To study the effect of aspect ratio, four different types of aspect ratios for laminated composite plates are considered i.e. for a/b value (1.0, 1.5 and 2.0).For different aspect ratios, the plate dimension varies, whereas the thickness of the plate i.e. (h=0.0031m) remains unchanged. The Variations of natural frequencies of Experimental results with present FEM results of different aspect ratio of woven GFRP under free-free boundary condition are shown in fig7

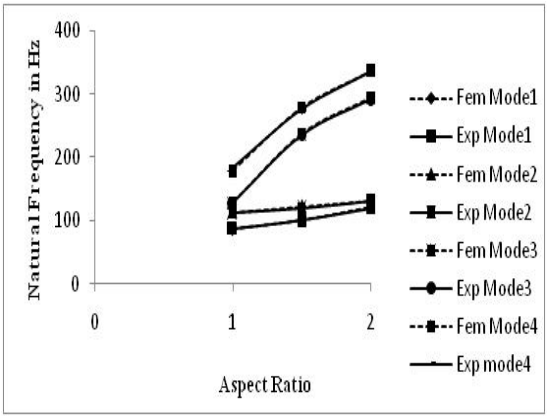

Fig. 7 : Variation of natural frequency of Experimental and numerical results with different aspect ratio.

V. CONCLUSION:

In the present study, both experimental and numerical study is conducted for woven roving G/E composite plates. Quantitative results are presented to show the effect of different Parameter like no. of layers, aspect ratio and fiber orientation in free-free boundary conditions. Based on the first order shear deformation theory, a finite element formulation is presented for the analysis of the free vibration of composite plates. The percentage of difference between numerical results and experimental results are due to non uniformity in the specimens properties (Voids, variations in thickness, non uniform surface finishing) and also positioning of the accelerometers. This experimental method represents to predict the dynamical behavior of woven composite, in order to design panels or other similarly structure used in different applications such as automotive industry, aerospace, civil, marine and other high performance structures.

PULSE REPORT:

Pulse report for 12-layer Woven Fiber Glass/Epoxy Cantilever Composite Plate

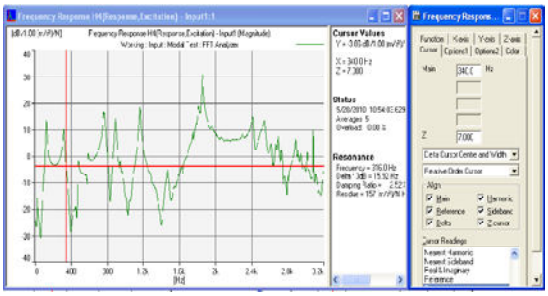

Fig. 8 : Typical FRF of test specimen.

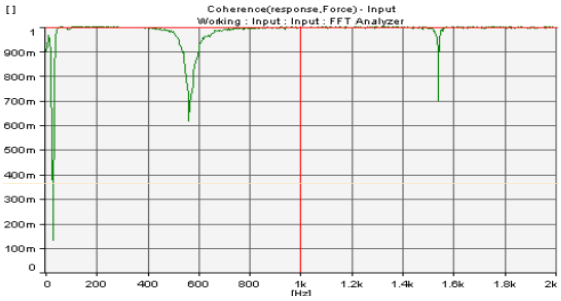

Fig. 9 : Typical coherence of test specimen.

Table 3. Geometrical dimensions of composite plate: The plate dimensions are 24cmx24cm with different thickness as the no. of layers varies.

Plate no	Stacking sequence	h (m)	ρ(kg/m^3)
1	$[0]_8$	0.0031	1580
2	$[0]_{12}$	0.0047	1650
3	$[0]_{16}$	0.0056	1686
4	$[0]_8$ (a/b=0.5)	0.0031	1523
5	$[0]_8$ (a/b=1)	0.0031	1580
6	$[0]_8$ (a/b=1.5)	0.0031	1512

VI. ACKNOWLEDGMENTS

The authors gratefully acknowledge the financial support provided by the Department of science and

Technology (DST), New Delhi, India. (Project No.SR/S3/MERC/009/2008).

NOMENCLATURE:

a, b, h Plate dimensions along x, y and z axes respectively

E_1, E_2 Young's moduli of a lamina along and across the fibers, respectively

G_{12} Shear moduli of a lamina with respect to 1 and 2 axis

$[K_e]$ Elastic stiffness matrix

$[M_e]$ Element mass matrix of the plate

[B] Strain displacement matrix of the plate

[N] Shape function of the plate

ν_{12} Poisson's ratios

ρ Mass density

ω_n Natural frequency

REFERENCES:

[1] R.L.Clary, "Vibration characterstics of Aluminium plates Reinforced with Boron-Epoxy composite material", Journal of Composite Materials, Vol-7, 1975, pp-348-365.

[2] P.Cawley and R.D. Adams, "The Predicted and experimental natural modes of free-free CFRP plates", Journal of Composite Materials, Vol.12, 1978, pp-336-347.

[3] K.M.Dutt and H.K.Shivanand, "An experimental approach to free vibration response of carbon composite laminates", Journal of Advanced Engineering & Applications, (2011), pp- 66-68.

[4] S. Chakraborty, M. Mukhopadhyay and A. R. Mohanty, "Free Vibrational Responses of FRP Composite Plates: Experimental and Numerical Studies", Journal of Reinforced Plastics and Composite, Vol-19, 2000, pp- 535-551.

[5] ASTM D 3039/D 3039 M (2008), Standard test method for tensile properties of polymer matrix composite materials.

[6] Jones R. M., "Mechanics of Composite Materials", McGraw Hill, (1975), New York.

[7] F. Ju, H.P. Lee and K.H. Lee "Finite element analysis of free vibration of delaminated composite plate" Composite Engineering, vol.5, 1995, pp-195-209.

◈◈◈

Comparative Performance of Elevated Isolated Liquid Storage Tanks (With Shaft Staging)

Pravin B.Waghmare, Atul M. Raghatate & Niraj D.Baraiya
Civil Engg. Dept, A.S. Polytechnic, Pipri (M), Wardha (MH)-India

Abstract **-** Liquid storage tanks are important components of lifeline and industrial facilities. They are critical elements in water supply scheme and fire fighting system, and extensively used for storage and processing of variety of liquid like material such as petroleum product, liquefied natural gas, chemical fluid and wastage of different forms. In this paper, the seismic response of base isolated cylindrical liquid storage tanks is investigated under real earthquake ground motion. The isolation systems considered is elastomeric bearings (without lead core), the specific objectives of the study are to carry out the comparative performance of the tanks with isolation and without isolation (i.e. Fixed tanks) also to investigate the response of the tanks for varying capacity with varying heights. For this study forty tanks of varying heights such as 8m,10m,11m,11.5m,12.5m,14m,16m with varying capacities of 500kl,265kl,200kl,100kl,50kl are considered. For this a time history analysis has been carried out by using a three time history of varying magnitude with varying peak ground acceleration. It is observed that the base shear of elevated liquid storage tanks supported on shaft is significantly reduced due to isolation. The drift of the tank relation to base of shaft is also significantly reduced due to isolation. The earthquake response of isolated short tanks is relatively more, i.e. Isolation is not effective for stiffer shafts, and however in general, the effectiveness of base isolation is achieved for tall tanks. Although the effectiveness of seismic isolation increases with the increase of bearing flexibility and damping these properties needs to be modified for desired response.

Keywords- *liquid storage tanks, shaft, earthquake ground motion, elastomeric rubber bearing*

I. INTRODUCTION

The tanks come under variety of configuration; it may be ground supported, elevated or partly buried. In recent years the number, the size and importantance of these structure have been increased and there is need to understand their seismic behavior and to formulate rational and efficient method of their analysis and design to resist earthquake ground motion. Over period of times failure of large number of tanks has attributes the need of more clear understanding and assessment of behavior of tanks during an earthquake ground motion.

Reinforced concrete circular shafts type support (staging) is widely used for elevated tanks of low to a very high capacity for its ease of construction and more solid form it provides compared to frame construction. In recent past earthquakes Bhuj,Gujarat (2001)and Jabalpur (1997)thin shell of circular shaft have perform unsatisfactory, thin shaft shell when used as a column (or pedestal)are vulnerable because they not only possess a very low ductility but also lack redundancy of alternate load path that are present in framed structure. For structure in high Seismicity regions earthquakes loading is considered the most significant and possibly the most destructive external loads, particularly for low to medium rise tanks. Seismic isolation consist essentially the installation of mechanism which decouple the tanks and or its content from particularly damaging earthquakes induces ground or support motion. This decoupling is achieved by increasing the flexibility of the system, together with providing appropriate damping to resist the amplitude of the motion caused by the earthquakes. The advantages of seismic isolation includes the ability to significantly reduces structural and non structural damage to reduce seismic design forces. The past studies of the dynamics behavior. This includes (i) the effect of aspect ratio on for further study of base isolated liquid storage tanks to understand tanks reducing the earthquake response of tanks. However, there is need. Liquid storage tanks confirm the effectiveness of base isolation in (ii) the effectiveness of isolation System for liquid storage tanks.

II. MODEL OF SEISMIC ISOLATED LIQUID STORAGE TANKS

For the presents study, a practical range of tanks is considered. Five practical capacities of tanks viz, 50kl, 100kl, 250kl, 256kl, 500kl are considered for the analysis's height of the tanks is varied from 8m to 14m(various parameters of tanks are given in table No.3.1).Thus 8 tanks for each capacities are considered. Thus, in alls the performance of 40 tanks is examined using time history for each fixed base and isolated tanks.

Each of 40 tanks is designed to evaluate their geometrical parameters. The shaft and container is modeled as shell in SAP-2000. The isolation system, i.e. laminated rubber bearings (LRB) installed below the tower to decouple the structure from the ground.

A. Spring mass model for seismic analysis

It was observed that tank liquid vibrates in two distinct pattern[1] (a) The liquid in the lower region of tank behaves like a mass that is rigidly connected to tank wall, this mass is termed as impulsive liquid mass which accelerates along with the wall and induces impulsive hydrodynamic pressure on tank wall and similarly on base (b) Liquid mass in the upper region of tank undergoes sloshing motion, this mass is termed as convective liquid mass and it exerts convective hydrodynamic pressure on tank wall and base. Thus, total liquid mass gets divided into two parts, i.e., impulsive mass and convective mass. In spring mass model of tank-liquid system, these two liquid masses are to be suitably represented. In the present work convective mass is shown by spring with a mass at a height [h_c] and impulsive mass attach with the wall is shown by a mass at a height [h_i] of the container.

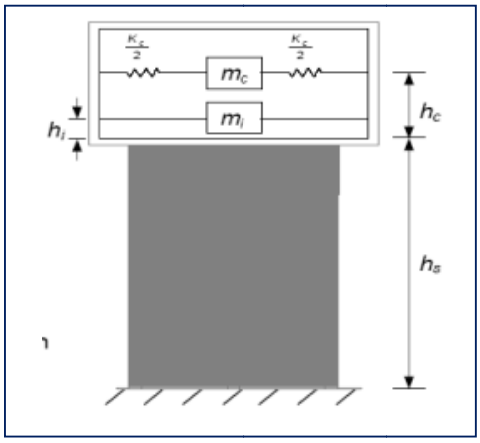

Fig.1.1 Mathematical Model of Tank with Various Masses

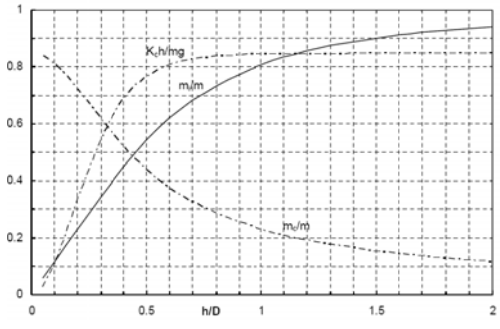

Fig, 1.2 Impulsive and Convective Masses and convective spring stiffness

Where, S =H/D (i.e. ratio of the liquid height to diameter of the tank) [1]

$$Y_c=m_c/m \quad (3.1)$$

$$Y_i=m_i/m \quad (3.2)$$

$$m=\pi R^3 H \rho_w \quad (3.3)$$

Time period of impulsive mode [47].

$$T_i = 2\pi\sqrt{\frac{m_i + m_s}{K_s}} \quad (3.4)$$

Where m_s- mass of container and one third mass of staging, m_i-impulsive mass of liquid,K_s- Lateral stiffness of staging.

Time period of convective mode [1].

$$T_c = 2\pi\sqrt{\frac{m_c}{K_c}} \quad (3.5)$$

Where, m_c- convective mass of liquid, Kc- stiffness of convective mass

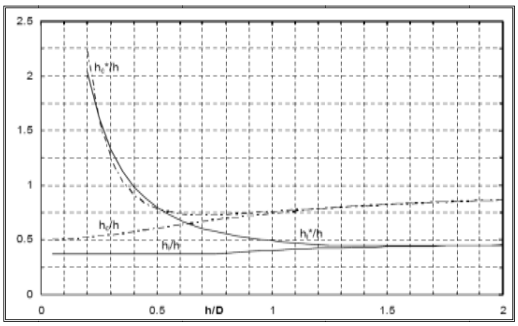

Fig, 1.3 Heights of Impulsive and Convective Masses

The effective heights H_c,H_i, in terms of liquid height are expressed as [fig.1.3].

$$H_c=\mu_c H \quad (3.6)$$

$$H_i=\mu_i H \quad (3.7)$$

Design Horizontal Seismic Coefficient:-

The Design horizontal seismic coefficient for impulsive mode,[47]

$$A_{hi}= (Z/2)\,(I/R)\,(S_a/g)_i \quad (3.8)$$

Where,

Z-zone factor=0.24, I-importance factor=1.5

Damping 5%,T_i-time period of impulsive mode.

$(S_a/g)_i$-spectral acceleration coefficient.

Design horizontal seismic coefficient for convective mode,[47]

$$A_{hc}= (Z/2)\,(I/R)\,(S_a/g)_c \qquad (3.\ 9)$$

Shaft is considered to have reinforcement in two curtains both horizontally and vertically. Hence, *R* – Response reduction factor is taken as 1.8. Damping 0.5% T_c-time period of convective mode.

A multiplication factor of 1.75 is used to get $(S_a/g)_c$ for 0.5% damping from that of 5% damping.

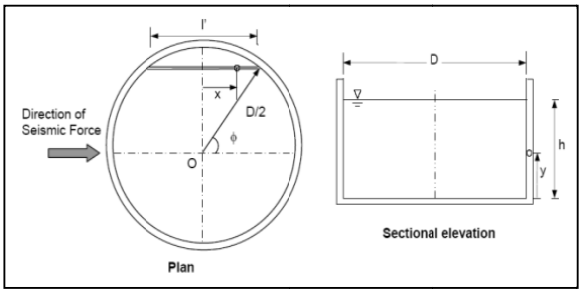

Impulsive hydrodynamic pressure on wall [1].

$$p_{iw}(y)=Q_{iw}(y)\,(A_h)_i\,\rho gh\cos\emptyset \qquad (4.\ 0)$$

where,

$$Q_{iw}(y)=0.866[1-(y/h)^2]\tanh(0.866D/h) \qquad (4.\ 1)$$

Maximum pressure will occur at φ=0, at base of wall y=0, Impulsive hydrodynamic pressure in vertical direction, on base slab (y=0) on a strip of length l',is given by[1].

$$p_{ib} =0.866\,(A_h)_i\,\rho gh\,\sinh(1.732\,x/h)/\cosh(0.866l'/h) \quad . \qquad (4.\ 2)$$

Where,

ρ = Mass density of liquid,φ = Circumferential angle, and

y = Vertical distance of a point on tank wall from the bottom of tank wall.

x=horizontal distance of a point on base of tank in the direction of seismic force, from centre of tank

Lateral Convective hydrodynamic pressure on wall [1].

$$p_{cw}=Q_{cw}(y)\,(A_h)_c\,\rho gD\,(1-1/3\cos^2\emptyset)\cos\emptyset \qquad (4.\ 3)$$

Where,

$$Q_{cw}(y) =0.5625\cosh(3.674y/D)/\cosh(3.674h/D) \qquad (4.\ 4)$$

Convective hydrodynamic pressure in vertical direction on base slab (y=0) [1].

$$p_{cb}=Q_{cb}(x)\,(A_h)_c\,\rho gD \qquad (4.\ 5)$$

Where

$$Q_{cb}(x) =1.125[(x/D)-4/3(x/D)^3]\,\mathrm{sech}\,[3.674\,h/D] \qquad (4.6)$$

Pressure on tank wall due to inertia is given by[47].

p-(wall inertia) = $(A_h)_i$ x mass density of wall x wall thickness

B. Governing equation of motion

Structure has been model by finite element method using SAP-2000 (version 9i).The equation of motion of elevated liquid storage tanks subjected to unidirectional earthquake ground motion are expressed in the matrix form as [3]

$$[m]\{\ddot{x}\} + [c]\{\dot{x}\} + [k]\{x\} = -[m]\ddot{u}_g \qquad (4.7)$$

Where {x}-displacement vector,

[m]-mass matrix

[c]-damping matrix

[k]-stiffness matrix

$\ddot{u}_g$ -earthquake acceleration

The convective and impulsive masses are calculated by using eq. (3.1) to (3.3) the self weight of tank and shaft is calculated automatically by the software at appropriate nodal points. The convective and impulsive masses lumped at appropriate heights by using equation (3.6) to (3.7).For non isolated tanks the bottom nodal points are given zero degrees of freedom i.e. fixed.

For isolated tanks L.R.B. types of isolation has been used, the time period of isolation is considered as 2 sec in horizontal motion. The total stiffness of isolation is equally divided among all nodal points.

C. Earthquake ground motion

The seismic response of isolated liquid storage tanks is investigated for near fault earth quake ground motions recorded on rock. For the present study, three recorded earthquake ground motions considered are Kern Country (1952/07/21), Imperial Valley (1979/10/15) and Sanfracisco (1957/03/22). For the purpose of the seismic behavior of the tanks, ground motions records are put in X-component. Records of acceleration for Kern Country (1952/07/21), Imperial Valley (1979/10/15), and Sanfracisco (1957/03/22) are as below [2].

Earthquake	Magnitude	Record/Component	PGA
Kern-Country (1952/07/21)	M(7.5)	KERN/HOL-UP	0.022(g)
Imperial-Valley (1979/10/15)	M6.5)	IMPAVAL/ H-AEP045	0.327(g)
Sanfracisco (1957/03/22)	M(5.3)	SANFRAN/GGP-UP	0.112(g)

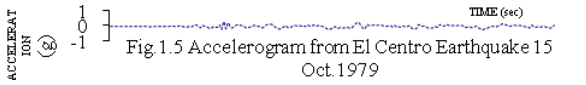

Fig.1.5 Accelerogram from El Centro Earthquake 15 Oct.1979

Fig1.6 Accelerogram from Sanfrancisco Earthquake22 March 1957

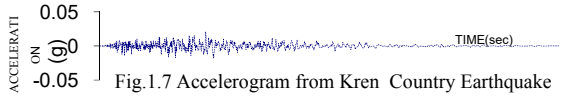

Fig.1.7 Accelerogram from Kren Country Earthquake 21 JULY 1952

III. DESIGN OF ISOLATORS

A practical seismic isolation system should meet the fallowing requirements.

1. Sufficient horizontal flexibility to increase the structural periods and spectrum demands accepts for very soft soil sites
2. Sufficient energy dissipitation capacity to limit the displacement across the isolators to a practical level.
3. Adequate rigidity to make the isolated structure not much different from a fixed base structure under general service loading.

Based on above mentioned requirements and codal procedure, as per UBC -1997, LRB isolator design properties like damping, hardness, modulus of rigidity, and poissoins ratio for rubber are considered from UBC 1997.

Tanks under consideration here requires different size of isolators, as gravity loads acting on the column are different for different sizes of tanks, different sizes of bearings are required.

The basic equation of LRB is as fallows [4].

The effective horizontal stiffness of the isolators is [4]

$$k_{eff}=(W/g)(2\pi/T_D)^2=GA/t \quad (4.7)$$

Where W- total weight of the tank,

G-gravitational force and taken as 9.81m/s,^{2}

T_D- effective isolation period,

G- Shear modulus of the rubber,

A-cross sectional area of the bearing,

t- total thickness of rubber layer.

The design displacement D_D of the isolation system along each main horizontal axis at design basis earthquake level is calculated according to the UBC97 [5]

$$D_D=(g/4\pi^2)(C_{VD}T_D)/B_D \quad (4.8)$$

C_{VD}- Seismic coefficient C_D as set forth in Table 16-R [5],

B_D - Numerical coefficient related to the effective damping of the isolation system at the design displacement $ß_D$ as set forth in Table A-16-C [5],

The total design displacement including additional displacement due to accidental torsion is calculated according to the UBC [5]

$$D_{TD}=D_D[1+(12ey/b^2+d^2)] \quad (4.9)$$

e-actual eccentricity plus accidental eccentricity which is taken as maximum tank direction perpendicular to the direction of force under consideration,b-shortest plan dimension, d -longest plan dimension, y- distance between the center of rigidity of the isolation system[6]. The characteristics force Q is [7]

$$Q = (\pi/2)k_{eff}ß_D D_D \quad (5)$$

$ß_D$ – damping of the isolation system

The post yield horizontal stiffness k_2 is [7]

$$k_2=k_{eff}-(Q/D_D) \quad (5.1)$$

Post yield to pre yield stiffness ratio is taken as 0.1

i.e. $k_2 /k_1 = œ$

The yield displacement D_Y [7]

$$D_Y = Q/ (k_2- k_1) \quad (5.2)$$

The yield force F_Y [7]

$$F_Y=Q+k_2D_Y \quad (5.3)$$

The pre-yield horizontal stiffness k_1 [7]

$$k_1 =F_Y / D_Y \quad (5.4)$$

The vertical stiffness of the laminated rubber bearings is expressed by

$$k_v =E_rA / t \quad (5.5)$$

E_r—compression modulus of elasticity of rubber [7],

A-c/s area of LRB, t. total thickness of LRB. [7],

$$E_r=[1/(6GS_H^2)]+1.333K \qquad (5.6)$$

K- Bulk modulus. For circular LRB, shape factor is taken as [7]

$$S_H=Ø/(4t_r) \qquad (5.7)$$

where Ø- diameter of LRB, t_r- thickness of each rubber layer in LRB.The details calculations of base isolators are omitted here and final design parameters are listed in table no 1.5-1.6. It is important to note that analysis and design of all different types of base isolator was done using excel spread sheet

Table1.1 (A) Geometric Properties of All Water Tank

.		Geometry of shaft support		Bottom slab		Vertical slab		
Sr No	Capacity	thickness	height	Diameter	thickness	height	Diameter	thickness
	KL	(m)	(m)	(m)	(m)	(m)	(m)	(m)
1	50 KL	2.628	0.175	8	4.38	0.1	3.285	4.38
2		2.628	0.175	10	4.38	0.1	3.285	4.38
3		2.628	0.175	10.5	4.38	0.1	3.285	4.38
4		2.628	0.175	11	4.38	0.1	3.285	4.38
5		2.628	0.175	11.5	4.38	0.1	3.285	4.38
6		2.628	0.175	12.5	4.38	0.1	3.285	4.38
7		2.628	0.175	14	4.38	0.1	3.285	4.38
8		2.628	0.175	16	4.38	0.1	3.285	4.38

Table1.1 (B) Geometric Properties Of All Water Tanks

.		Geometry of shaft support		Bottom slab		Vertical slab		
Sr No	Capacity	thickness	height	diameter	thickness	height	diameter	thickness
	(KL)	(m)	(m)	(m)	(m)	(m)	(m)	(m)
1	100 KL	3.312	0.15	8	5.52	0.2	4.14	5.52
2		3.312	0.15	10	5.52	0.2	4.14	5.52
3		3.312	0.15	10.5	5.52	0.2	4.14	5.52
4		3.312	0.15	11	5.52	0.2	4.14	5.52
5		3.312	0.15	11.5	5.52	0.2	4.14	5.52
6		3.312	0.15	12.5	5.52	0.2	4.14	5.52
7		3.312	0.15	14	5.52	0.2	4.14	5.52
8		3.312	0.15	16	5.52	0.2	4.14	5.52

Table1.1(C) Geometric Properties Of All Water Tanks

.		Geometry of shaft support		Bottom slab		Vertical slab		
Sr. No	Capacity	thickness	height	diameter	thickness	height	diameter	thickness
	(KL)	(m)	(m)	(m)	(m)	(m)	(m)	(m)
1	200 KL	4.176	0.16	8	6.96	0.2	5.22	6.96
2		4.176	0.16	10	6.96	0.2	5.22	6.96
3		4.176	0.16	10.5	6.96	0.2	5.22	6.96
4		4.176	0.16	11	6.96	0.2	5.22	6.96
5		4.176	0.16	11.5	6.96	0.2	5.22	6.96
6		4.176	0.16	12.5	6.96	0.2	5.22	6.96
7		4.176	0.16	14	6.96	0.2	5.22	6.96
8		4.176	0.16	16	6.96	0.2	5.22	6.96

Table1.1 (D) Geometric Properties Of All Water Tanks

.		Geometry of shaft support		Bottom slab		Vertical slab		
Sr. No	Capacity	thickness	height	diameter	thickness	height	diameter	thickness
	(KL)	(m)	(m)	(m)	(m)	(m)	(m)	(m)
1	265 KL	4.59	0.16	8	7.65	0.23	5.737	7.65
2		4.59	0.16	10	7.65	0.23	5.737	7.65
3		4.59	0.16	10.5	7.65	0.23	5.737	7.65
4		4.59	0.16	11	7.65	0.23	5.737	7.65
5		4.59	0.16	11.5	7.65	0.23	5.737	7.65
6		4.59	0.16	12.5	7.65	0.23	5.737	7.65
7		4.59	0.16	14	7.65	0.23	5.737	7.65
8		4.59	0.16	16	7.65	0.23	5.737	7.65

Table 1.1 (E) Geometric Properties Of All Water Tanks

	Geometry of shaft support		Bottom slab		Vertical slab		
Capacity	thickness	height	diameter	thickness	height	diameter	thickness
KL	(m)	(m)	(m)	(m)	(m)	(m)	(m)
500 KL	5.676	0.2	8	9.46	0.2	7.095	9.46
	5.676	0.2	10	9.46	0.2	7.095	9.46
	5.676	0.2	10.5	9.46	0.2	7.095	9.46
	5.676	0.2	11	9.46	0.2	7.095	9.46
	5.676	0.2	11.5	9.46	0.2	7.095	9.46
	5.676	0.2	12.5	9.46	0.2	7.095	9.46
	5.676	0.2	14	9.46	0.2	7.095	9.46
	5.676	0.2	16	9.46	0.2	7.095	9.46

Table 1.2 Time Period Of Convective Mass

Capacity KL	E_c (KN/m^2)	ρ_s (KN/m^3)	k_c kg/m	T_c sec	H_c (m)	H_i (m)	Mass of container (kg)
50KL	22.3 x10^6	25	121928	2.1	2.29	1.23	17.87 x10^3
100KL	22.3 x10^6	25	193680	2.4	2.8	1.55	47.80 x10^4
200KL	22.3 x10^6	25	307814	2.7	3.6	1.95	59.83 x10^4
265KL	22.3 x10^6	25	372240	2.9	4.01	2.14	71.93 x10^4
500KL	22.3 x10^6	25	567720	3.2	4.9	2.65	109.6 x10^4

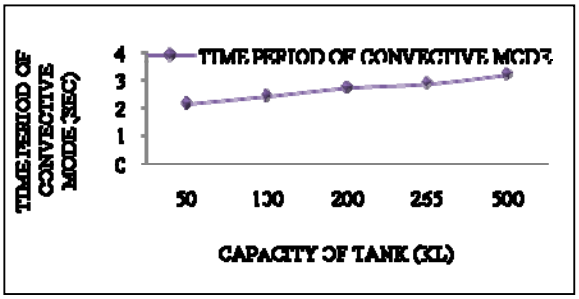

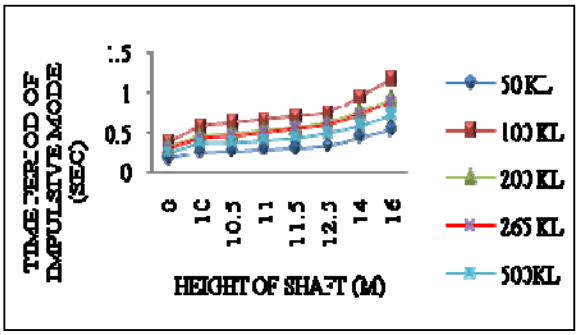

Fig.1.9 Time Period Of Impulsive Mass of All Tanks

Table 1.4 Properties Of Lrb (As Per Ref. [7])

Capacity (KL)	Height of staging (m)	k_{eff} (KN/m)	D_{TD} (m)	Q (KN)	k_2 (KN/m)	k_1 (KN/m)	F_Y (KN)	D_Y (mm)
50 KL	8m	989	0.2	46.	787.1	7871	51.	6
	10m	1057.3	0.2	49.	841.	8415.	55.5	6
	10.5m	1073.4	0.2	50.	854.	8543.	55.3	6.5
	11m	1092.4	0.2	51.	865	8695.	56.3	6.5
	11.5m	1107.5\\	0.2	51.	881.5	8815.	57	6.5
	12.5m	1134.7\	0.2	53.	903	9031	59	6.5
	14m	1190.9	0.2 0.2	55	947.9	9479	62	6.5
	16m	1258.3	0.2	59.	1001.	1001	651	6.5
100 KL	8m	1826.1	0.26	85	1453.	1453	95.8	6.5
	10m	1860.	0.2	87.	1480.	1480	97	6.5
	10.5m	1878.	0.2	88.	1495.	1495.	99	6.5
	11m	1900.5	0.26	89.	1512.	1512	99	6.5
	11.5m	1915.6	0.26\	89.	1524.	1524	99.4	6.5
	12.5m	1947.7	0.26	91.	1550.	1550	101.5	6.5
	14m	2007.0	0.26	94.	1597.	1597	107	6.5
	16m	2079.4	0.26\\	97.6	1655.0	16550	108	6.6
200 KL	8m	3001.0	0.2	140	2388	2388	152	6.5
	10m	3108.6	0.26	145	2474	2474	162.1	6.5
	10.5m	3120.6	0.26	146	2483	2483	162.7	6.5
	11m	3156.8	0.26	148	2512.	2512	164.6	6.5
	11.5m	3192.0	0.26	149	2540.5	25405	166.49	6.5
	12.5m	3260.4	0.26	153	2594	2594	170.0	6.5
	14m	3315.6	0.26	155	2638.	2638	172.9	6.5
	16m	3415.1	0.26	160	2718	2718	178.	6.5

Table 1.4(B) Properties Of Lrb (As Per Ref. [7])

Capacity KL	Height of staging (m)	k_{eff} (KN/m)	D_{TD} (m)	Q (KN)	k_2 (KN/m)	k_1 (KN/m)	F_Y (KN)	D_Y (mm)
265 KL	8m	3827.	0.26	179	3046.	30461	199	6.5
	10m	3935.	0.26	184	3132.	31325	205	6.5
	10.5m	3962.	0.26	186	3154.	31541	206	6.5
	11m	3991	0.26	187	3176.	31764	208	6.5
	11.5m	4018.	0.26	188	3198	31980	209	6.5
	12.5m	4072.	0.26	191	3241.	32412	212	6.5
	14m	4153	0.26	194	3306	33060	216	6.5
	16m	4235	0.26	198	3370.	33708	220	6.5
500 KL	8m	6782	0.26	318	5397.	53978	353.	6.5
	10m	6954	0.26	326	5535.	55354	362.	6.5
	10.5m	7044	0.26	330	5606.	56066	367.	6.5
	11m	7051	0.26	330	5608	56088	367	6.5
	11.5m	7065	0.26	331	5623.	56234	368	6.5
	12.5m	7178	0.26	336	5713.	57130	374	6.5
	14m	7278	0.26	341	5793.	57930	379	6.5
	16m	6782	0.26	348	5913	59138	387	6.5

TABLE 1.5 Properties of LRB

Capacity (KL)	Height Of Staging (m)	K_v (KN/m)	S_H	A (m^2)	t (m)	t_r (m)
50 KL	8	131633	14	0.24725	0.25m	0.01
	10	141758	14	0.26433	0.25m	0.01
	10.5	144143	14.	0.26835	0.25m	0.01
	11	146977	14.	0.273124	0.25m	0.01
	11.5	149215	15	0.276893	0.25m	0.01
	12.5	15324	15	0.28367	0.25m	0.01m
	14	16160	15	0.29774	0.25m	0.01
	16	17161	14	0.31458	0.25m	0.01
100 KL	8	256301	19	0.456547	0.25m	0.01
	10	261405	19	0.46509	0.25m	0.01
	10.5	264108	19.	0.469612	0.25m	0.01
	11	267412	19.	0.47514	0.25m	0.01
	11.5	269665	19	0.478909	0.25m	0.01
	12.5	274471	19	0.48695	0.25m	0.01
	14	283334	19	0.501774	0.25m	0.01
	16	294153	20	0.519865	0.25m	0.01
200 KL	8	432082	24	0.750274	0.25m	0.01
	10	448188	24	0.77716	0.25m	0.01
	10.5	449994	25	0.780175	0.25m	0.01
	11	455414	25	0.78922	0.25m	0.01
	11.5	460683	25	0.798015	0.25m	0.01
	12.5	470920	25	0.8151	0.25m	0.01
	14	479200	25.	0.82892	0.25m	0.01
	16	494106	26	0.853795	0.25m	0.01
265 KL	8	555848	27.600	0.956813	0.25m	0.01
	10	572114	27.989	0.98395	0.25m	0.01
	10.5	576180.6	28.085	0.990734	0.25m	0.01
	11	580397.9	28.185	0.997769	0.25m	0.01
	11.5	584464.6	28.28	1.004554	0.25m	0.01
	12.5	592598.2	28.471	1.018122	0.25m	0.01
	14	604798.9	28.754	1.038474	0.25m	0.01
	16	617000.1	29.034	1.058827	0.25m	0.01
500KL	8	998822.8	36.741	1.69553	0.25m	0.01
	10	1024745	37.206	1.738747	0.25m	0.01
	10.5	1038158	37.445	1.761109	0.25m	0.01
	11	1039123	37.123	1.761109	0.25m	0.01
	11.5	1041323	37.501	1.766386	0.25m	0.01
	12.5	1058203	37.798	1.794528	0.25m	0.01
	14	1073275	38.062	1.819654	0.25m	0.01
	16	1096033	38.457	1.857595	0.25m	0.01

IV. RESPONSE OF TANKS ISOLATED BY ELASTOMERIC BEARINGS SUBJECTED TO REAL EARTHQUAKES

The seismic response of isolated and fix base tanks system is investigated for the three real earthquakes excitation. The time history analysis is carried out by giving excitation in lateral direction of tank (shaft).

A. Maximum Bearing Displacement

The bearing displacement increases with increase of isolation period. It becomes more flexible leading to more displacement. In the present study, time period of isolation system (target period) is T_D=2 sec, damping ratio i.e. ß$_D$=0.13and normalized yield strength i.e. F_O= F_Y/W is equal to 0.05.It is found that the maximum displacement of the bearing depends upon the stiffness properties of the bearing, in present work stiffness properties of the bearings varies due to increase in the total seismic weight of the structure. Also, the vertical to horizontal stiffness ratio for 50kl, 100kl,200kl, 265kl,500kl,increase to 134,140,144,147,

148 respectively, there is a slight difference in maximum displacement in the bearing which is under the permissible limits. The maximum permissible limits for the lateral displacement of the bearing are equal to the height of the bearing. All the bearing for all the tanks did perform as desired i.e. the displacement of the bearing are well controlled by the design of the bearing.

B. Maximum Acceleration Response

Response of both fixed base (non isolated tanks) and isolated tanks are investigated for three different earthquakes having different characteristics. The normalized response gives a clear idea of effectiveness of isolation for the given tanks in fig 2.4 to fig 2.6. It is observed that tanks with fixed base attracted greater ground acceleration. It is also found that all the isolated tanks performed as desired i.e. they attracted lesser ground acceleration as compared to fixed base(normalized acceleration value below 1). Isolation tanks especially the shorter height did not perform well i.e. the ground acceleration were amplified after isolation.

C. Base Shear Response

Each earthquake record considered for the time history are having properties like peak ground acceleration (PGA), frequency composition and duration varying significantly so that the inherent variability of earthquake can be accounted in the analysis. In the present study, time period of isolation system (target period) is T_D=2 sec,damping ratio i.e. $ß_D$=0.13 and normalized yield strength i.e. $F_O = F_Y/W$ is equal to 0.05, From above study it is observed that the percentage reduction of base shear under Imperial Valley (1979/10/15) earthquake for 50kl tank of height 8m, 10m, 10.5m, 11m, 11.5m, 12.5m, 14m,16m are 72,73,68,67,70,71, 78,77 which are less as compared to base shear 81,81,79,82,80,82,82,87 under Kern-Country (1952/07/21) and base shear 84,82,84,84,82,80,81,86 under Sanfracisco(1957/3/22) earthquake.

In 100kl tank the percentage reduction of base shear under Imperial Valley (1979/10/15) earthquake for 8m,10m,10.5m,11m,11.5m,12.5m,14m,16m,are,64,68,70, 74,74,78,81,83 which are less as compared to base shear,88,89,88,89,89,88,88,90,under,Kern-Country, (1952/7/21)earthquake,and,base shear, 94,87,90,87,87, 87,91,95,under. Sanfracisco-(1957/03/7) earthquake.

In 200kl tank the percentage reduction of base shear under Imperial Valley (1979/10/15) earthquake for 8m, 10m, 10.5m, 11m, 11.5m, 12.5m,14m,16m,are 71,66,66,78,78,78,77,80 which are less as compared to base shear, 89, 89, 89, 87, 90, 90, 92,87under,Kern-Country (1952/07/21)earthquake&base-shear, 85, 89, 85, 89 88,89,92,94 under Sanfracisco (1957/03/22) earthquake.

In 265kl tank the percentage reduction of base shear under Imperial Valley (1979/10/15) earthquake for 8m,10m,10.5m,11m,11.5m,12.5m,14m,16m,are,81,83, 83,85,83,83,81,75 which are less as compared to base shear 90,93,86,84,90,91,91,94 under Kern-Country (1952/07/21) earthquake and base shear 90,93,92, 93,95, 95, 95, 95 under Sanfracisco (1957/03/22) earthquake.

In 500kl tank the percentage reduction of base shear under Imperial Valley (1979/10/15) earthquake for 8m,10m,10.5m,11m,11.5m,12.5m,14m,16m,are,81,88, 89,91,89.4,89.5,88.2,87.7which are less as compared to base shear,93,94,95,95,94,94,94,95,under,Kern-Country (1952/07/21)earthquake,and,base-shear,93,96, 96, 95,94, 95, 94, 95 under Sanfracisco(1957/03/22) Earthquake.

Base shear values for all the tanks are considerably reduced after isolation. It is found that all the tanks behave satisfactory under Kern-Country (1952/07/21) earthquake, and Sanfracisco (1957/03/22) earthquake as compared to Imperial Valley (1979/10/15) earthquake. It is also observed that the designed isolation system decreases the base shear value as damping of the isolation system maintains constant. In fig. 2.7 to fig. 2.9 shows the comparative graphs with height and normalized base shear for considered time history**.**

In fig. 3 to fig.4.1 shows the comparative graphs with time and base shear values of isolated and fixed base tanks for considered time history.

V. CONCLUDING REMARKS

1. Comparative performance of elevated liquid storage tanks supported on shafts by putting the base isolation system at bottom of the supporting shaft is investigated using real earthquake motions. The earthquake response of isolated tanks is compared with the non isolated (fixed base) tanks to measure the effectiveness of the isolation.
2. It is observed that the base shear of elevated liquid storage tanks supported on shaft is significantly reduced due to isolation.
3. The drift of the tank relation to base of shaft is also significantly reduced due to isolation.
4. The earthquake response of isolated short tanks is relatively more, i.e. isolation is not effective for stiffer shafts, and however in general, the effectiveness of base isolation is achieved for tall tanks.
5. Although the effectiveness of seismic isolation increases with the increase of bearing flexibility and damping these properties needs to be modified for desired response.

REFERENCES

[1] Jain S.K., Jaiswal O. R. IITK-GSDMA Guidelines for seismic design of liquid storage tanks.

[2] http://peer.berkeley.edu/research/motions

[3] Shrimali M. K. And Jangid R.S. Earthquake response of isolated elevated liquid storage steel tanks, Dept.Of Civil Engg. IIT, Bombay.

[4] 4.Cenk A. and Metin A. Performance of non linear base isolation systems designed according to uniform building code, 5th international advanced technologies symposium (IATS'09) May13-15, 2009, Karabuk, Turkey.

[5] International building code, UBC 1997

[6] IS 3370-1967-PART I, "Code of practice for concrete structure for storage of liquids" Bureau of Indian standards, New Delhi.

[7] Kelly, J.M., Earthquake resistant design with rubber, Springer Publishers, New York, USA (1997).

[8] SAP-2000 Version-9 COMPUTRS AND STRUCTURES, INC, Berkeley, California

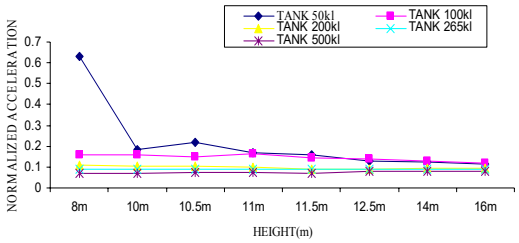

Fig.2.4 Normalized Acceleration Response Spectra for Imperial Valley (1979/10/15) Earthquake

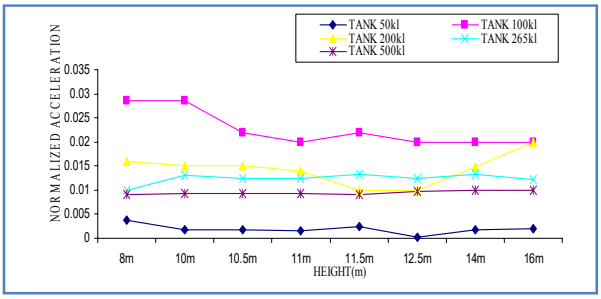

Fig.2.5 Normalized Acceleration Response Spectra for Kern Country (1952/7/21) Earthquake

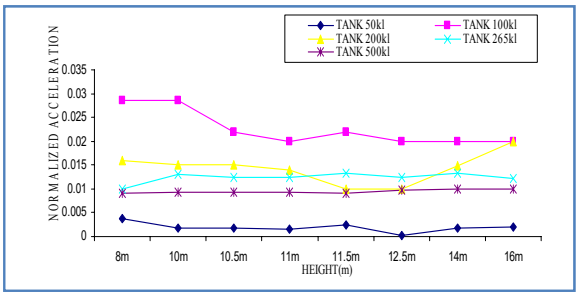

Fig.2.6 Normalized Acceleration Response Spectra for Sanfracisco (1957/03/22) Earthquake

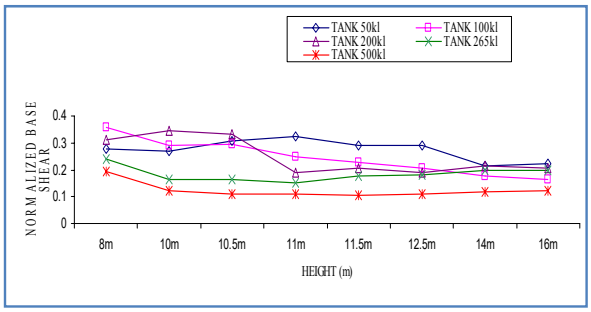

Fig.2.7 Normalized Base Shear Response Spectra for Imperial Valley (1979/10/15) Earthquake

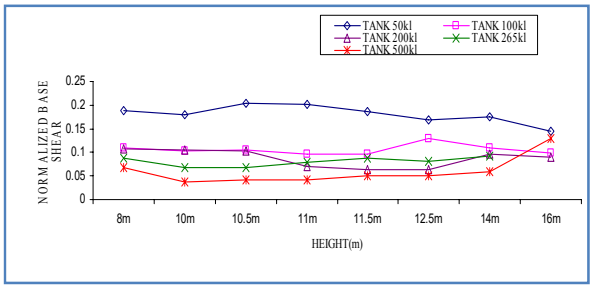

Fig.2.8 Normalized Base Shear Response Spectra for Kern Country (1952/7/21) Earthquake

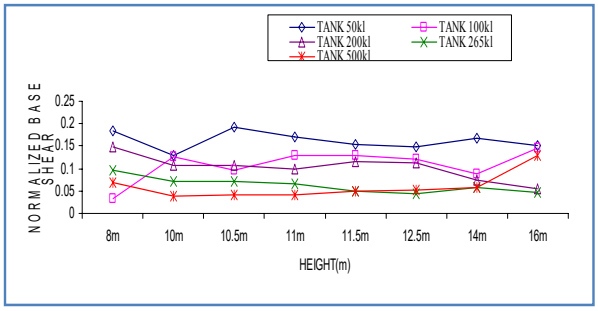

Fig.2.9 Normalized Base Shear Response Spectra for Sanfracisco (1957/03/22) Earthquake

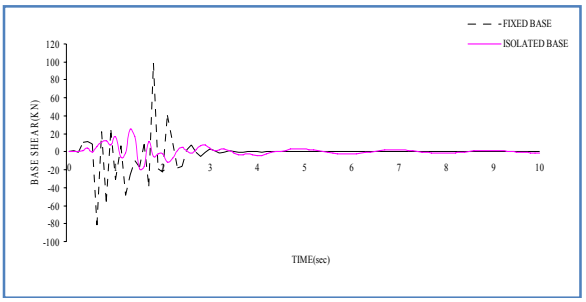

Fig.3 Variation of Base Shear Response Spectra against Time of 50kl Tank (Height 8m) For Imperial Valley (1979/10/15) Earthquake

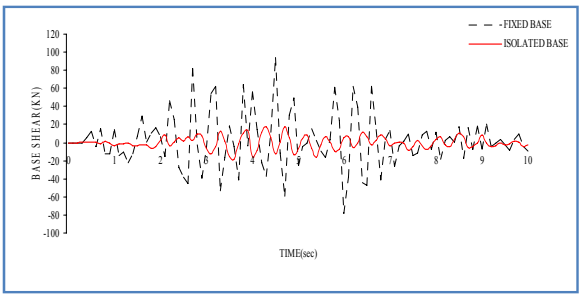

Fig.3.1 Variation of Base Shear Response Spectra against Time of 50kl Tank (Height 8m) For Kern Country (1952/7/21) Earthquake

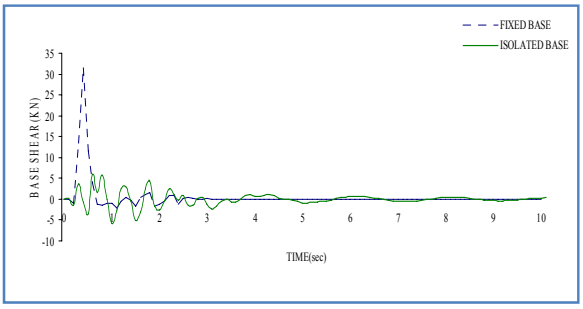

Fig.3.2 Variation of Base Shear Response Spectra against Time of 50kl Tank (Height 8m) For Sanfracisco (1957/03/22) Earthquake

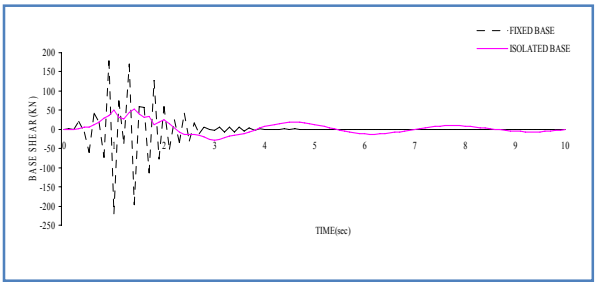

Fig.3.3 Variation of Base Shear Response Spectra against Time of 100kl Tank (Height 10m) For Imperial Valley (1979/10/15) Earthquake

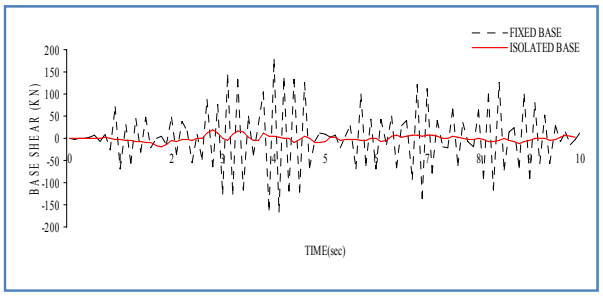

Fig.3.4 Variation of Base Shear Response Spectra against Time of 100kl Tank (Height 10m) For Kern Country (1952/7/21) Earthquake

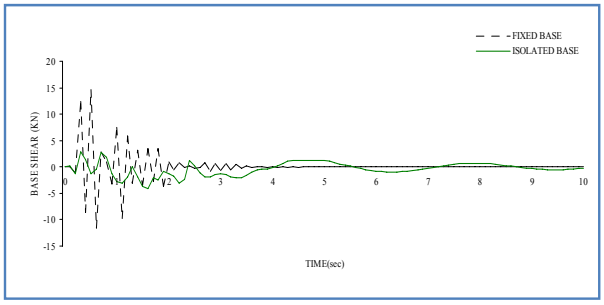

Fig.3.5 Variation of Base Shear Response Spectra against Time of 100kl Tank (Height 10m) For Sanfracisco (1957/03/22) Earthquake

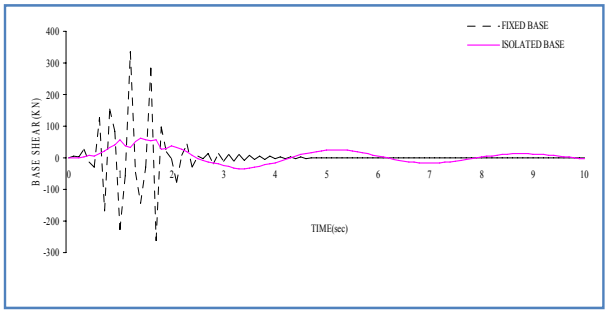

Fig.3.6 Variation of Base Shear Response Spectra against Time of 200kl Tank (Height 11m) For Imperial Valley (1979/10/15) Earthquake

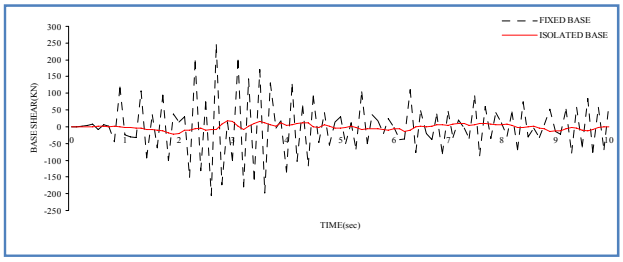

Fig.3.7 Variation of Base Shear Response Spectra against Time of 200kl Tank (Height 11m) For Kern Country (1952/7/21) Earthquake

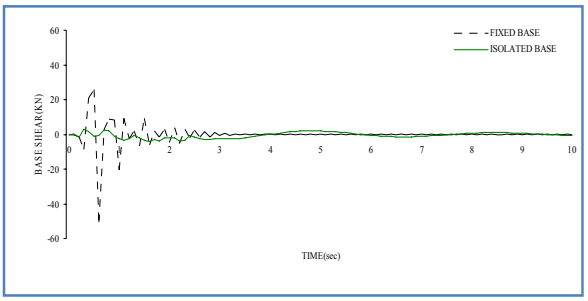

Fig.3.8 Variation of Base Shear Response Spectra against Time of 200kl Tank(Height 11m) For Sanfracisco (1957/03/22) Earthquake

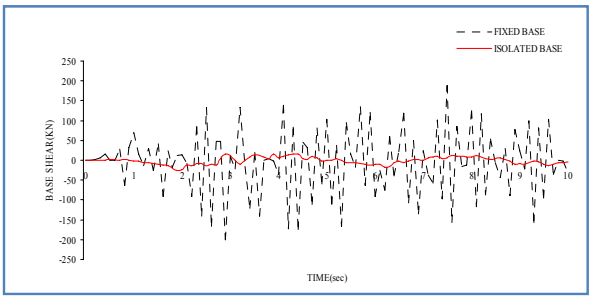

Fig.4 Variation of Base Shear Response Spectra against Time of 265kl Tank (Height 12.5m)For Kern Country (1952/7/21) Earthquake

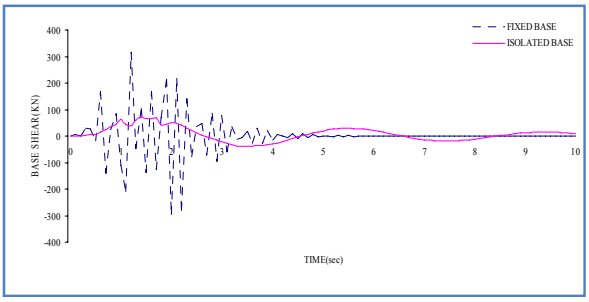

Fig.3.9 Variation of Base Shear Response Spectra against Time of 265kl Tank (Height 12.5m) For Imperial Valley (1979/10/15) Earthquake

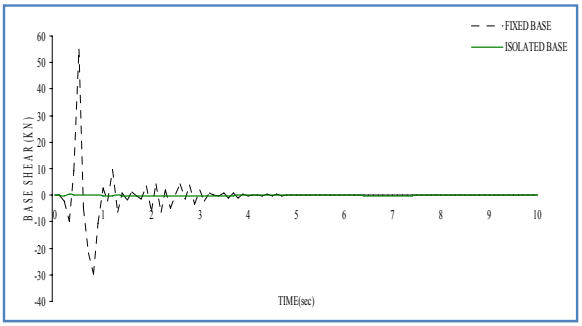

Fig4.1 Variation of Base Shear Response Spectra against Time of 265kl Tank (Height 12.5m) For Sanfracisco (1957/03/22) Earthquake

Performance of FRP Confined Concrete Columns In Fire

Jivesh Kumar & RamanshBajpai
Infrastructure Engineering, University of Petroleum and Energy Studies, Dehradun, India

Abstract **-** Over the past decade, research has shown that fiber reinforced polymers (FRP's) can be efficiently, economically and safely be used for strengthening and rehabilitation of reinforced concrete RC structures. However little is known about the behaviour of FRP materials, at high temperature and this is a primary factor limiting the widespread application of FRP materials in buildings, parking garages and industrial structures. This paper presents the results of a numerical program to investigate the fire performance of FRP wrapped confined RC columns. The primary objective of this research paper is -: to develop numerical models to simulate the behavior in fire of these members; to investigate techniques to improve their behavior in fire; and to use data from numerical studies to provide fire design guidance. A numerical model is presented which is capable of predicting the thermal and structural response of FRP wrapped confined RC columns under exposure to standard fire.

Keywords*-FRP; numerical program; thermal and structural response.*

I. INTRODUCTION

Externally bonded fiber reinforced polymers (FRP) are now widely accepted as an effective and efficient means of repairing and upgrading deteriorated or under strength reinforced concrete (RC) structures. One of the most efficient and widely implemented, of these FRP repair techniques is circumferential wrapping (confinement) of RC columns, which has shown to increase both axial strength and ductility of these members. Design recommendations are now available for repair and upgrade of concrete columns with FRP wraps, and the technique has, in the last 10 years, been used in hundreds of field applications around the world. Despite the numerous advantages of the FRP wrapping technique, it has yet to see widespread applications in buildings, due in large part to uncertainties associated with the FRP materials during fire. This paper presents results of an ongoing numerical research program investigating the behavior in fire of FRP wrapped RC columns. The current discussion focuses on column strengthening applications, although slab and beam slab assembly strengthening applications are also being investigated within the overall program.

II. FRP'S IN FIRE

All structural materials, including concrete and steel, experience some degradation in mechanical properties and elevated temperature, and this is true also of FRP's. At elevated temperatures, beyond the GTT of the FRP's polymer matrix component, mechanical properties deteriorate rapidly, this results reduction in the strength and stiffness of the FRP. In addition, in extremely-bonded FRP applications, it is likely that exposure to elevated temperatures would lead to rapid and severe deterioration of the FRP/concrete bond, resulting in delamination of the FRP and loss of its effectiveness as tensile or confining reinforcement. To accomplish this goal, a database of results from tensile tests on FRP at high temperature was assembled from the literature. For each type of FRP, a sigmoid function was fitted to the data using a least squares regression analysis. As an example, the resulting curves for the strength and stiffness deterioration of carbon/epoxy FRP (CFRP) with temperature are shown in fig.1. also included in fig1 are equivalent curves for reinforcing steel and concrete.

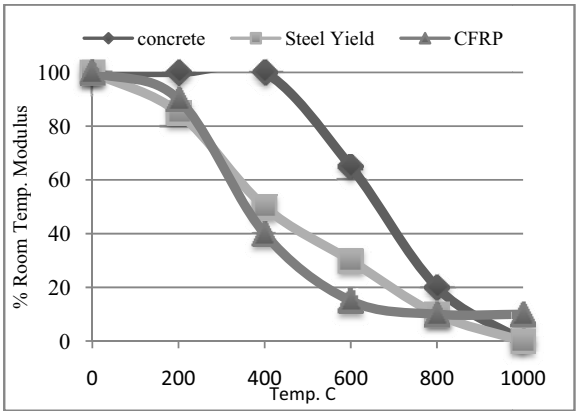

Fig. 1(a) Reduction of strength.

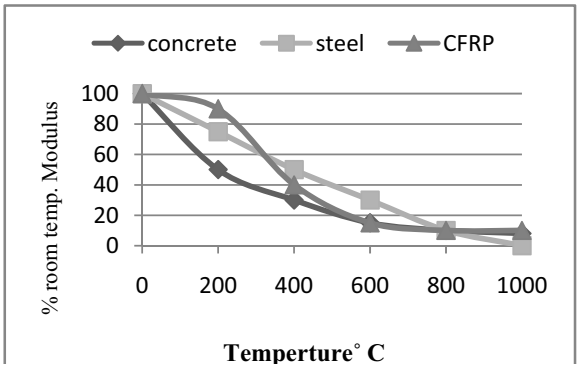

Fig 1(b) Reduction of stiffness of Carbon/Epoxy FRP at elevated temperatures.

III. NUMERICAL MODEL

Fire resistance experiments on loaded full-scale columns are relatively complex and costly to perform, with the advent of powerful computing capabilities, however, it is now possible to develop detailed numerical models which, once verified by relatively few full-scale experiments, can be used to conduct parametric studies and examine the influence of various factors on member behavior in a more cost effective manner. For current study, a numerical model has been developed to stimulate both the heat transfer and load capacity of FRP wrapped RC columns.

A. Heat Transfer

The transfer of heat within the column during fire is treated using an explicit finite difference methodology wherein the column is divided into a series of ring elements. For each ring, an energy balance is formulated such that the heat entering into minus the heat going out of the element (due to conduction) is equated to the energy stored in the element during some finite time interval. This allows the development of a series of equations which, once programmed into a computer, can be used to predict the temperature at any location within an FRP-wrapped and insulated RC column during exposure to fire following a known time- temperature curve. The thermal analysis ignores the contribution of the reinforcing steel to temperature propagation since its effect is negligible due to the small cross-sectional area of rebars.

B. Load Capacity

The load capacity of a structural member in fire can be evaluated once the distribution of internal temperatures is known (using heat transfer model described above). The analysis tools developed in the current program allow for the calculation of column strength based on pure axial crushing or on buckling. The buckling generally governs failure in fire for column lengths that would be encountered in practice. The analysis accounts for the thermal deterioration of mechanical properties of all materials involved, except for the insulation which is assumed to provide negligible strength to the column. The output of the load capacity analysis consists of curves showing the variation in axial strength, buckling strength, or overall axial elongation, with time during exposure to fire.

IV. RESULTS AND DISCUSSION

A. Temperatures

Figure 2 presents the temperature recorded at various key locations. Included also in figure 2a are equivalent temperatures as predicted by the numerical model. For both columns, the temperature at the level of the FRP is seen to increase fairly rapidly within the first 15-45 minutes of exposure, at which point the rate of temperature rise decreases and a temperature plateau is seen near 100 degree centigrade. The duration of this plateau, which can be attributed to the evaporation of both free and chemically combined moisture from the insulation at temperature near the boiling point of water is longer for column 2, which has greater insulation thickness, as should be expected. Indeed the FRP temperature in col. 2 remains less than 100 degree centigrade for more than 3 hours under fire exposure. Once all of the moisture has evaporated, the temperatures at the level of the FRP increase more rapidly until the end of the test. This behavior implies that one way to significantly improve the fire performance of the columns would be to increase the GTT of the polymer matrix to even slightly above 100 degree centigrade. The temperature at the level of the FRP remained less than the matrix ignition temperature for the full duration of fire exposure for col.2. For column 3, the ignition temperature was exceeded about 3 hours of exposure (a factor which may have contributed to its sudden failure at slightly more than 4 hours). For all 3 columns, the thermal insulation provided by the supplemental insulation was excellent, and temperatures within the concrete and reinforcing steel remained less than 350 degree centigrade for the full duration of the fire (until failure). Thus, it is likely that the columns retained essentially all of their unwrapped strength till the insulation was lost late in the fire exposure (beyond 4 hours for col.5 and beyond 5 hours for cols. 1 &2). Hence, the columns satisfied the ASTM E119 fire endurance requirement for 4 or 5 hours for the square and circular columns respectively.

Figures 2a and 2b show that, while the predictions of the numerical model generally is in agreement with test data, the model does not precisely capture the 100 degree centigrade temperature plateau exhibited in the experimental thermal profiles. This can be attributed to

the fact that, while the model does account for the evaporation of moisture from individual elements at 100 degree centigrade, it does not account for the migration of free moisture in the concrete away from the fire.

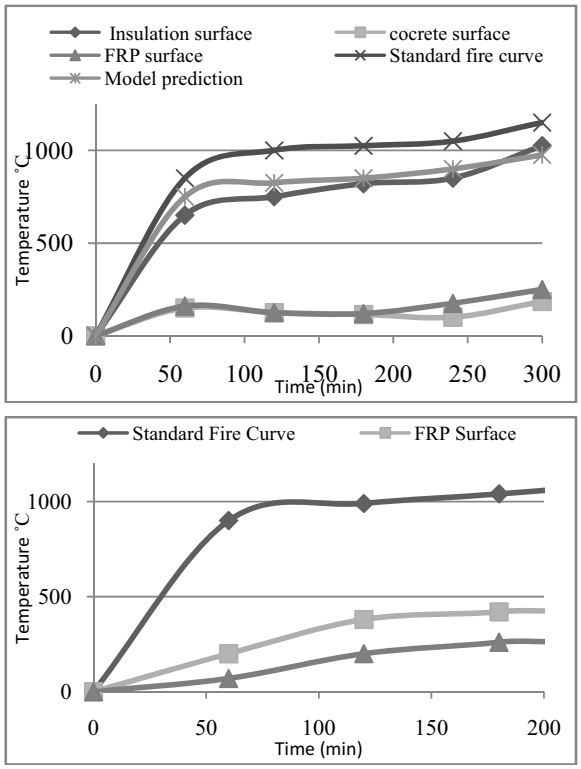

Figure 2 – temperature observed (or predicted) in (a) Col.2 (57mmVG) and (b) Col.3 (38mm VG).

B. Fire Endurance

All columns tested were able to carry their full service load for at least 4 hours of exposure to the standard fire. Cols. 1 and 2 both failed at approximately 5.5 hours of fire exposure, and only once the applied load has been increased to about 1.8 times the required service load. Failure was sudden and explosive, and was accompanied by extensive spalling. Thus, as expected given the thermal profiles of concrete discussed above, these two columns indeed retained virtually all of their room- temperature unwrapped strength for the full duration of fire exposure. Col. 3(the square column) failed in an explosive manner at about 4.25 hours of fire exposure while under only its applied service load. The resulting combustion of the fire-exposed FRP directly exposed the substrate concrete, which had previously been at less than 400*C, to the full heat of the fire (at about 1100*C). This result in an extreme thermal shock to the concrete and caused explosive spalling resulting in rapid and catastrophic failure of column.

To demonstrate the use of the numerical model for the prediction of fire endurance of an FRP-wrapped RC column, Fig. 3a shows the predicted axial crushing strength of a concrete column with fire exposure time, and Fig. 3b shows a similar plot for the column's predicted buckling strength.

The following points are worthy of note with respect to fig. 3:

1. The model reasonably predicts the strength of the two circular FRP-wrapped RC columns tested to date after 5.5 hours of fire exposure (based on the buckling analysis).
2. For all cases shown the predicted axial crushing strength is greater than the predicted buckling strength for the full duration of the fire exposure (note that the buckling analysis assumes an initial eccentricity of 27 mm).
3. Loss of structural effectiveness of the FRP is predicted to occur very rapidly during the fire exposure for a wrapped but uninsulated column. Once the wrap is lost, the strength of the column is only slightly greater than that of an equivalent unstrengthened column. Loss of the wrap is seen to be more significant for the crushing strength analysis as opposed to the buckling strength analysis. This is because confinement of concrete with an FRP wrasp cannot be expected to significantly increase the concrete's modulus, and hence the buckling strength is not substantially improved by FRP wrapping.
4. Even a small amount of supplemental insulation (32mm for col.1) is predicted to significantly improve the retention of strength during fire. This is due primarily to the fact that the concrete and reinforcing steel in the column remain at sufficiently low temperatures to prevent degradation of their mechanical properties, and not to the effectiveness of the FRP warp being maintained. Thus, the columns are predicted to retain a significant portion of their unwrapped strength even if the FRP is lost.

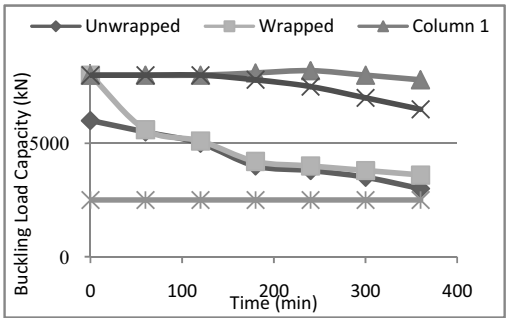

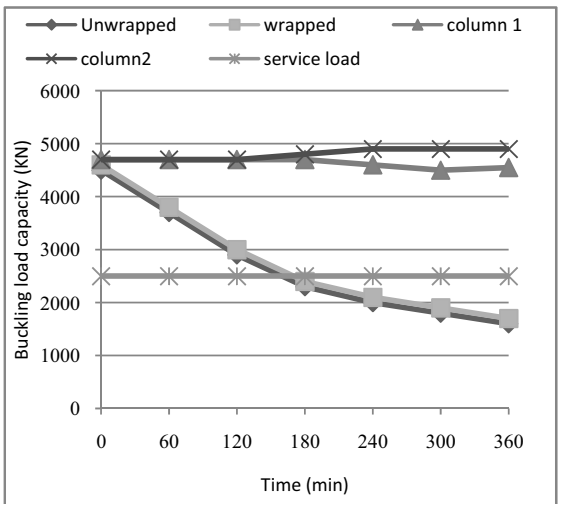

Fig.3 – Observed and predicted structural fire endurance for various column configurations based on (a) crushing strength and (b) buckling strength.

V. CONCLUSIONS

- FRP materials used as externally – wounded reinforcement for concrete structures are sensitive to the effects of elevated temperatures.
- FRP's experience degradation in strength, stiffness, and the bond at temperatures exceeding the GTT of the polymer matrix.
- Appropriately designed (and in the most cases supplementally- insulated) FRP wrapped circular RC columns can achieve satisfactory fire endurances in excess of 5 hours.
- The numerical models presented briefly herein can be used to predict the heat transfer within, and load capacity of, unwrapped and FRP wrapped and insulated RC columns under exposure to a standard fire.
- Parametric studies conducted using the model (not discussed here) indicate that the most important factors influencing the fire endurance of FRP wrapped RC columns are the thickness and thermal conductivity of the insulation applied to the exterior of the FRP wrap.
- While no explicit requirement currently exists that the temperature of an FRP wrap must remain below its matrix GTT during fire, it is not known what temperatures are allowable in the FRP such that it retains sufficient residual properties to remain effective after a severe building fire.
- Further work is required in this area.

REFERENCES :

1. Apicella, F., &Imbrogno, M., "Fire performance of CFRP-composites used for repairing and strengthening concrete," Materials and Construction, Cincinnati, OH, USA, May, 1999, pp 260-266.
2. Saadatmanesh, H.; Ehsani, M.R.; and Li, M.W, "Repair of earthquake damaged RCC columns with FRP wraps," ACI Structural Journal, No. 94, S-20,1996,pp. 206-214.
3. Benichou, N. "Results of Fire Resistance Experiments on FRP-Strengthened Reinforced Concrete Columns – Report No. 2", Research, Report, Institute for Reseach in Construction, National Research Council Canada, pp. 39, 2007.
4. Benichou, N. "Fire Performance of FRP-strengthened concrete systems", short course, Response of Materials and Structures to Fires, Carleton University, Ottawa, Ontario, May 20-22, 2009.
5. FOSTA PVT LMT, "FRP for Structural Strengthening in Land and Marine Environment", Singapore.
6. Krishna Conchem Pvt. Ltd., http:// www.krishnaconchem.com/products.html
7. Mukherjee, Abhijeet, and Joshi, Mangesh. "Recent Advances In Repair And Rehabilitation of RCC Structures". Department of Civil Engineering, IIT Bombay.
8. Limaye.R.G., and KAMAT M.K., Experimental studies on polymer modificationof cement mortar, The Indian Concrete Journal, March1992.
9. Sorathia, U., Dapp, T., & Beck, C., "Fire performance of Composites," Mat. Engrg., 9, 1992, pp. 10-12.
10. Lie, T., Structural Fire Protection, ASCE, New York, NY, USA, 1992, pp. 241.
11. ISIS, Design Manual No. 4, ISIS Canada, Winnipeg, MB, Canada, 2001.

◈◈◈

System Identification with Noisy Data

U. K. Dewangan[1] & S. V. Barai[2]

[1]Dept. of Civil Engineering, National Institute of Technology, Raipur, India
[2]Dept of. Civil Engineering, IIT Kharagpur, Kharagpur -721 302, India

Abstract - System identification from the field obtained data is not successful till date because of the noise in the sensor or measured. The unknown system parameter for any unknown damage is still a long way to move. In this paper finite element technique is applied on the simulated damaged structures. The damage detection for the noise free data is extended and tried for the random noisy sensor data. The proposed algorithm is used to predict the system parameter on static deflection data with introduction of some random noisy data using simulated structure. The developed algorithm is applied on bridge truss structure for the identification of the damaged system parameter prediction.

Key words - *Damage, System identification; Noisy data; Finite element.*

I. INTRODUCTION

The prediction of the damaged parameters from the field data having noise is still an open challenge in the field of structural identification. The Structural Health Monitoring (SHM) of large space structures like aerospace structure; satellite vehicles, where once the damage had occurred cause the uncertainty due to unknown damaged parameter. Finite element methods are universally accepted as fast computation tools for structural behavior prediction. Development in the field of computational technology and sensing instruments has also progressed a lot. Field data are usually noisy. The damage detection, location and damage extent prediction are among the important aspect of structural behavior prediction. The main aim of researchers is concentrated on the suitable identification algorithms based on uncertain available sensor data which may be linear or nonlinear, noisy or noise free sensor data.

There are two kinds of parameter identification namely static and dynamic parameter identification. In the dynamic parameter identification there are three unknowns. They are mass, stiffness and damping. The relationship between the dynamic coefficients (mass, stiffness and damping) and also its sensitivity effects of one property on another are still unknowns. Such a system makes the analysis very complicated. For uncertain damage with uncertain noisy data, no certain techniques are available. The static identification method seems to be better than dynamic identification as it is having only one unknown (stiffness).

A brief review on damage detection mainly using the static method or static combined with dynamic method is presented here. The static damage parameter identification approaches by the error term reduction includes minimum deviation, sensitivity analysis, output error optimization etc. were approached by [2] , [4], [7], [12], [14] and [15]. Damage detection in composite materials using system identification technique proposed by [14]. The output error approach of system identification was employed to determine the changes in the analytical model in order to minimize the distance between measured and predicted response. [2] Used force error estimator and displacement error estimator for static parameter grouping scheme to identify the error by least squares minimization. Static strain measurement from multiple loading models for identification of the hole and cracks in linear anisotropy elastic materials with nonlinear optimization was presented by [4]. [15] applied a linear constrained nonlinear optimization problem using the minimization of error between the measured and computed displacement to find damage.

Error sensitivity analysis is found to be a popular method for finding the damage existence [9], [11], [13], [1. On analyzing the sensitivity coefficients for natural frequency, mode shapes and modal flexibility, [9] found that modal flexibility is more sensitive as damage indicator. Sensitivity with some other term approach like orthogonal sensitivity, non-linearity, modal updating were approached by[3], [16], [20] etc. The orthogonal condition sensitivities was developed by [16]

for the damaged and undamaged structure mode shapes using FEM in laminated rectangular plate of composite structures. [20] presented a sensitivity-based finite element (FE) model updating for damage detection. The modal flexibility residual formulation and its gradient were used for formulation. The damage detection procedure was illustrated on a simulated example with noisy data and on a reinforced concrete beam model.

Dmage detection of cable-stayed bridges by changes in cable forces, was optimized on cable force error between measurement results and analytical model by [17]. [10] developed a method used continuous strain data from fiber optic sensor and neural network model. [18] used sensitive characteristic of strain to identify damage in structures for strain-based damage identification. [8] Used conventional single-objective optimization approach defines the objective function by combining multiple error terms into a single one, for weaker constraint in solving the identification problem.

The above literature review indicates that both static as well dynamic methods were used in the system parameter prediction of structure using simulated, experimental and from the field data. Static methods used either strain or displacement as measured data, while in case of dynamic methods frequency and mode shapes data were used popularly. Sensitivity method, analyses the effect of parameter changes on the other parameters. When the structural parameters are unknown, the sensitivity analysis has no meaning. In addition, noise in the measured data may completely change the matrix property using matrix inversion. The structural parameter identification from the field data has no well-established solution, until now.

The paper is attributed to the static parameter identification process with the noisy sensor data. The objective of this paper is to develop a new modified approach for the noisy sensor data with few measurement. The initial parameter identification algorithm has been taken from [13] but some noise were introduced in the sensor data. This will lead to near realistic field situation. Finite element method for damage detection using static test data for smaller subgroups of matrix was applied [3] for damage existence prediction with only few measurements. The noise values were varied between ± 4 % errors in the sensor data. A finite element model of bridge truss structure presented for the demonstration.

II. INITIAL AND DEDELOPED APPROACH

An algorithm to find the parameter extent for noise free data was developed by [13]. Assuming the structure behavior of structure is linear throughout the test, the force displacement relationship in the static case for undamaged structure is given by

$$[F] = [K][U] \tag{1}$$

and for damaged structure by

$$[F] = [K_d][U] \tag{2}$$

Partitioning into measured and unmeasured displacements

$$\begin{bmatrix} \boldsymbol{f_a} \\ \boldsymbol{f_b} \end{bmatrix} = \left[\begin{array}{c|c} \boldsymbol{K_{daa}} & \boldsymbol{K_{dab}} \\ \hline \boldsymbol{K_{dab}} & \boldsymbol{K_{dbb}} \end{array}\right] \begin{bmatrix} \boldsymbol{U_a} \\ \boldsymbol{U_b} \end{bmatrix} \tag{3}$$

$$[f_a] = [[K_{aa}] - [K_{ab}]^{-1}[K_{bb}]^{-1}[K_{ab}]\,][U_a] + [K_{ab}][K_{bb}]^{-1}[f_b] \tag{4}$$

$[f_a]$, $[f_b]$ and $[U_a]$ are measured from test. The difference between the measured and theoretically calculated value will be the error term. If the stiffness parameters are correct, then error matrix $[E(p)]$ will be zero, otherwise non-zero.

$$[E(p)] = [[K_{aa}] - [K_{ab}]^{-1}[K_{bb}]^{-1}[K_{ab}]\,][U_a] + [K_{ab}][K_{bb}]^{-1}[f_b] - [f_a] \tag{5}$$

$$[E(p)] \approx \{E(p)\} + \{S(\delta p)\}[\Delta p] \tag{6}$$

The error sensitivity expression was calculated using first order Taylor series expansion of error matrix $[E(p)]$. The stiffness parameters were obtained by minimization of error function with respect to unknown parameter ***(p)*** using the least square optimization.

The error sensitivity expression has been modified for noisy sensor data as the displacement gets modified due to sensor noise and unknown damaged. The unknown parameters become the function of both displacements. The sensitivity matrix was recalculated with this new modified expression,

$$[S(p_i)] = [\frac{\partial [k_{aa}]}{\partial p_i} - \frac{\partial [k_{ab}]}{\partial p_i}[k_{bb}]^{-1}[k_{ba}] - [k_{ab}][k_{bb}]^{-1}\frac{\partial [k_{ab}]}{\partial p_i}$$
$$+ [k_{ab}][k_{bb}]^{-1}\frac{\partial [k_{ab}]}{\partial p_i}[k_{bb}]^{-1}[k_{ba}]\ ][U_a] + \left[[k_{aa}] - [k_{ab}][k_{bb}]^{-1}[k_{ab}]\right]\frac{\partial [U_a]}{\partial p_i}$$
$$+ \left[\frac{\partial [k_{ab}]}{\partial p_i}[k_{bb}]^{-1} - [k_{ab}][k_{bb}]^{-1}\frac{\partial [k_{bb}]}{\partial p_i}[k_{bb}]^{-1}\right] *$$
$$\left[[f_a] - \left[[K_{aa}] - [K_{ab}]^{-1}[K_{bb}]^{-1}[K_{ab}]\right][U_a]\right] * [K_{ab}]^{-1}[K_{bb}]$$
$$+ \left[[K_{ab}][k_{bb}]^{-1}[f_b] - [f_b]\right]\left[[f_a] - \left[\frac{\partial [k_{aa}]}{\partial p_i}[k_{bb}]^{-1} + [K_{aa}]\frac{\partial [k_{aa}]}{\partial p_i} - \right][U_a]\right] * [K_{ab}]^{-1}[K_{bb}]$$
$$+ \left[[f_a] - \left[\frac{\partial [k_{aa}]}{\partial p_i}[k_{bb}]^{-1} + [K_{aa}]\frac{\partial [k_{aa}]}{\partial p_i} - \right]\left[\frac{\partial [U_a]}{\partial p_i}\right]\right] * [K_{ab}]^{-1}[K_{bb}] \qquad (7)$$

The present method is able to predict the damage existence in structure with only few measurements. Using least square optimization technique, all the unknown damaged parameters can be identified after some iteration successfully with the noisy sensor data. The finite element method revisited and a row-echelon form of matrix developed for damage detection using static displacement and force data, Dewangan U. K. (2010) [4]. The row-echelon form has an advantage of partitioning matrix into smaller subgroups.The noise values were varied between ± 4 % errors in the sensor data. A finite element model of bridge truss structure presented for the demonstration. The modified algorithm is implemented using MATLAB [21].

III. EXAMPLES

Based on the algorithm discussed in the above section, the computer program was written in MATLAB and tested Bridge Truss Structure Bridge Truss Structure Structural Details: All elements are having the modulus of elasticity $E = 210\,GPa$ and initial undamaged cross sectional area $A = 1.61X10^5\ mm^2$. The structural configuration is shown in Fig. 3.8. A single concentrated load is applied at each joint. The deflections at each joint are measured. The force matrix $[F]$ is found out and corresponding displacement matrix $[U]$ is measured.

For bridge truss structure, [1] as shown in Figure 1, the modulus of elasticity of all elements was 206.8 GPa and initial undamaged cross sectional area of all members was 500 mm^2. The noise was introduced up to ± 5 % error in the sensor data for sensor numbers 5, 6, 7 and 8 displacement d.o.f. Different load combinations are considered and they are tabulated in the Table 2 with sensor noise value. Previously discussed algorithms were applied to this problem and results are given in Table 2 and Figure 4 for typical cases. For the noisy sensor data set combination on tower truss the computed parameter values were compared with the actual parameter value. From the plotted graph as shown in Figure 2, it is clear that with the noisy sensor data, [13] algorithm values are far away from the actual value of the parameter. The modified proposed algorithm values are nearly close to the actual value of the parameters. The algorithm could identify the damage extent for members away from the supports.

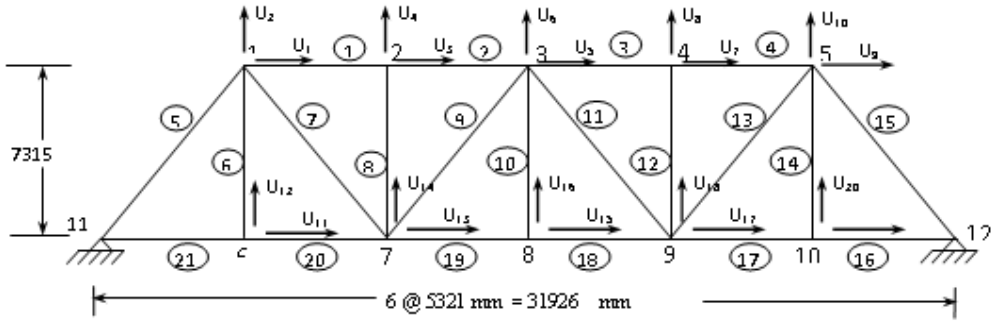

Fig. 1 : Railway bridge truss

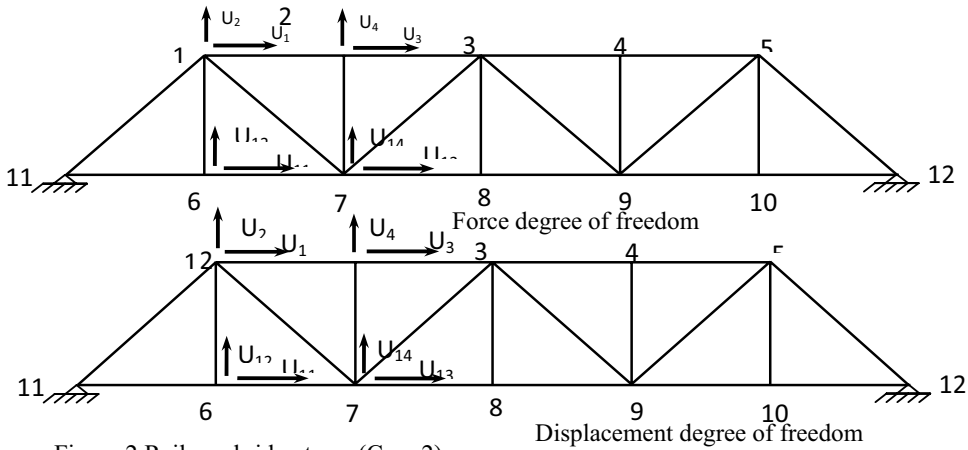

Figure 2 Railway bridge truss (Case 2)

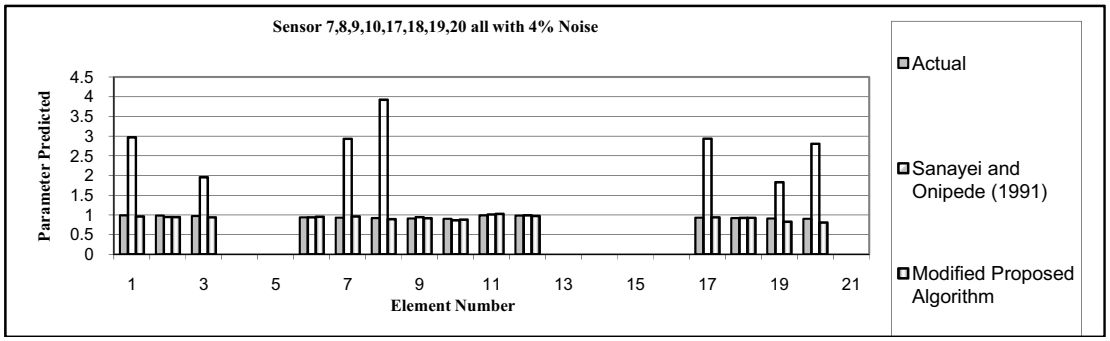

Fig. 3 : Comparative study of damage extent prediction (Bridge truss Structure)

TABLE I: RESULTS OF NOISY SENSOR DATA WITH MODIFIED ALGORITHM ON BRIDGE TRUSS

Case	Member damaged	Applied force d.o.f.	Measured displacement d.o.f.	Noise in Sensor	Members Converged	Members Diverged
1	All	1-20	1-20	8 up to 5%	1-4, 6-14, 17-20	5,16,15 and 21
2	All	7-10, 17-20	7-10, 17-20	1- 8 up to 5%	1-4, 6-14, 17-20	5,16,15 and 21
3	All	7-10, 17-20	1-4, 11-14	4 up to 5%	1-4, 6-14, 17-20	5,16,15 and 21
4	All	1-20	1-20	5,6,7 and, 8	1-4, 6-14, 17-20	5,16,15 and 21

				up to 4%		

.

IV. RESULTS

Considering the various multiple damaged member combinations, the existence of damage is detected.

Different combinations of force DOF and displacement DOF used are given in Table 1for various cases.

From the plotted graph as shown in Figure 4, it is clear that with the noisy sensor data, the modified proposed algorithm values are nearly close to the actual value of the parameters. The algorithm could identify the damage extent for members away from the supports.

V. DISCUSSION

In this study, it was clearly observed from the demonstrated examples that the modified algorithm could predict damage extent in the presence of noise in structural response. Further it was found that the algorithms failed to predict damage extent in the members, which were near to the support. Hence, the present work is very well justified for the large space structures where except the support connected members, all other members, damage extent could be predicted. The failure of the algorithm in identifying the damage extent in members near support is a matter of further investigation.

VI. CONCLUSION

The damage parameter identification with the noisy sensor data was carried out for different random noise value. Algorithm developed by [13] has been modified for the noise in sensor value. Finite element method for damage detection using static test data for smaller subgroups of matrix was applied [3] for damage existence prediction with only few measurements. The noise values were varied between ± 4 % errors in the sensor data. The algorithm works well for lower noise level up to a value ± 4 % errors in the sensor data and the unknown damaged parameter could be extracted even from the noisy data set of structural response using above technique for the members with only few measurements. Hence the algorithm is useful for damage prediction with noisy sensor data on large structures for the members, which are away from the supports.

NOTATION

d.o.f. = Degree of freedom

d.d.o.f. = Displacement degree of freedom

f.d.o.f. = Force degree of freedom

{E(p)} = Error function vector

[Fa] = Applied force matrix at force d.o.f. at measured d.o.f.

[Fb] = Unapplied force matrix at force d.o.f. for unmeasured displacement d.o.f.

F.E.M. = Finite element method

[K] = Undamaged global stiffness matrix

[Kdaa] = Sub matrix of [K] corresponding to measured d.o.f. and applied force d.o.f.

[Kdab] = Sub matrix of [K] corresponding to measured d.o.f. and unapplied force d.o.f.

[Kdbb] = Sub matrix of [K] corresponding to unmeasured d.o.f. and unapplied force d.o.f.

[Kdba] = Sub matrix of [K] corresponding to unmeasured d.o.f. and applied force d.o.f.

[Kd] = Damaged global stiffness matrix

n = Number of elements

p = Unknown parameter's values

r = Row number

[Sd] = Damaged global stiffness matrix

[S] = Undamaged global stiffness matrix

[Saa] = Sub matrix of [S] corresponding to measured d.o.f. and applied force d.o.f.

[Sab] = Sub matrix of [S] corresponding to measured d.o.f. and unapplied force d.o.f.

[Sbb] = Sub matrix of [S] corresponding to unmeasured d.o.f. and unapplied force d.o.f.

[Sba] = Sub matrix of [S] corresponding to unmeasured d.o.f. and applied force d.o.f.

{S(p)} = Sensitivity matrix

[U] = Transformation matrix

[Ua] = Measured displacements matrix

[Ub] = Unmeasured displacements matrix

REFERENCES

[1] S. R. Agrawal, "Steel Bridges In Indian Railways. Advances in Steel Structures," (Ed.) V. Kalyanraman, Proc. of the National Symposium on Advances in Steel Structures, Tata McGraw Hill, Publishing Company Ltd., New Delhi, ,1990, pp. 227–243.

[2] M. R. Banan, M. R. Banan and K. D. Hjelmstad, " Parameter Estimation of Structures From Static Response II: Numerical simulation studies,"

Journal of Structural Engineering, vol. 120, Nov,1994, pp. 3259–3283.

[3] U. K. Dewangan, "Structural Damage Existence Prediction with Few Measurements" International Journal of Engineering Science and Technology, Vol. 3, 2011 No.10, pp. 7587–7597.

[4] C. Hwu and Y. C. Liang, "Hole Crack Identification By Static Strains from Multiple Loading Modes," AIAA Journal, vol. 39, 2, 2001, pp. 315–324.

[5] D. Bernal and B. Gunes, "Flexibility Based Approach for Damage Characterization: Benchmark Application," Journal of Engineering Mechanics, vol. 130, 1, 2004, pp. 61–70.

[6] E. Udwadia, "Structural Identification and Damage Detection From Noisy Modal Data," Journal of Aerospace Engineering, vol. 18, 3, 2005, pp. 179–187.

[7] J. H. Jang, I. Yeo, S., Shin, and S. P. Chang, "Experimental Investigation of System – Identification – Based – Damage Assessment on Structures," Journal of Structural Engineering, vo. 128, 3, 2002, pp. 390 – 399.

[8] J. Sungmoon et al., "Structural Damage Identification Based on Multi–Objective Optimization," Conference Proceedings of the Society for Experimental Mechanics Series, 12, 2011, pp. 1239–1244.

[9] J. Zhao and J. T. Dewolf, Sensitivity study for vibrational parameters used in damage detection, Journal of Structural Engineering, 125,4 ,1999, pp. 410–416.

[10] J.W. Lee, C. kwang–Ho and Huh Y. C., "Damage Detection Method For Large Structures Using Static and Dynamic Strain Data From Distributed Fiber Optic Sensor," International Journal of Steel Structures , vol. 10, 2010, pp. 91–97.

[11] L. H. Yam, Y.Y. Li, and W.O. Wong, "Sensitivity Studies Of Parameters For Damage Detection Of Plate – Like Structures Using Static And Dynamic Approaches," Engineering Structures, vol. 24, 11, 2002, pp. 1465–1475.

[12] M. D. Paola and C. Bilello, "An Integral Equation For Damage Identification Of Euler – Bernoulli Beams Under Static Loads," Journal of Engineering Mechanics, vol. 130, 2, 2004, pp. 225–234.

[13] M. Sanayei and O. Onipede, "Damage Assessment Of Structures Using Static Test Data," AIAA Journal, vol. 29, 7, 1991, pp. 1174–1179.

[14] P. Hajela and F. J. Soerio, "Recent Developments in the Damage Detection Based On System Identification Methods," Structural Optimization, vol.2,1990, pp. 1–10.

[15] S. Shin, and H.M. Koh, "A Numerical Study on Detecting Defects in a Plane – Stressed Body by System Identification, Nuclear Engineering and Design, vol. 190, 1999, pp. 17 – 28.

[16] V. Santos, M. Soares, and C, A. Pina, "Damage Identification Numerical Model Based On The Sensitivity Of Orthogonality Conditions And Least Squares Techniques." Computers and Structures, vol. 78, 1, 2000, pp. 283–291.

[17] X. G. Hua, Y. Q. Ni, Z. Q. Chen, and J. M. Ko, "Structural Damage Detection Of Cable–Stayed Bridges Using Changes In Cable Forces And Model Updating, J. Struct. Eng, vol. 135, 9, 2009, pp. 1093–1107.

[18] Y. Y. Li, "Hypersensitivity of strain–based indicators for structural damage identification: A review," Mechanical System and Signal Processing, vol. 24,3, 2010, pp. 653–664.

[19] B. Vanlanduit, E. Parloo, and P. Guillaume, "Combined Damage Detection Techniques," Journal of Sound and Vibration, 266, vol. 4, 2003, pp. 815–831.

[20] B. Jaishi, and W.X. Ren, "Damage Detection by Finite Element Modal Updating Using Modal Flexibility Residual." Journal of Sound and Vibration, vol. 290(1 – 2), 2006, pp. 369 – 387.

[21] R. Pratap, "Getting Started with MATLAB." 3rd Ed., 2001, Oxford University Press. New York.

◈◈◈

Accident Analysis and Prediction of Model on National Highways

Rakesh Kumar Singh & S.K.Suman

Department of Civil Engineering, National Institute of Technology Patna, Patna, Bihar, India

Abstract **-** Rapid growth of population coupled with increased economic activities has favored in tremendous growth of motor vehicles. This is one of the primary factors responsible for road accidents. It is observed that few works have been carried out on statistical analysis of accidents particularly on two-lane National Highways.

For this paper stretch of NH-77 has been selected from Hajipur to Muzaffarpur. The accidental data was collected for last eleven years, 2000-2010 from the Police Stations where FIR was lodged. The collected data were analyzed to evaluate the effect of influencing parameters on accident rate. Heavy vehicles like truck are involved in maximum number of accidents on the selected stretch. It is estimated that a heavy vehicles is involved in almost 48% accidents followed by two-wheelers 16%, car 12% and bus 10%. There is no definite trend for monthly variation in accident on a study section but the accidents in month of July and January are generally higher. Accident rate in terms of number of accidents per km-year increases with traffic volume. But the accidents rate in terms of number of accident per million-vehicle kilometer-year (MVKY) decreases with increase in traffic volume. Accident rate per MVKY increases during the study year, whereas both injury and fatality rate per MVKY show a declining trend over the study period. The developed model for accident prediction represents that the number of accidents per-km-year increases with AADT and decreases with improvement in road condition.

Key word - *FIR, Statistical analysis, Regression model*

I. INTRODUCTION

The highway network is accelerated at a fast rate and the safety of vehicular movements becomes a concern for everybody due to reporting of loss of lives and properties along with fatal injuries and periodical obstruction of traffic flow. National highways provide the efficient mobility and accessibility function. The increasing road accidents have created social problems due to loss of lives and human miseries. Road accidents are essentially caused by interactions of the vehicles, road users and roadway conditions. Each of these basic elements comprises a number of sub elements like pavement characteristics, geometric features, traffic characteristics, road user's behavior, vehicle design, driver's characteristics and environmental aspects.

Valli & Sarkar (1997) examined the possibility of using the speeds formula on accidents rate estimation for Indian condition and proposed a model for road accidents in India based on that. Victor & Vasudeman (1998) made a detail study and analysis on bus related accident in Tamil Nadu taking data from fine bus Transport Corporations. Chand (1999) made an attempt to examine the accident frequently and trend of bus related accidents with special references to public Road Transport under takings in India.Baviskar (1999) studied road accidents in Nashik Municipal corporation area and highlighted the distribution and accidents pattern in the city at micro level during the period 1980-1989.Saija et al (2000) had made a detailed study on road accident spectrum analysis of Gujrat.Singh & Misra (2000) analyzed the road accident spectrum for the city of Patna.Chakraborty et al (2001) studied the aggression to risk taking behaviors that leads a threat to road safety. Jenna et al (2001) developed a model for prediction of accidents in Indian urban roads taking field data from Ernakulum. Mohan Dinesh (2007) deals a **s**ustainable transport system that provide mobility and accessibility to all urban residents in a safe and environment friendly mode of transport.

A. NEED AND OBJECTIVES OF STUDY

As per the NATPAC number of road accidents in India is three times higher than that prevailing in developed countries. The number of accidents for 1000 vehicles in India is as high as 35 while the figure ranges from 4 to 10 in developed countries.

The objectives of the present study are listed below:

1. To study the monthly and annual variation in accident rate on selected stretch.
2. To study the effect of traffic volume on accident rate.

3. To develop an accident prediction model based on AADT and road condition.

II. DATA COLLECTION

The busiest NH-77 passing through two cities namely Hajipur and Muzaffarpur, the stretch of this road has length 70km is selected for data collection and statistical analysis of accidents, as road shown in Bihar Road Map [Fig. -1].With the prior permission of the concerned Senior Superintendent of Police (S.S.P), the accident data were collected from the six Police stations situated along the NH-77. These Police stations are Hajipur, Sarai, Bhagwanpur, Goraul, Kudhani and Turki.The police stations have their own FIR records of several years. Accident, Fatality and Injury data were collected month wise in every year from each police station records during year 2000 to 2010. The type of vehicles involved in accidents as recorded in the FIR was also noted down. The categories of vehicles include Tuck, Bus, Tractor, Jeep, Car, Tempoo, Motorcycle and Bicycle etc. Further, monthly-obtained data were sorted out year wise, represented in percentage over the study year as shown in Table-1.

Year	Fatality in %	Injury in %	Total Accident in %
2000	6.15	2.33	3.15
2001	1.54	3.00	2.56
2002	7.69	8.33	8.27
2003	15.38	9.00	9.25
2004	15.38	10.00	10.43
2005	13.85	11.33	11.81
2006	10.77	12.00	12.00
2007	7.69	11.67	10.43
2008	6.15	14.00	13.58
2009	10.77	13.33	13.39
2010	4.62	5.33	5.31

Table -1: Accident, Injury & Fatality in % on NH-77

A. DATA COLLECTED FROM P.W.D. RECORDS

P.W.D. (Public works Department) records are the main source for traffic volume data & road map. In addition to the above, road conditions information were also obtained from PWD records. Traffic survey was conducted at Sarai market on NH-77 at about 8km from Hajipur. Traffic volume for the year of count 2008 was extracted and represent in form of Commercial Vehicles per day (CVPD) & PCU/day, shown in Table-2.It is assumed that the traffic volume is uniform throughout the study stretch.

As the yearly traffic census data was not available for all the years, the available data were used to predict traffic volume on a road in each year for the period 2000-2010 as shown in Table-3.A growth rate (r) of 7.5 % per year was assumed for this purpose. A formula was used for forecasting as follows:

$$A = P(1 \pm \frac{r}{100})^n$$

where A = Predicted year traffic volume, P = Present year traffic volume, n = years of count and minus sign indicates before the present year traffic count and plus sign indicates after the present year traffic count.

Table -2: Traffic Volume Data

Name/No. of the road	Year of count	Traffic Volume	
		CVPD	PCU/day
NH-77	2005	9507	15128

Table-3: Predicted Traffic Volume

Year	PCU/day
2000	7499.93
2001	8108.03
2002	8765.44
2003	9476.15
2004	10244.49
2005	11075.12
2006	11973.10
2007	12943.90
2008	13993.40
2009	15128.00
2010	16262.60

III. ANALYSIS OF DATA AND DISCUSSION OF RESULTS

The data collected reflects the view of the reporting Police Officer. According to the literature review accidental data collected from the Police Station is not the complete information because all accidents are not recorded in their FIR (First information report). Therefore, all accidental data may be increased by 25-30%.

In this paper all accidental data are increased by 30%. All accidental data were analyzed, using the software MS EXCEL. As per the pilot survey, accidents cause has been recognized that occur due to (i) Driver's fault (ii) Failure of the motor vehicle (iii) Road condition and, (iv) Environmental condition.

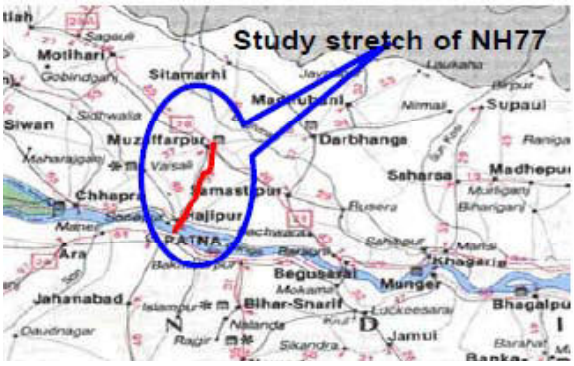

Fig.1: Map showing the study stretch

A. ANNUAL VARIATION IN ACCIDENTS

Fig.-2 shows the annual variation in accidents during 2000-2010.It is observed that percentage accidents are increasing relatively in most of the year. In year 2010 accident rate fall down suddenly, this type of situation occur may be due to the maintenance of the road is executed in the same year.

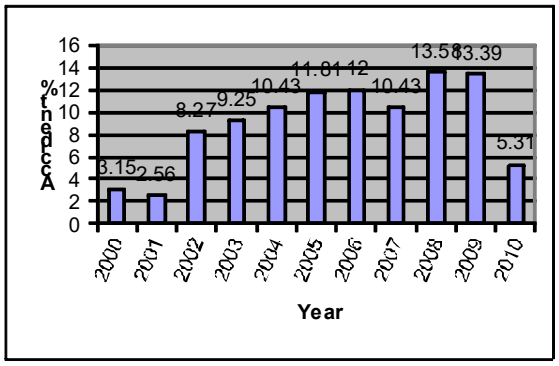

Fig.2: Annual Variation in accidents during 2000-2010 on NH-77

B. MONTHLY VARIATION OF ACCIDENTS

Average monthly variation in accidents during year 2000-2010 on NH-77 road section is shown in bar chart; Fig.-3.These results indicate that there is no definite trend for monthly variation in accidents. Accidents in the month of July are quite high. It may be due to rainy season in this month. The earthen shoulder gets deteriorated in rains and pavement surface becomes slippery. Also, it is observed that accidents rate is comparatively higher in the month of December – January of the year. No definite reason can be attributed to this trend but it might be due to poor or low visibility (fog condition) in winter seasons

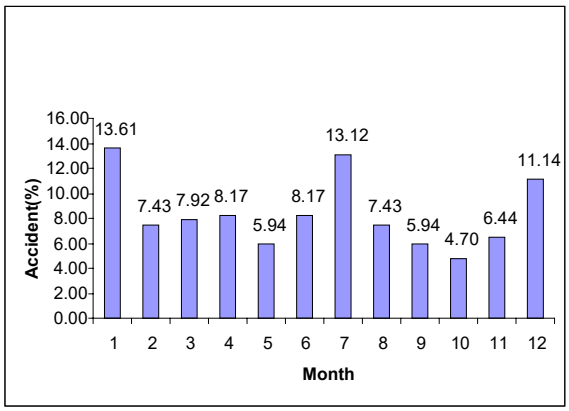

Fig.3: Average monthly variation in accidents during 2000-2010 on NH-77

C. ANNUAL VARIATION IN FATALITY, INJURY AND ACCIDENTS

Fig.-4 shows the comparison of Fatality, Injury and Accidents in percentage. Fatality in the year 2003 and 2004 is quite high. Injury rate during the whole study year are increasing relatively and the accident rate is as mentioned in the fig-4. However, High fatality rate gives the challenge to the Traffic Engineer to prevent the casualty. Therefore, Traffic Engineer has to study the cause of casualty and to suggest corrective treatment at potential locations.

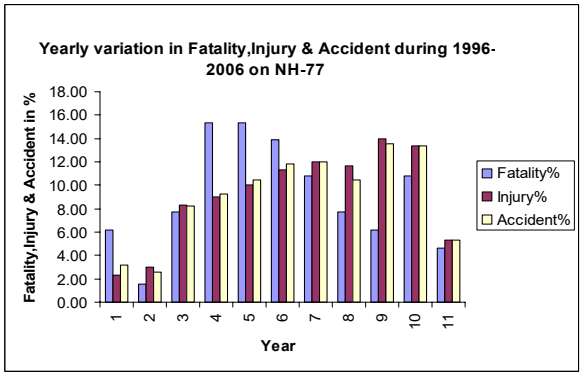

Fig.4: Yearly variation in fatality, injury & accident during 2000-2010 on NH-77

D. VEHICLES INVOLVED IN ACCIDENTS

Fig.-5 shows the percentage accidents involving a particular type of vehicle. It is observed that Truck are involved in maximum number of accidents almost 48%. It may be due to the most of the Truck driver are driving their vehicles after drink of alcohol or they are not aware about the condition /maintenance of their vehicles. It is followed by Motorcycle (16%), Car

(12%), Bus (10%), Tempo (5%), Jeep & Tractor (3%), cycle (2%) and Pedestrian (1%).

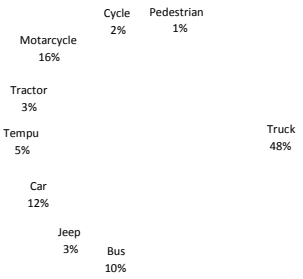

Fig.-5: Vehicles composition involved in accidents

E. ACCIDENTS AS RELATED TO TRAFFIC VOLUME

To observe the relationship between accident rate and traffic volume, accident rate is presented in two forms. In first case, it was the number of accidents that occurred in a road section per km per year and presented as accident per km-year. In second case, it was the number of accidents that occurred in a road section per million vehicles (MV) taken in terms of PCU per kilometer (k) per year (y), represented as accident per MVKY (Accidents per million vehicles-km-years).

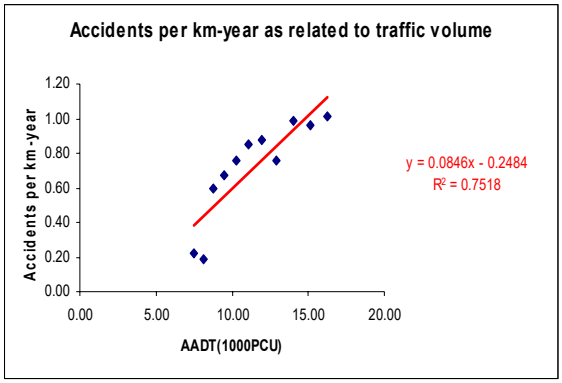

Fig.6: Accidents per km-year as related to traffic volume

It is observed that accident rate increases with increase of AADT.The data supporting the linear trend line relationships may be sensitive to the design and operational feature of the Highway.

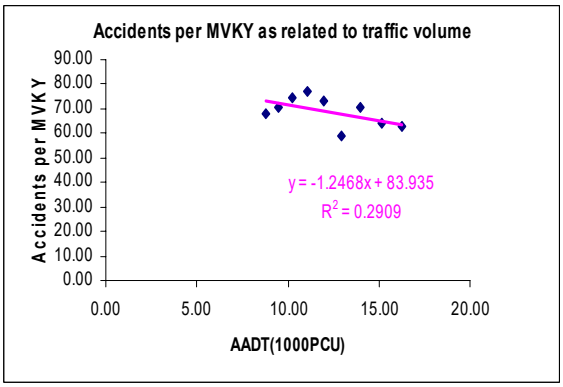

Fig.-7: Accident per MVKY as related to traffic volume

Figure-7 shows the accidents per million-vehicle-kilometer –year decreases slowly with increase in the AADT.It may again be due to design and operational features of the highway and influence of other parameters like roadside features, degree of side slope, climate condition and operational environment.

F. TREND OF ACCIDENTS DURING 2000-2010

The annual trend of MVKY is shown in fig.8.Linear variation means accident rate per MVKY increases in each subsequent year. This increasing trend in accident rate may be due to detoriation in road and shoulder conditions and the road users did not adopt general awareness. Even though the failures of the motor vehicle are mainly driver's fault, result the accidents.

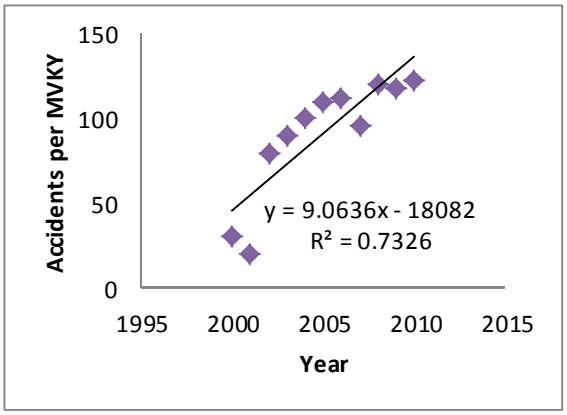

Fig.-8: Trend of accidents during 2000-2010

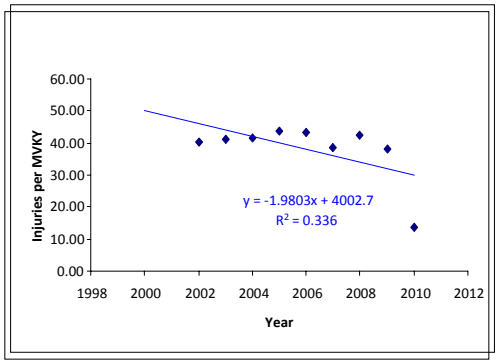

Fig-9: Trend of injuries during 2000-2010

G. TREND OF INJURIES DURING 2000-2010

The annual trend of injuries is shown in Fig.9.Scattered points do not show the definite trend, this may be due to the insufficient relatively closer values. A linear trend line is fitted to show the trend because logically true but have coefficient of determination/correlation is very less. It was found that injuries per MVKY decrease over the period 2000-2010.This trends may be attributed to incautiousness driving of small sized vehicles and also priority goes to motorcyclists.

H. TREND OF FATALITIES DURING 2000-2010

The observed values are not showing the definite trend of fatalities. The fatality rate per MVKY has decreased substantially over the years. Ref Fig.10.

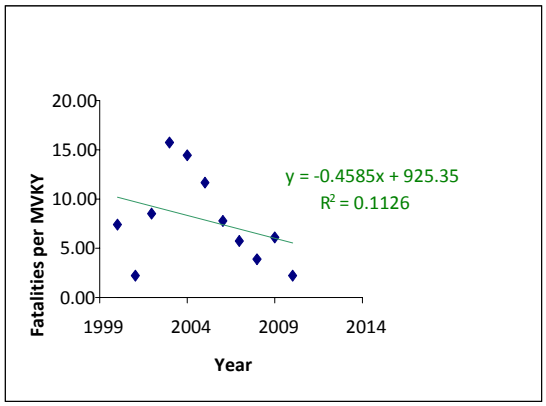

Fig.10: Trend of fatalities during 2000-2010

IV. ACCIDENT PREDICTION MODEL

The portion of the Highways and shoulder, where maintenance work was carried out in a particular year were noted down from the PWD records. Chandra and Dev Raj (1999) suggested that the section of a road and its shoulder may be ranked on a 5-point scale as shown below:

Excellent = 5, Good = 4, Average = 3,

Poor = 2 and Bad = 1

The excellent means road and shoulders was maintained very recently and bad means road and shoulders were not maintained within last four years and these have deteriorated to the extent that vehicles cannot use them. This decimal way of ranking is primarily due to the maintenance works not being carried out in a single year for the whole stretch of a road. The accidents per km-year were regressed with AADT and road shoulder conditions rank.

The general form of equation is represented as:

Accident /km-year =C_0 + C_1 (AADT) + C_2 (Road and Shoulder Condition Rank [CR])

Accidental data collected for the study stretch of NH-77 was used to develop the Accident Model. Regression analysis is used in the present study, for finding out a best prediction model for accidents on National Highways. The accident data collected from different police stations were regressed against the AADT and CR.

C_0 =1.21, C_1 = 4 x 10^{-6},

C_2 = 0.183, R^2 = 0.895

The prediction model for NH-77 may be represented as

Accident/km-year = 1.21 + 4 x 10^{-6}(AADT)

-0.183(CR)

The above equations indicate that the accident/km-year increases with AADT, but decreases with improvement in condition of road or shoulders or both.

A. VALIDATION OF THE MODEL

Using the AADT of the selected stretch of the road and road and shoulder condition rank (CR) are assigned as per site visit. The accident prediction model was validated for the road stretches between Kudhani to Sitamardhi road on NH-77.The estimated values from the accident prediction model were tested by Chi-squared test.

Table-4: Estimated accidents at 5 locations for validation

Locations	1	2	3	4	5
Accidents estimated from prediction model	0.87	0.70	0.70	0.51	0.69

Sum of the accidents rate = 0.87+0.70+0.70+0.51+0.69 =3.47, the expected number of accidents rate = 3.47/5 =0.69, Chi-square = 0.87, Degree of freedom, d_f = 5-1= 4 and H_0 = it is a good fit, Chi-square for d_f = 4 and 5% significance level = 9.488, since 0.87 <<9.488

Hence,H_0 is correct. Therefore, It was found that estimated accident rate from accident prediction model were significant at 5% level of significance.

V. CONCLUSIONS

The following conclusions are drawn:

1. There is no definite trend for monthly variation in accident on a section of highway. But the accident in months of July is generally higher. It may be due to fast deterioration of earthen shoulder by rain in these months. Accident in month of January has relatively high value; it may be due to the foggy weather.
2. Heavy vehicles like truck are involved in maximum number of accidents on National Highways. It is estimated that a heavy vehicles is involved in almost 48 % accidents followed by two-wheelers (motorcycle) 16%, car12% and Bus10%.
3. Accident rate in terms of number of accidents per km-year increases with traffic volume. But the accidents rate in terms of number of accident per million-vehicle kilometer-year (MVKY) decreases with increase in traffic volume.
4. Accidents rate per MVKY increases during the study year, whereas, both injury and fatality rate per MVKY show a declining in trend over time.
5. Accident prediction model developed in the present study show that number of accidents per km-year increases with AADT and decreases with improvement in road/shoulder condition.

Accident prediction model was validated by Chi-squared test and found to have a good linear relationship between AADT and CR.

REFERENCES

[1] Bavikar, S.B. (1999), "Road Accidents in Nashik Municipal Corporation Area: A Case Study," Indian Journal of Transport Management, 2319,pp543-555.

[2] Chandra, S and Dev. Raj (1999), "Role of shoulders in Traffic operation," Indian Highways, 27(11), Indian Roads Congress, New Delhi, pp31-38.

[3] Chand M (1999), "An analytical study of bus – related accidents in India," Indian Highways, (2799), 9-20.

[4] Chakraborty, S. et al (2001), "Accident Characteristics of roadway Vehicles in Kolkata,"ROTRAN, Vol.2, pp6.39-6.45

[5] Chandra, S et al (2004), "Accident Analysis on two lane roads," Highway research bulletin, Highway research Board, IRC, pp77-92

[6] Kadiyali, L.R. et al (1983), "Effect of road characteristics on accident rates on rural highways in India," Highway research bulletin, IRC, 20, 1-38.

[7] Kadiyali L.R., "Traffic engineering and transport planning," Khanna publishers Delhi-110006, ed1999, 411-483

[8] Mohan D., (2007),"Traffic safety and health in Indian cities', Research and Injury prevention Programme," IIT Delhi, New Delhi

[9] Saija, K.K. et al (2000), "Spectrum analysis of road accidents a case study," Indian highways, 28(9), 29-41.

[10] Singh S.K. (2004), "Road accident analysis: A case study of Patna city," Urban Transport Journal, Vol.2, No.2, pp.60-75.

[11] Tula Dhār, S.B.S and Justo C.E.G. (1981), "Analysis of accidents rates-A case study," Highway research bulletin', Indian road congress,(56),1-11.

[12] Victor, D.J. and Vasudenan, J (1998), "Factors affecting bus related accidents case study of five corporations in Tamilnadu,"HRB, IRC, 4088, pp39-52.

[13] Valli P. and Sarkar P.K. (1997), "Models for road accidents in India," Highway research bulletin, IRC 16

◈◈◈

Innovations in Concrete Technology of High-Rise Buildings

Rinu Mary Abraham & B. S. Srinivasa Prabhu
Department of Civil Engineering, Manipal Institute of Technology (MIT), Manipal, India

Abstract - Skyscrapers and High-rise buildings are an increasingly common sight where land is expensive, as in the centers of big cities, because they provide such a high ratio of rentable floor space per unit area of land. Not only do they define the skyline, they help to define the city's identity. In this paper a brief history of the prominence of concrete in the construction of tall buildings is closely examined. We have attempted to bring out the merits of concrete and the usage of composites in concrete for high rise structures. Important advancements in concrete technology involved in high rises including high performance concrete and light weight concrete are described. In this connection, prominent concrete high rise structures like Ingalls Building, Marina City Towers and their crucial features are discussed. Through this paper an attempt is made to bring out the various advancements of concrete construction to enable futuristic construction for high rises with prospects of using appropriate concrete technology.

Keywords-*skyscraper;concrete; high-rise construction;*

I. INTRODUCTION

Development of tall buildings underlines and accentuates the prosperity of the urban communities all around the globe. They are built not just for economy of space; like temples and palaces of the past, skyscrapers are considered symbols of a city's economic power. The choice for construction material for high-rises has been strongly influenced by economical and structural stability factors which include the ability to withstand natural calamities such as windstorms. Traditionally, the primary concern of the structural engineer designing a building has been the provision of a structurally safe and adequate system to support the vertical loads. This is understandable since the vertical load-resisting capability of a building is its reason for existence. However, this is only true for the buildings involved if they are not too high, are not in seismic zones, or have been constructed with adequate built-in safety margins in the form of substantial nonstructural masonry walls and partitions. A structure must be designed to carry loads due to gravity, wind, equipment and snow; resist high or low temperatures and vibrations; protect against explosions; and absorb noises. Adding to this the human factor means considering rentable spaces, owner needs, aesthetics, cost, safety and comfort. Although one set is not mutually exclusive of the other, careful planning and consideration are essential in an attempt to satisfy and integrate both. Considering structure alone, there are two main categories for high-rise buildings - structures that resist gravity and lateral loads and those that carry primarily gravity loads. Since skyscrapers have the greatest need for resisting high magnitudes of wind, the lateral load resisting system becomes the most important and hence, it is essential to also take into account the lateral forces such as wind loads, seismic inertia-forces, blast loads, etc. to ensure the stability of buildings.

Concrete, inspite of being a relatively recent construction material has become an indispensable part of the modern construction industry. Engineers are coming to realize how concrete can be utilized to build seemingly impossible structures with relative ease and efficiency. Ransome, Hennebique, Fazlur Khan initiated the emergence of concrete to the modern age. With the advent of concrete technology involving high- strength concrete, light weight concrete, slag cement and such, the presence of concrete in superstructures was established. From the Ingalls building, concrete skyscrapers have graced the skyline over the years. Johnson Wax Tower, Place Victoria, Lake Point Towers are but a few examples. The structural aspects of the Ingalls building, and modern skyscrapers such as the Burj Khalifa, provide insights into how far we've come from single storeyed stone structures and how we continue to dream on.

II. EMERGENCE OF CONCRETE AS A SIGNIFICANT CONSTRUCTION MATERIAL

Concrete in its present form is the youngest of the three basic structural materials (steel, concrete and masonry materials) of construction. While steel has been much favored in the construction of high-rises, concrete is gaining fast popularity in the field. According to CEMBUREAU, in 1900, the total world production of cement was about 10 million tons; in 1998 it was 1.6 billion tons. If we suppose that on average 250kg of

cement are used to produce 1 m3 of concrete, in 1900 only 40 million m3 of concrete were used, whereas in 1997 the amount produced was about 6.4 billion m3.[4]

The baseline from which to measure the history and development of the skyscraper is the 1876 Centennial Exposition in Philadelphia. Specimens of reinforced concrete were exhibited at the Centennial as a usual curiosity in the field of specific possibilities, but as yet unrecognized for any general use, although a few obscure but adventurous leaders had begun to catch the vision [1].

Reinforced concrete started gaining popularity in construction from the late 1900s. The parallel development of reinforced concrete frame construction by Ernest L. Ransome in the United States, and by Francois Hennebique in France is a significant example. Ransome, first used reinforcing in 1877, and in 1884 he patented a system using twisted square rods to help the development of bond between the concrete and reinforcing. Between 1901 and 1902, Ransome first patented a system with an exterior belt course to hold up walls from stories above. The Ingalls Building, a landmark structure in Cincinnati, was built in 1904 using a variation of the Ransome system. Designed by the firm of Elzner and Henderson, it was the first concrete skyscraper, reaching 16 stories (210 feet). He also developed the first precast wall units that were placed integrally with cast-in-place floors and columns. Precast systems were initially popular making erection quicker and more efficient as well as avoiding cold weather problems [2]. These two innovations changed the exterior walls from ones that carried their own loads to ones that bore integrally with the rest of the system. This encouraged the use of concrete as framing with a curtain wall sealing the building from external forces.

On the other side of the Atlantic, Francois Hennebique, a successful mason turned contractor in Paris, had started to build reinforced concrete houses in the late 1870s. His method of construction involved integrating separate elements of construction, such as the column and the beam, into a single monolithic element. He took out patents in France and Belgium for the Hennebique system of construction and proceeded to establish an empire of franchises in major cities. He promoted the material by holding conferences and developing standards within his own company network. Most of his buildings were industrial. More than any other individual he was responsible for the rapid growth of reinforced concrete construction in Europe.

Frank Lloyd Wright declared the prime assets of reinforced concrete to be its formability and monolithic property of construction, but he did not take advantage of this until late in his career. He was the first to exploit the cantilever as a design feature made possible by the continuous nature of reinforced concrete construction. The Kaufman House (Falling water), built in 1936, is a tour de force in the use of the cantilever.

The most significant contribution to concrete high-rise construction however, was made by Fazlur Rahman Khan with the introduction of the concept of tubular structures. The framed-tube structure has its columns closely spaced around the perimeter of the building, rather than scattered throughout the footprint, while stiff spandrel beams connect these columns at every floor level. This structural system was first implemented in 1964 in the construction of the DeWitt-Chestnut Apartments in Chicago, a 43-story reinforced concrete tower designed by Fazlur Khan and his colleagues at Skidmore, Owings & Merrill (SOM). Because of its great relative strength and stiffness, the tubular form immediately became a standard in high-rise design. Furthermore, crafting rational architecture in cooperation with Bruce J. Graham, chief design architect in SOM's Chicago office, Fazlur Khan united an exceptionally efficient "trussed-tube" structural system with an articulate, graceful form for Chicago's 100-story John Hancock Center. Another groundbreaking structural system, the "bundled tube", was later introduced by him. This structural design for Chicago's 110-story Sears Tower was structurally efficient and economic; at a height of 1,450 feet, it provided more space and rose higher than the Empire State Building, yet cost much less per unit area. Equally important, the new structure type was innovative in its potential for versatile formulation of architectural space. Efficient towers no longer had to be box-like; the tube-units could take on various shapes and could be bundled together in different sorts of groupings.

III. UNIQUE CHARACTERISTICS OF CONCRETE

Flexibility in mode of production as well as material properties of concrete enables various types of architectural structures.

Cast-in-place concrete reduces project start-up time and start-to-finish time as compared to steel. Concrete provides structural economy in many other ways too; including reduced material costs and improved cash flow. It can also maximize marketable space and increase Return on Investment (ROI).

During construction, the new generation of concrete admixtures and super plasticizers make concrete flow more easily. Today's concrete solutions set in lower temperatures. So, site-cast concrete construction can proceed year round. With super plasticizers high concrete strengths can be achieved rapidly, and pouring on successive floors can proceed more quickly. Cast-in-place concrete construction can finish off, and other trades can get on the floor sooner. Electrical,

mechanical, plumbing and HVAC (heating, ventilation, and air conditioning) systems as well as interior partitions can be installed while the frame is progressing upward.

High-strength mixtures and advanced reinforcing design technologies allow engineers and architects to design longer spans with fewer and smaller columns making more useable floor space available. Moreover, concrete has a shorter floor-to-floor height than steel by up to two feet per floor. Because concrete can withstand catastrophic loading and there is less movement with concrete structures, buildings have a longer life expectancy. Concrete constructions, also are weather-tight, require lower maintenance and have greater resale value than other structures. Concrete is naturally fire-resistant. Concrete buildings typically qualify for reduced fire insurance rates—up to 60 percent less on fire and extended coverage for warehouses and storage buildings. New coloring admixtures provide attractive, economical alternatives to exterior finishing. And concrete is adaptable to a variety of surface treatments and shapes resulting in structures that set graciously into any environment.

IV. ADVANCEMENTS IN CONCRETE TECHNOLOGY

Today's concrete technologies provide innovative solutions for architectural interest and versatility in design. A few of the prominent are mentioned here.

High performance concrete (HPC): This type of concrete possesses high workability, high strength and high durability. ACI (American Concrete Institute) has defined HPC as a concrete in which certain characteristics are developed for a particular application and environment. HPC is a concrete made with appropriate materials combined according to a selected mix design; properly mixed, transported, placed, consolidated and cured so that the resulting concrete will give excellent performance in the structure in which it is placed, in the environment to which it is exposed and with the loads to which it will be subject for its design life. Mix proportions for high-performance concrete (HPC) are influenced by many factors, including specified performance properties, locally available materials, local experience, personal preferences, and cost. With today's technology, there are many products available for use in concrete to enhance its properties. Under the ACI definition durability is optional and this has led to a number of HPC structures, which should theoretically have had very long services lives, exhibiting durability associated distress early in their lives. ACI also defines a high-strength concrete as concrete that has a specified compressive strength for design of 6,000 psi (41 MPa) or greater.

Ready-mix concrete: It is defined as the type of concrete that is manufactured in a factory or batching plant, according to a set recipe, and then delivered to a work site, by truck mounted transit mixers. This results in a precise mixture, allowing specialty concrete mixtures to be developed and implemented on construction sites. The first ready-mix factory was built in the 1930s, but the industry did not begin to expand significantly until the 1960s, and it has continued to grow since then. Ready-mix concrete is sometimes preferred over on-site concrete mixing because of the precision of the mixture and reduced work site confusion.

Lightweight Concrete: One of the disadvantages of conventional concrete is the high self-weight of concrete. Density of normal concrete is in the order of 2200 to 2600 kg/m3. Light weight concrete however, has a density of 300-1850 kg/m3. The advantages of low density concrete include reduction of dead load, lower haulage and handling costs. Construction using light weight concrete results in considerable economy, especially in framed tall structure, where the beams and columns have to bear the weight of walls and floors. Another characteristic feature of this type of concrete is its relatively low thermal conductivity, a property which improves with decreasing density. In high rises, where extreme climatic conditions are encountered this comes as a considerable advantage.

Self-compacting Concrete: Shortage of skilled labour and savings in construction time were the main factors for development of self-compacting concrete. High fluidity and segregation resistance were obtained by the simultaneous use of a super plasticizing admixture and a viscosity-increasing admixture. In France, the ready-mixed concrete industry is using self-compacting concrete as a noise-free product that can be used around the clock in urban areas. Due to noise reduction, labour savings, and longer life of steel molds, the precast concrete products industry is also investigating the use of the material.

Cathodic protection of reinforced concrete: Cathodic protection techniques involve the suppression of current flow in the galvanic cell either by external supply of current in the opposite direction or by using sacrificial anodes. The externally applied current method is commonly used for corrosion protection in chloride-contaminated reinforced concrete structures. Researchers including Rasheduzzafar have reported the degradation of bond between steel and concrete probably due to a buildup of sodium and potassium ions which results in the softening of concrete at the steel-concrete interface [5]. The degradation of steel-concrete

bond was found to increase with the increase in the impressed current density and chloride content of concrete.

Slag cement: Ground granulated slag is often used in concrete in combination with Portland cement as part of blended cement. Ground granulated slag reacts with water to produce cementitious properties. Concrete containing ground granulated slag develops strength over a longer period, leading to reduced permeability and better durability. Since the unit volume of Portland cement is reduced, this concrete is less vulnerable to alkali-silica and sulfate attack. This previously unwanted recycled product is used in the manufacture of high performance concretes, especially those used in the construction of bridges and coastal features, where its low permeability and greater resistance to chlorides and sulfates can help to reduce corrosive action and deterioration of the structure. [6]

Another innovation that improved the utilization of concrete structures is the Hardy Cross Method for determination of indeterminate structures. Most concrete structures are highly statically indeterminate, which makes them difficult to analyze. In 1930, Hardy Cross, a professor of structural engineering at the University of Illinois, published a 10-page paper outlining a method of successive approximation called moment distribution. The Hardy Cross Method took ten years to develop and is noteworthy for its straightforwardness and elegance.

V. CONCRETE SKYSCRAPERS SINCE THE 20TH CENTURY

High-rise construction in concrete progressed slowly forward from the Ingalls Building in 1904. The giants and mid-giants of the 1930s were all of steel construction. The Johnson Wax Tower, however, provided the impetus for Bertrand Goldberg's twin towers of Marina City, though on a vastly different scale. The Chicago 60 storey high-rise, erected in 1962, heralded the beginning of the use of reinforced concrete in modern skyscrapers and with it, competition for the steel frame. Place Victoria in Montreal, constructed in 1964, reached a height of 624 ft. utilizing 6000 psi concrete in the columns. Concretes of higher strength proved to be the key to increased height, permitting as they do a reasonable column size on the floors below. One Shell Plaza in Houston topped out at 714 ft. in 1970 using 6000 psi concrete. The Chicago area, with its plentiful supply of high quality fly ash (which helps to achieve a more workable concrete at lower water/cement ratios), has spawned the greatest concentration of tall reinforced concrete buildings. The 70-story Lake Point Towers used 7500 psi concrete to reach 645 ft. in 1968. Water Tower Place reached 859 feet in 1973 with concrete strengths as high as 9000 psi thanks to a super plasticizing admixture. Maybank Menara came up in 1988 incorporating concrete on an entirely new level of construction paved way for the construction of taller structures such as the Petronas towers (1998) in Kuala Lumpur. In 1989 the Scotia Plaza Building in Toronto was completed to a height of 907 ft. In 1990 two more towers in Chicago exceeded 900 ft. The taller of these is the building at 311 S. Wacker Drive which is located next to the Sears Tower. The latest jewel in the crown of concrete skyscrapers is the Burj Khalifa, a marvel in concrete, steel and glass.

VI. CASE STUDY OF A FEW CONCRETE HIGH-RISE STRUCTURES

The Ingalls Building - This building was considered a daring engineering feat at the time, but its success contributed to the acceptance of concrete construction in high-rise buildings in the United States. Many people from both the public and the engineering community believed that a concrete tower as tall as the plan for the Ingalls Building would collapse under wind loads or even its own weight. Ingalls and engineer Henry N. Hooper were convinced, however, that Ernest L. Ransome's system of casting twisted steel bars inside of concrete slabs as reinforcement (patented in 1884) and casting slab, beams and joints as a unit allowed them to create a rigid structure. Hooper's design consisted of a monolithic "concrete box of eight-inch [200 mm] walls, with concrete floors and roof, concrete beams, concrete columns, concrete stairs - no steel. It consisted merely of bars embedded in concrete, with the ends interlaced" [1]. The amount of concrete produced during construction - 100 cubic yards (76 m^3) in each ten-hour shift was limited by the rate at which the builders could place it. An extra wet mix was used to insure complete contact with the rebars and uniform density in the columns. Floor slabs were poured without joints at the rate of three stories per month. Columns measured 30 by 34 inches (760 by 860 mm) for the first ten floors and 12 inches (300 mm) square for the rest. Three sets of forms were used, rotating from the bottom to the top of the building when the concrete had cured. Completed in eight months, the finished building measured 50 by 100 feet (15 by 30 m) at its base and rises 210 feet (64 m) tall. The exterior concrete walls are eight inches thick (200 mm) in unbroken slabs 16 feet (5 m) square with a veneer 4 to 6 inches (100 to 150 mm) thick. The Beaux Arts Classical exterior is covered on the first three stories with white marble, on the next eleven stories with glazed gray brick, and on the top floor and cornice with glazed white terra cotta.

Marina City Towers- The 60-story Marina Towers of 1962 in Chicago designed by Bertrand Goldberg, reached 588 ft. (180m). According to Schueller (1990), these towers may be considered the first true reinforced

concrete skyscrapers expressing the character of the material. The cylindrical forms of the twin towers offers a true tube geometry (although the structural tube concept was unknown at that time), providing three-dimensional structural action and making it highly efficient, aerodynamically [8]. A cylindrical building also has a smaller exposed projected surface or "sail" perpendicular to the wind direction and thus encounters lower magnitudes of wind forces as compared to other shapes [3].

Lake Point Tower -The race for height in concrete began in 1968, with the 70-story, 645-ft. (197-m) high Lake Point Tower apartment building in Chicago, which utilized the flat plate–shear wall principle [3]. Designed by Schipporeit-Henrich Architects with Graham, Anderson, Probst & White, the high-rise residential tower is based on a cloverleaf geometry that takes advantage of the unique plastic characteristics of concrete and its ability to be modeled into organic shapes. In a manner similar to Wright's Johnson Wax Building, the floor plates of Lake Point Tower is cantilevered from a central core buried deep in the earth. The exterior is wrapped in a dark glass curtain wall emphasizing its monolithic form and curvilinear surfaces.

311 South Wacker Drive - Completed in 1990, the 75-story, 969-ft. (296-m) high 311 South Wacker Drive office tower in Chicago was officially acknowledged, at the time, the tallest concrete high-rise building. It is also a good example of the application of a shear wall and interactive frame structural system [8]. A basic requirement for such interaction is that the relative stiffness properties of each shear wall and each frame remain unchanged throughout the entire height of the building. In practice it is rarely possible to comply strictly with this requirement for various architectural and functional reasons. With the availability of sophisticated computer programs, which can simulate the actual interaction of the idealized elements, this is no longer a problem.

Burj Khalifa - Designers purposely shaped the structural concrete Burj Khalifa - 'Y' shaped in plan - to reduce the wind forces on the tower, as well as to keep the structure simple and foster constructability. The structural system can be described as a 'buttressed' core. Each wing, with its own high performance concrete corridor walls and perimeter columns, buttresses the others via a six-sided central core, or hexagonal hub. The result is a tower that is extremely stiff laterally and torsionally. Skidmore, Owings & Merrill (SOM) applied a rigorous geometry to the tower that aligned all the common central core, wall, and column elements. Each tier of the building sets back in a spiral stepping pattern up the building. The setbacks are organized with the tower's grid, such that the building stepping is accomplished by aligning columns above, with walls below to provide a smooth load path [7]. This allows the construction to proceed without the normal difficulties associated with column transfers. The setbacks are organized such that the tower's width changes at each setback. The advantage of the stepping and shaping is to 'confuse the wind'. The wind vortexes never get organized because at each new tier the wind encounters a different building shape.

VII.INFERENCES AND RECOMMENDATIONS

Skyscrapers and other high-rises are fast becoming part of our living environment thus influencing our living conditions, social well-being and health. Hence, it is important to explore sound and economical design and development techniques for buildings and infrastructure for them to be sustainable and affordable, and also which encourage innovation in construction. Shown in Fig. 1 are some of the prominent concrete high-rises since the 1950's. The figure clearly indicates on the average the growth both in terms of height and number of floors for concrete high rises over the past five decades. This is indicative of the efforts taken in the direction of new concrete technologies over the years and the need to further it.

VII.CONCLUSIONS

Concrete is fast becoming an indispensible part for several concrete high rise construction projects. In this respect, it is crucial to understand its characteristics and capabilities. This paper has roughly covered the basic advantageous properties of concrete in the construction of concrete skyscrapers.

ACKNOWLEDGMENT

The authors would like to thank Dr. Sarath Chandra Rao Sanku and Dr. Ranjit Abraham for their assistance in the research work.

REFERENCES

[1] Mir M. Ali, "Evolution of Concrete Skyscrapers: from Ingalls to Jin Mao", Electronic Journal of Structural Engineering, Vol. 1, No.1, pp. 2-14, 2001.

[2] Harries, K. A., "Reinforced Concrete at the Turn of the Century," Concrete International, January, 1995, pp. 58-62.

[3] Paul J. Armstrong, "Architectural Issues for Concrete Design and Construction", CTBUH Review 3, Journal of the Council on Tall Buildings and Urban Habitat, 2001, Vol. 1, No. 3

[4] Pierre-Claude AõÈtcin, "Cements of yesterday and today, Concrete of tomorrow", Cement and Concrete Research 30 (2000), pp 1349±1359

[5] Rasheeduzzafar; Ali, M. G.; and Al-Sulaimani, G. J., "Degradation of Bond Between Reinforcing Steel and Concrete Due to Cathodic Protection Currents," ACI Materials Journal, V. 90, No. 1, January- February 1993, pp. 8-15.

[6] "High Performance Cement for High Strength and Extreme Durability" by Konstantin Sobolev, 2009.

[7] "Burj Dubai: Engineering The World's Tallest Building", William F. Baker, D. Stanton Korista and Lawrence .C. Novak, Skidmore, Owings & Merrill LLP, Chicago, Illinois, USA.

[8] Ali, M. ve Armstrong, P., Architecture of Tall Buildings, Council on Tall Buildings and Urban Habitat Committee (CTBUH), New York: McGraw-Hill Book Company, 1995.

◈◈◈

.

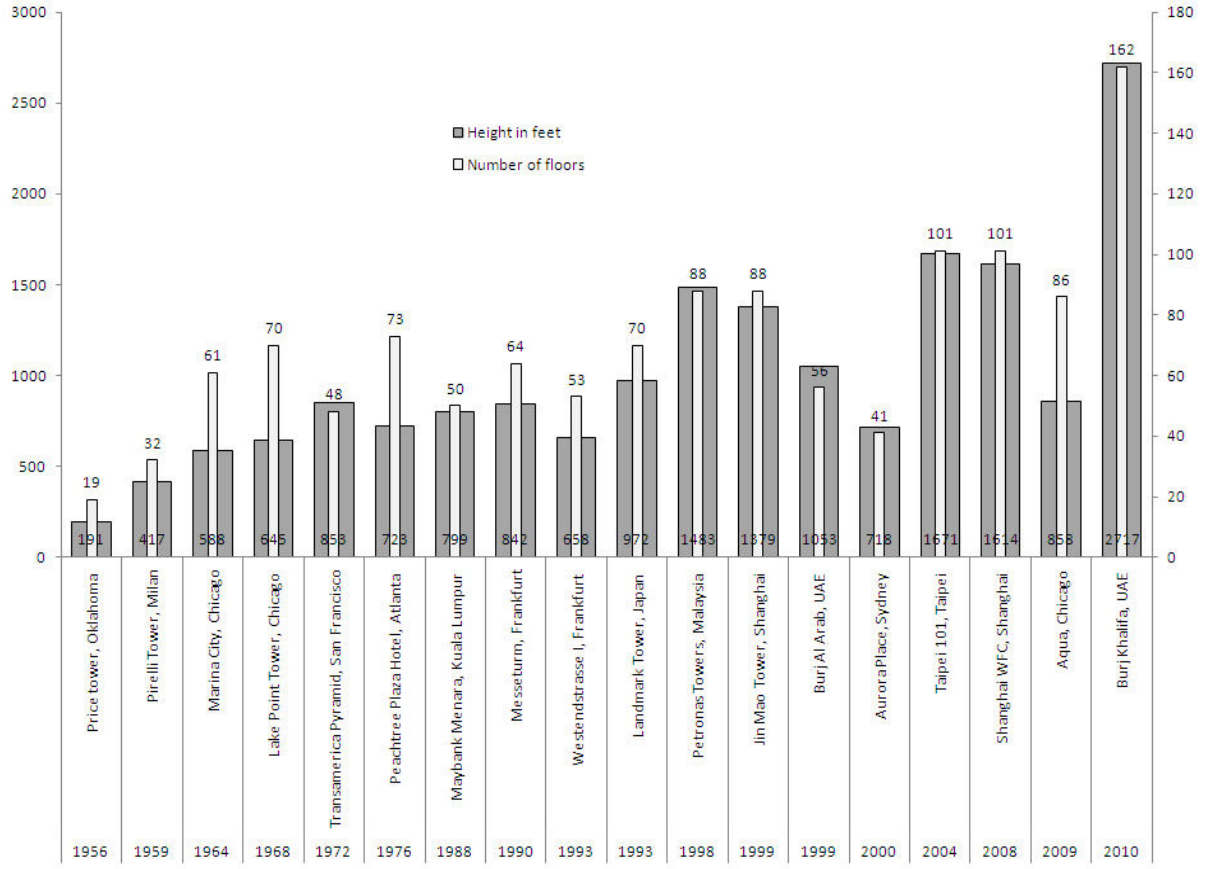

Fig. 1 Popular Concrete high rises since the 1950's

…..

Statistical Evaluation of Induced Seismicity In Karkheh Dam, Iran

S. M. Mir Mohammad Hosseini & Pegah Rajaei

Civil Engineering, AmirKabir University of Technology, Tehran, Iran

Abstract - Karkheh dam is the largest dam in Iran with a capacity of about 7.4×10^9 cubic meters and height of 127 meters. Since the first impoundment, increasing in seismic activity in the dam area has been observed that indicates the possible occurrence of reservoir-induced seismicity (RIS).In the present work, a preliminary evaluation is conducted firstly in order to investigate these observations. Based on the assessment of the number of earthquakes occurred in equal time periods before and after reservoir impoundment and their focal depths, it is concluded that RIS is happening in the dam site. Secondly, a cross-correlation method is applied in order to find the relationship between water level fluctuations and the variations of seismic activities. This analysis confirms a strong relationship between fluctuation of the water level and the number of seismicity events in the dam area.

Keywords - *reservoir-induced seismicity (RIS); Karkheh dam; dam impoundment; cross-correlation method*

I. INTRODUCTION

Since the first case of reservoir induced seismicity at Lake Mead (Hoover Dam) in the mid-1930, there have been many reports of this phenomenon from all around the world. RIS caused by not only the initial impoundment of artificial reservoir but also by seasonal water level changes. In many cases, changing in seismicity has been observed immediately after the first filling of the reservoir, while in others, it took several years for RIS to occur[4, 5].Thereafter, major earthquakes had occurred at some large artificial dams such as, Xinfengjiang reservoir in China, the Kariba reservoir in Zambia-Zimbabwe, the Koyna reservoir in India, and the Kremasta reservoir in Greece [6], which caused loss of human life, injuries and property damages. By increasing the number of large reservoirs and their potential hazards in the economical and social matters, RIS has attracted the attention of the scientists, over the past decades. Consequently, many analytical and numerical models have been developed to study reservoir induced seismicity. [7, 8, 9]

The scope of the current work is to study the RIS in Karkheh dam site. Karkheh storage dam is considered as the largest dam in Iran due to its capacity of about 7.4 billion cubic meters at the maximum water level. Karkheh dam is an earth core rock-fill dam with a height of 127 m and a length of 3030 m which is located on Karkheh river, the third largest river in Iran based on the river flow discharge, in southwest of Iran. The filling of the dam was started on Feb. 12, 2000. The water height and total reservoir volume are more than 100 m and about 5.6 billion cubic meters at the normal water level, respectively. From seismo-tectonic point of view, the Karkheh dam is located in the Zagros fold and thrust belt whose deformation appears to be concentrated on basement thrusts and a few transverse strike-slip faults [1]. The majority of the project area in a distance of 30 km from the dam reservoir is located within the Zagros foredeep (Dezful Embayment unit). Some reverse and thrust faults are presented at the dam area, including Lohbari fault at the east of the dam, Kabir-Kuh anticline fault at the north, Dal-pari anticline fault at the south, and the Dezful thrust at the southeast, as seen in Fig1.

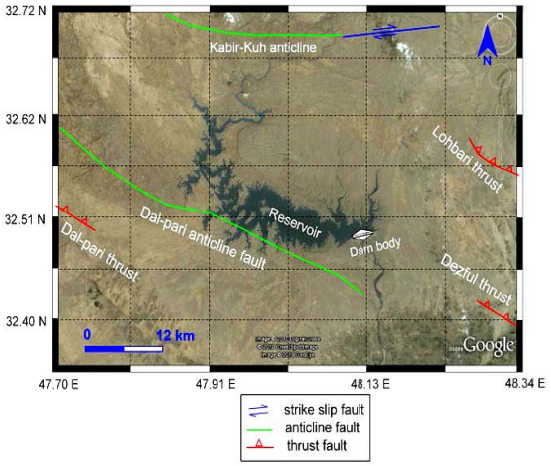

Figure 1 : Active faults in the vicinity of Karkheh reservoir

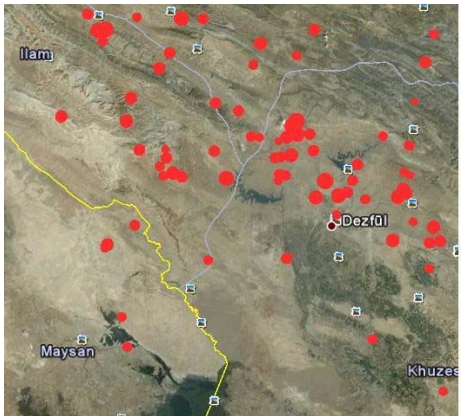

a) before impoundment

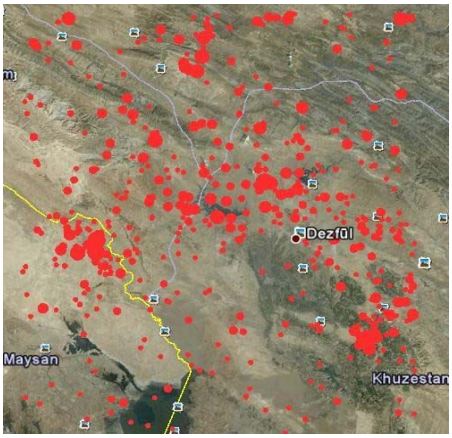

b) after impoundment

Figure 2. Seismic events before and after impoundment whose epicenter were located with 100 kilometers from reservoir, The red circles represent earthquake epicenters whereas earthquake magnitudes are proportional with the diameters of the circles. (ISC catalog)

Since insufficient efforts have been made to study this phenomenon and also dam's characteristics augment the probability of causing RIS, in the current work, a preliminary evaluation of RIS at the Karkheh dam is conducted. And then, a statistical approach, cross-correlation method, is applied for verification of the rudimentary assessment.

II. DATA ANALYSIS

For primary analysis, the database has been provided by using NEIC (National earthquake Information Center), ISC (International Seismological Center), USGS (U.S. Geological Survey), IRSC (Iranian Seismological Center). A 10-year period before the impoundment and a 10-year period after the impoundment are considered. Furthermore, according to the number of events before and after the impoundment, the earthquakes whose epicenters are located within 100 kilometers from the reservoir have been included in the database. For the second part of the investigation, data which recorded by the Karkheh dam network station (5 station were installed) has been added to the database, the sequence of seismic events between 2000 and 2008 with magnitude m>1 has been considered. The daily water level fluctuation data in the reservoir, measured by Mahab Ghods Consulting Engineering Co., has been also used.

III. PRELIMINARY EVALUATION

According to Simpson et al. [10], two types of respond to the large dams impoundment can be observed, namely rapid and delayed seismic responses. Two main mechanisms corresponding to these responses are: a) the increase in stresses due to the load of the reservoir and b) the diffusion of pore pressure. The water weight stresses could lead to change the seismic activity, also the active faults in the reservoir area (Fig. 1) are susceptible to lose their effective normal stresses because of increase in pore pressure. Therefore it can be concluded that both mechanisms could cause reservoir induced earthquakes.

To roughly evaluate the mechanism which is responsible for RIS in Karkheh dam site, the annual cases of RIS have been shown in Fig. 3. It indicates that the annual number of events has increased significantly after the impoundment. As can be seen, despite the effect of shear strength decrease, due to increased pore pressure, the first mechanism (rapid increase in elastic load) cannot be neglected. Moreover, for the case of Karkheh dam, the maximum load from the reservoir water is about 10 bars, whereas the already-developed pressure at the hypocentral depth exceeds 2000 bar. Thus, it can be concluded that the water load cannot directly cause earthquake. As discussed by Beck [11], reservoir water load only accounts for nearby faults which are close to their critical stress to fail and cause earthquake.

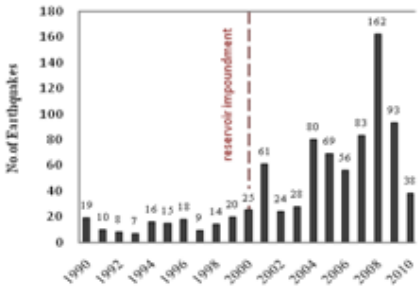

Fig. 3. The Number of earthquakes within 100 km around the reservoir in a 10 year period before and after the reservoir filling

RIS is characterized by shallow hypocentral depths [2]. To study the behavior of RIS depth and magnitude at the Karkheh dam, these parameters are shown in Figs. 4 and 5 for the periods before and after reservoir impoundment, respectively. According to Fig. 4, the average earthquake depth before the impoundment is about 30.5 km, whereas it decreases to about 22 km after the impoundment.

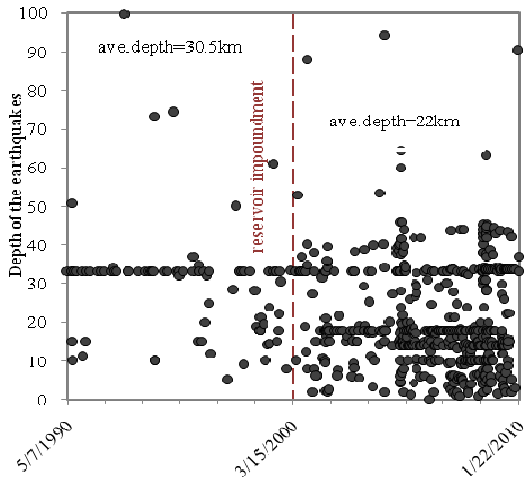

Figure 4. Earthquake depth distribution before and after impoundment

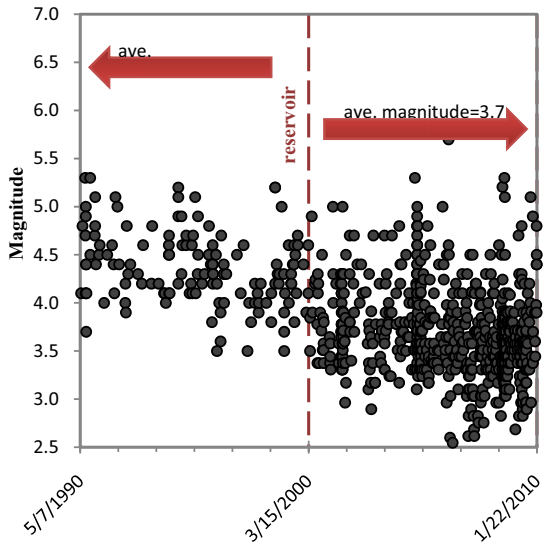

Figure 5. Magnitude of earthquakes occurred before and after impoundment

Since the earthquake magnitudes of the current database have been obtained from different earthquake catalogs, the relationships proposed by Utsu [3] are used to make them compatible with each other. Fig. 5 shows that the average earthquake magnitudes in the region are 4.5 and 3.7 before and after the reservoir impoundment, respectively. Gutenberg and Richter presented the equation, $\text{Log}_{10}N = a - bM$, which is applicable to the frequency of seismic events. In this equation, N is the cumulative total number of earthquakes with magnitude equal to or greater than M that occur in a given region within a certain time period, and a and b are constant parameters that depend on the region. In most cases RIS shows relatively high b values compared to non-RIS. It is reported that b values in reservoir-induced earthquakes is increased up to 1 or even more [2].

To investigate the b value of RIS at the Karkheh dam, the aforesaid equation is applied for the earthquake data after the impoundment.

The b value for the Karkheh dam is 0.61 which is lower than the values observed in other cases of RIS in the world. Therefore, it may be concluded that the behavior of RIS at the Karkheh dam is an example indicating that the conclusion about the high b values for RIS is not always true. A similar result was reported by Papazachos [12], who stated that the b for RIS shows some tendency to the larger values but this cannot be considered as a discriminatory property of RIS.

IV. SEISMICITY AND RESERVOIR WATER LEVEL

In previous studies [2, 11], it has been shown that a very high correlation between reservoir water level and RIS exists. There are more effective factors in RIS than the local tectonic setting of the dam area, such as rate of water level increase, duration of loading, maximum level achieved, and duration for which high levels are maintained [13].

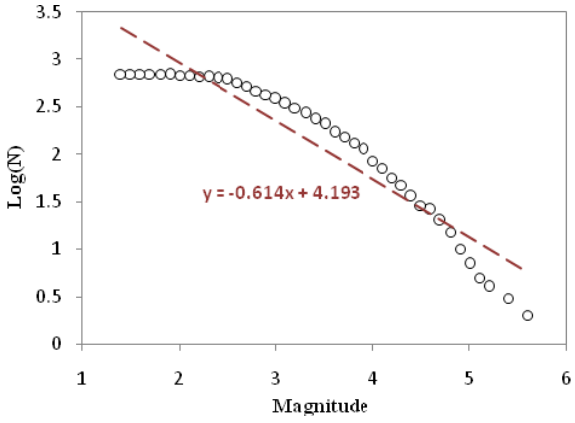

Figure 6. Gutenberg-Richter (G-R) relationship for Karkheh dam seismicity after the reservoir impoundment

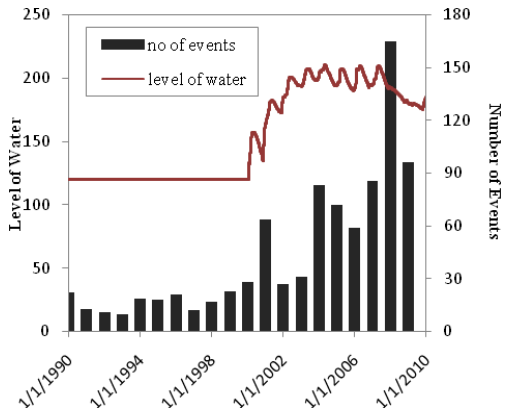

Fig. 7.Annual number of earthquakes with water level fluctuations before and after the reservoir impoundment

To examine the effect of reservoir water load on the RIS at the Karkheh dam, the daily fluctuations of reservoir water level is presented along with annual seismicity in Fig. 8. Overall, a strong correlation can be seen between reservoir water level and seismicity.

Cross correlation method

Cross-correlation method is a standard approach for estimating the correlation coefficient between two different series, as follows:

$$r(d) = \frac{\sum_i [x(i) - mx) \times (y(i-d) - my]}{\sqrt{\sum_i (x(i) - mx))^2} \sqrt{\sum_i (y(i-d) - my))^2}} \quad (1)$$

Where *mx* and *my* are the means of two series, *x(i)* and *y(i),* respectively, and *d* is the time lag between the corresponding series.

M. M. Selim *et* al. [9] carried out a cross-correlation method to find out whether the fluctuation of water level could influence the seismicity activities in the Aswan dam area or not. For the first series, they took the monthly average of daily reservoir's water level into account and calculated the deviations of these values from moving average of a 13-month interval in order to obtain the fluctuation data. For the second series, they computed the daily average numbers of events for every month and attained the fluctuation data via the same methods as other series. Their computations involved three principle parameters, namely the earthquake depths, their location and the period in which the earthquakes happened. In most of the cases they found very low correlation between two series.

This method is applied in this context; however, since 95 percent of rainfalls in the Karkheh dam area occur in the first half of a year, a model based on moving average of a 7 month interval is also used in addition to the Selim model.

The correlation coefficients for the first model are obtained for depths of 0-18km, 18-40 km and 0-40km, the periods of 1 year to 8 years and within the distances of 30, 50, 100 kilometers from the reservoir. In the second model, time periods are considered from 6 months to 5 years at a 6 month step. Time lags for both models are assumed in the range of 1 to 12 months by an increment of one month.

The analysis results indicate that the best correlation coefficients can be obtained via second model in the distance up to 100 kilometers, with the depth ranging from 0 to 40 km and in a 6-month period. As seen in the table.1 and table.2, the correlation coefficients for the second half of the year in all periods are above 0.56 and in most of the years the maximum coefficients are attained at a 0 month time lag. For the first half of the year the correlation coefficients in some periods are below 0.5 and the time lags are also oscillated in the range of 0-4 months.

On the other hand, in the first model the maximum correlation coefficient is 0.58. Moreover the results show that even in the longer periods these coefficients are lower in the first model.

In order to compare these two models in a typical longer period, the cross-correlation coefficients are plotted in Fig.8.

TABLE I. CORRELATION COEFFICIENT FOR THE FIRST HALF OF THE YEARS

Year	Cross-correlation coefficient	Time Lag
2000	0.89	0
2001	0.4	0
2002	0.67	2
2003	0.59	1
2004	0.63	3
2005	0.53	0
2006	0.5	0
2007	0.37	4
2008	0.78	2

TABLE II. CORRELATION COEFFICIENT FOR THE SECOND HALF OF THE YEARS

Year	Cross-correlation coefficient	Time Lag
2000	0.76	0
2001	0.68	0
2002	0.69	0
2003	0.56	0
2004	0.81	1
2005	0.56	0
2006	0.7	0
2007	0.71	1
2008	0.66	2

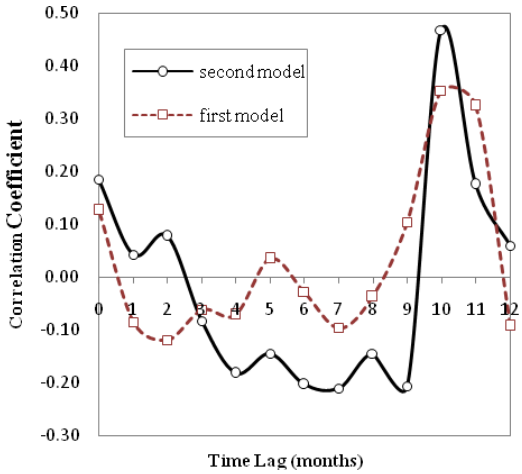

Figure. 8. Correlation coefficients between fluctuation of water level and number of earthquakes, which happened in 2002-2003, versus time lag for the distance of up to 100 km and depth of up to 40 km, between these two series. The results for both models are shown for comparison.

V. CONCLUSION

Investigating the RIS phenomenon is of great interest because of the potential hazards that may cause. Therefore, RIS in Karkheh dam due to impoundment is studied. Based on the evaluation of seismicity in the dam site, the number of earthquakes in a 10-years period after the filling of the dam is 5 times greater in comparison to an equal time interval before the impoundment. Furthermore, the reservoir impounding has changed the seismic behavior of the dam site so that the region experiences more earthquakes with less magnitudes.

As other case of RIS, strong correlation between the fluctuation of water level and number of events can be observed in Karkheh dam. For further investigation, a cross-correlation method is applied. According to the results, the correlation is better during the drawdown phase of the reservoir.

REFERENCE :

[1] M. Berberian, Seismotectonic Map of Iran, Geological and Mining Survey of Iran:, 1976, report NO.39.

[2] H. K. Gupta, B. K. Rastogi, and H. Narain, "Earthquakes in the Koyna region and common features of the reservoir-associated seismicity," Geophys. Monogr. Ser., vol. , edited by W. C. Ackermann et al.,1973, pp. 455–467

[3] International Association of Seismology and Physics of the Earth's Interior. Committee on Education, International Association for Earthquake Engineering, "International handbook of earthquake and engineering seismology, Part2 ," Academic Press, 2003

[4] H.K. Gupta and H.M. Iyer, "Are reservoir-induced earthquakes of magnitude greater than or equal to 5.0 at Koyna, India, preceded by pairs of earthquakes of magnitude greater than or equal to 4.0," Bulletin of the Seismological Society of America, vol. 74 (3), June. 1984, pp. 863- 873.

[5] D.W.Simpson,"Seismicity changes associated with reservoir loading," Engineering Geology, vol. 10, Jun. 1976, pp. 123-150,doi:10.1016/0013-7952(76)90016-8

[6] H.K.Gupta, "A review of recent studies of triggered earthquakes by artificial water reservoirs with special emphasis on earthquakes in Koyna, India," Earth-Science Reviews, vol.58, July. 2002,pp. 279-310,doi:10.1016/S0012-8252(02)00063-6

[7] E.A.Roeloffs,"Fault stability changes induced beneath a reservoir with cyclicvariations in water level," J. Geophys. Res, vol.93(B3), 1988,pp. 2107-2124,doi: 10.1029/JB093iB03p02107.

[8] L. Telesca, "Analysis of the Cross-Correlation between Seismicity and Water Leve l i n the Koyna Area of India," Bulletin of the Seismological Society of America, vol. 100, october. 2010, pp. 2317-2321,doi: 10.1785/0120090392.

[9] M. M. Selim,M.Imoto, and N.Hurukawa, "Statistical investigation of reservoir-induced seismicity in Aswan area, Egypt," Earth, Planets and Space, vol. 54, April. 2002, pp. 349-356,doi: 10.1785/0120090392

[10] D.W.Simpson,"Two types of reservoir induced seismicity ," Bulletin of the Seismological Society of America, vol. 78, December. 1988, pp. 2025-2040.

[11] J. L. BECK, "Weight-induced stresses and the recent seismicity at Lake Oroville, California," Bulletin of the SeismologicalSociety of America, vol. 66, August. 1976, pp. 1121-1131.

[12] B.C. Papazachos,"On the relation between certain artificial lakes and the associated seismic sequences," Engineering Geology, vol. 8, August. 1974, pp. 39-48, doi:10.1016/0013-7952(74)90010-6

[13] H.K. Gupta, B.K. Rastogi,"Investigations of the behaviour of reservoir-associated earthquakes," Engineering GeologyEngineering Geology, vol. 8, August. 1974, pp. 29-38, doi:10.1016/0013-7952(74)90009-X .

Swell And Compressibility of Fiber Reinforced Expansive Soils

Mona Malekzadeh & Huriye Bilsel

Department of Civil Engineering, Eastern Mediterranean University, Gazimagusa, Mersin 10, Turkey

Abstract - This paper presents an experimental study evaluating the effect of polypropylene fiber on swell and compressibility of expansive soils. The initial phase of the experimental program includes the study of the effect of polypropylene fiber on maximum dry density (MDD) and optimum moisture content (OMC) with different fiber inclusions. Static and dynamic compaction tests have been conducted on an expansive soil sample with different percentages of 0%, 0.5%, 0.75%, and 1% polypropylene fiber additions (by dry weight of the soil). The second phase of the experimental program focuses on the compressibility and hydraulic characteristics of the soils. The unreinforced and reinforced specimens have been prepared statically and the swell and compressibility behavior of the samples have been analyzed. Finally it is concluded that mitigation of expansive soils using polypropylene fiber might be an effective method in reducing the swell potential and compressibility of subsoils on which roads and light buildings are constructed.

Keywords: expansive soils, polypropylene, compaction, compressibility, swell potential.

I. INTRODUCTION

Expansive soils which include montmorillonite-rich clays, over- consolidated clays and shales are problematic soils found in many parts of the world (Nelson and Miller, 1992). They may cause serious problems in the behavior of light buildings associated with the seasonal cycles of wetting and drying. Moisture variations play important role in the swell-shrink potential of soils, and are dependent on climate, permeability of soil deposits, temperature, groundwater, vegetation, drainage and manmade water sources [9],[13].

There has been a growing interest in recent years in the influence of chemical modification of soils which upgrades and enhances the engineering properties. The transformation of soil index properties by adding chemicals such as cement, fly ash, lime, or combination of these, often alter the physical and chemical properties of the soil including the cementation of the soil particles. Especially use of lime admixture has proved to have a great potential as an economical method for improving the geotechnical properties of expansive soils [2],[3],[14],[10]. Rao, S. M and Shivananda, P. (2005) has examined the compressibility behavior of lime-stabilized soils [4]. According to Gordon and McKeen, (1976), cement and lime show different behavior in soil stabilization [6]. Cement contains the necessary ingredients for the pozzolanic reactions, whereas lime can be effective only if there are reactants in the soil.

Recently there is a growing attention to soil reinforcement with different types of fiber. However, there is limited research done on fiber reinforcement of fine grained soils particularly its effect on swelling, consolidation settlement, hydraulic conductivity, and desiccation characteristics. In this experimental investigation, the aim was to study the effect of polypropylene fiber reinforcement on the improvement of physical and mechanical properties of a clay sample obtained from an expansive clay deposit in Famagusta, North Cyprus. The experimental program was carried out on compacted soil specimens with 0%, 0.5%, 0.75%, and 1% polypropylene fiber additives, and the results of one-dimensional swell and consolidation tests are discussed. Despite the difficulties encountered in representative specimen preparation due to random distribution of fiber filaments, it is observed that there is a future prospect in the use of this environmental friendly additive for soil mitigation.

II. LITERATURE REVIEW

Reference [11] studied the behavior of lime-fiber stabilized soils, concluding the improvement in compression and shear strength, swelling and shrinkage. The addition of fiber is observed to transfer the failure characteristic of soil from brittle to ductile failure. Tang, C., Shi, B., Gao, W., Chen, F., Cai, Y. (2007) investigated on the effect of fiber and cement inclusions on unconfined compressive strength, shear strength parameters, stiffness and ductility of soil specimens. The

combined effect of fiber and cement have been observed to improve these properties, and fiber usage to impede the formation of dessication cracks [11]. Abdi, Parsapajouh, and Arjoman (2008)'s work on fiber reinforced soils substantiates the previous findings that consolidation settlements, swelling and dessication crack formation reduce substantially. They have also concluded that the hydraulic conductivities increased slightly by increasing fiber content and length [12]. Viswanadham, Phanikumar, and Mukherjee (2009) examined swelling behavior of geofiber-reinforced soils, using fibers of different aspect ratios and observed a reduction in heave. The swelling pressure was the maximum at low aspect ratios at both the fiber contents of 0.25% and 0.50%. Finally, the mechanism by which discrete and randomly distributed fibers restrain swelling of expansive soil was explained with the help of soil–fiber interaction [6]. Effect of freeze and thaw cycles on the strength behavior of expansive soils reinforced by polypropylene fiber has been studies by Ghazavi and Roustaie (2010). In cold climates freezing and thawing of the expansive soils is the main problem. Once the soil freezes most of its properties including permeability, water content, stress–strain behavior, failure strength, elastic modulus, cohesion, and friction angle will change accordingly. A method of static compaction is used for preparing samples with different percentages of polypropylene fiber to overcome the difficulty in sample preparation Finally, they have reported that an increase in the number of freeze–thaw cycles results in the reduction of unconfined compressive strength of clay samples by 20–25% [7].

III. MATERIALS AND METHODS

A. Soil

The soil that is used in this research has been obtained from the Eastern Mediterranean University campus in North Cyprus. The physical properties of the soils are as depicted in Table I. The high plasticity index indicates high swell potential, the most problematic soil type under light structures. Identification, description, and classification of this type of soils are based on preliminary assessment of their mechanical properties based on the Atterberg limits analysis. According to Nelson and Miller (1992) the soil used in this study has a high swell potential [1].

B. Polypropylene Fiber

The polypropylene fiber used in this study is the most commonly used synthetic material due to its low cost and hydrophobic and chemically inert nature which does not allow the absorbtion or reaction with soil moisture or leachate. The other properties are the high melting point of 160°C, low thermal and electrical conductivity, and high ignition point of 590°C. The physical properties also include the specific gravity of 0.91, and an average diameter and length of 0.06 mm and 20 mm respectively.

C. Sample Preparation

All the test specimens were compacted at their respective maximum dry density (MDD) and optimum moisture content (OMC), corresponding to the values obtained in the Standard Proctor compaction tests in accordance with ASTM D698-91. This is achieved by statically compacting the reinforced and unreinforced soil by applying the right amount of energy needed to reach to MDD at OMC. The static compaction is applied in a modified CBR instrument. To prepare unreinforced samples, water is added and the soil is statically compacted after 24 hours of mellowing. To obtain reinforced samples, the fiber is added after the mellowing time and blended in a mixer.

TABLE I. PHYSICAL PROPERTIES OF THE STUDIED SOIL

Property	
Specific Gravity	2.56
Gravel (>2000 μm), (%)	0
Sand (75-2000 μm), (%)	8
Silt (2-75 μm), (%)	40
Clay (<2 μm), (%)	52
Liquid limit, (%)	57
Plastic limit, (%)	28
Plasticity index, (%)	29
Linear shrinkage, (%)	20
Optimum moisture content, (%)	24
Maximum dry density, (kg/m^3)	1497
Soil classification(USCS)	CH

IV. RESULTS AND DISCUSSIONS

In order to assess the effect of random fiber inclusion on swelling, consolidation settlement, and hydraulic conductivity, oedometer tests were conducted according to ASTM D2435-96.

A. Effect of polypropylene fiber on swell potential

To investigate the swelling characteristics of unreinforced and fiber reinforced specimens, one dimensional swell tests were carried out. Samples were statically compacted in consolidation rings at optimum moisture obtained from Standard Proctor content in consolidation rings of 50 mm inner diameter and 19 mm of height. The samples were left under a low surcharge of 7 kPa and full swell was measured. Specimens of

different fiber inclusions have been swelled until the increase in free swell with time became marginal. Figure 1 presents the free swell response in percent swell (ΔH/H0) with respect to logarithm of elapsed time in minutes for different fiber percentages. The results show an increase of swell with 0.5% and 0.75% fiber content and a sudden reduction with 1% fiber content. According to Ghazavi and Roustaie (2009), a reduction in swell percentage has been obtained with 3% of polypropylene fiber and an enhancement of swell percent with 1% and 2% of polypropylene fiber. Sample size is a factor which can influence the swell percentage of the soil samples [7]. As Loehr, Axtell, Bowders (2000) pointed out, samples of 10.2 cm showed reduction in swell percentage versus time with the increase of fiber content and, the same soils have been tested with dimension of 6.4 cm which indicated an increase in swell percent of the soil specimens [8].

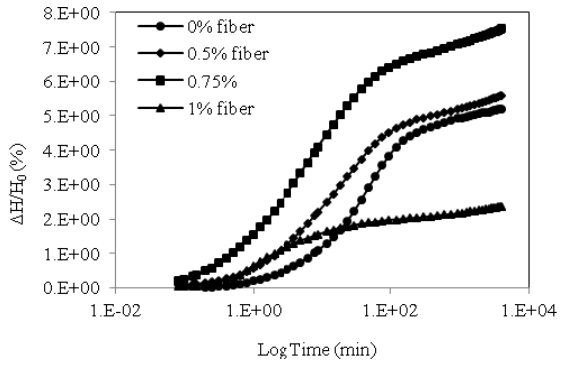

Fig. 1 : Percent swell of soil specimens versus log time with different polypropylene fibers.

Fig. 1 shows the swell percentage versus logarithm of time relationship for different fiber contents. The primary swell (s_w%), secondary swell and the primary swell times (t_s) are summarized in Table II. The results reveal that there is a marked reduction in primary swell potential with the increase in fiber inclusion. The secondary swell, which is the amount of swell beyond the completion of primary swell, has also been reduced with the increase of fiber content.

B. Compressibility Characteristics

The effect of polypropylene fiber on compressibility properties of expansive soils has been investigated by use of one-dimensional consolidation test. Consolidation pressures up to a maximum of 1568 kPa have been applied during the process. Table III indicates the results of this experiment in which a considerable reduction in the compression and rebound indices can be observed with the increase in fiber content. Expansive soil used in this study with high swell potential, was also highly compressible experiencing a noticeable reduction in volume change. Figure 2 gives the results of consolidation tests on increasing fiber contents as time versus logarithm of pressure. A distinct improvement can be observed on the compressibility of the soil which has been mixed with 1 % polypropylene fiber.

TABLE II. PRIMARY AND SECONDRY SWELL OF THE FIBER REINFORCED SPECIMENS

Fiber Content (%)	Primary swell (%)	Time of primary swell, t_s (min)	Secondary swell (%)
0	150	4.4	0.9
0.5	80	4.6	0.8
0.75	50	6.3	0.6
1.0	6	1.6	0.4

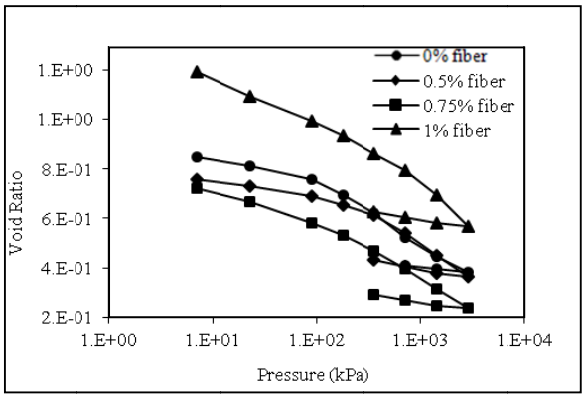

Fig. 2 : Void ratio versus effective consolidation pressure.

C. Hydraulic Conductivity

The hydraulic conductivity of the soil has been determined indirectly from the consolidation test results under low stress ranges. In pavement design, lower stress ranges are important for analysis since it is the surface soil that is in contact which the main layer of the pavement. The hydraulic conductivity of unreinforced and reinforced soils has been obtained using Equation 1.

$$k = c_v \; m_v \; \gamma_w \qquad (1)$$

Where *k* is the saturated hydraulic conductivity, c_v is the coefficient of consolidation, m_v is the coefficient of volume compressibility, γ_w is the unit weight of water. The results show variations of hydraulic conductivity with different fiber content, as presented in Figure 3. Comparing the k obtained for 0-200 ranges of stresses reveals that the addition of 0.5% and 1% fiber reduced the hydraulic conductivity. With 0.75% fiber content an appreciable increase in hydraulic conductivity is observed. Despite the inconsistency in the results, due to

random distribution of fiber in soil matrix, there is a tendency for hydraulic conductivity to increase with the increase of fiber content.

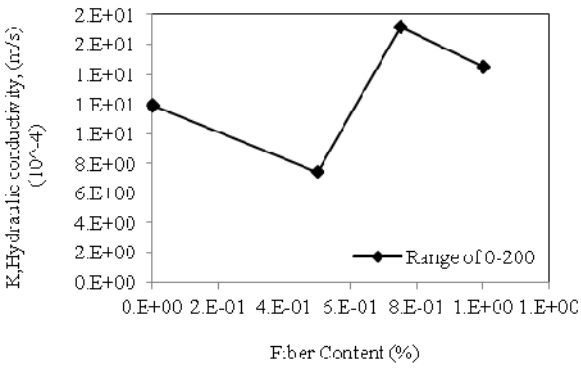

Fig. 3 : Hydraulic conductivity of low range stresses versus fiber content.

TABLE III. CONSOLIDATION PARAMETERS

Fiber content	Compression index (C_c)	Rebound index (C_r)	Preconsolidation pressure	Swell pressure
0%	0.317	0.131	830	200
0.5%	0.265	0.088	199	80
0.75%	0.230	0.058	505	68
1%	0.186	0.046	120	40

V. CONCLUSIONS

This study demonstrates the influence of polypropylene fiber on swelling, compressibility and hydraulic conductivity of expansive soils. The results indicate that primary swell and secondary swell percentages decreased considerably with increase in fiber addition. The time of primary swell, however increased with 0.5% and 0.75% fiber, while a marked reduction occurred with 1% fiber. The same behavior is observed in compression index results. Hydraulic conductivity shows another erratic behavior, increasing with 0.75% fiber, whereas with 1% a reduction in three fold occurs. It can be concluded that there is a potential for use of polypropylene fiber to reinforce expansive soils. 1% fiber content is suitable for the soil in this study to have low amount of swell, compressibility, and hydraulic conductivity. However, further research is required to substantiate these conclusions.

REFERENCES

[1] Nelson, J. D., & Miller, D. J. (1992). Expansive soils. New York: Wiley.

[2] Bilsel, H., Oncu, S. (2005). Soil-water characteristics and volume change behavior of an artificially cemented expansive clay. Proceedings of an International Symposium on Advanced Experimental Unsaturated Soil Mechanics, Trento, Italy, 27-29 June, A.A. Balkema Publishers, Taylor & Francis Group, London, pp. 331-335.

[3] Nalbantoglu Z., Tuncer, E. R. (2001). Compressibility and hydraulic conductivity of chemically treated expansive clay. Can.Geotech, 38, 154-160.

[4] Rao, S. M.. , Shivananda, P. (2005). Compressibility behaviour of lime-stabilized clay. Geotechnical and Geological Engineering, 23, 309–319.

[5] McKeen, R. G. (1976). Design and construction of airport pavements on expansive soils. Washington, D.C.: U.S. Department of Transportation, Federal Aviation Administration Systems Research & Development Service.

[6] Viswanadham., B. V. S., Phanikumar, B.R., Mukherjee, R. V. (2009). Swelling behaviour of a geofiber-reinforced expansive soil. Geotextiles and Geomembranes, 27(1), 73-76.

[7] Ghazavi, M., Roustaie, M. (2010). The influence of freeze and thaw cycles on the unconfined compressive strength of fiber reinforced clay. Cold Region science and technology, 61, 125-131.

[8] Loehr. , J. E., Axtell, P. J., Bowders, J. J. (2000). Reduction of soil swell potential with fiber reinforcement. GeoEng2000.

[9] Hanafy E.A.D.E. (1991). Swelling/shrinkage characteristic curve of dessicated expansive clays. Geotech. Testing J. GTJODJ. Vol 14, 206-211, 1991.

[10] Leroueil, S., and Vaughan, P.R. (1990). The general and congruent effects of structure in natural soils and weak rocks, Géotechnique, Vol 40, 467-488.

[11] Tang, C., Shi, B., Gao, W., Chen, F., Cai, Y. (2007). Strength and mechanical behavior of short polypropylene fiber reinforced and cement stabilized clayey soil. Geotextiles and Geomembranes 25 194–202.

[12] Abdi, M. R., Parsapajouh, A., Arjoman, M. A. (2008) . Effects of Random Fiber Inclusion on Consolidation, Hydraulic Conductivity, Swelling, Shrinkage Limit and Desiccation Cracking of

Clays. International Journal of Civil Engineering, Vol. 6, No. 4.

[13] Chen, F.H. and Ma, G.S. (1987). Swelling and shrinkage behavior of expansive clays. Proceedings of 6th International Conference on Expansive Soils, New Delhi, pp. 127-129.

[14] Basma, A.,A., and Tuncer, E. R. (1991). Effect of lime on volume change and compressibility of expansive clays. Transportation Research Record, Vol 1295, 52-61.

[15] McKeen, R.G. (1992). A model for predicting expansive soil behavior, Proceedings of the 7th International Conference on Expansive Soils, Dallas, Texas, pp. th1-6, August 3-5.

◈◈◈

Synchronization of Traffic Signals
"A Case Study – Eastern Ring Road, Indore"

H. S. Goliya & Nitin Kumar Jain

CE-AMD, S.G.S.I.T.S., Indore, India

Abstract **-** During the past decade major cities have under gone haphazard growth of Industrialization, urbanization of country. Consequently the urban population has to travel greater distances within minimum possible time. To manage travel demand the intersection should be give least resistance to traffic flow so that the travel time can be minimized. The present requirement of metropolitan cities is to absorb the growing traffic demand but within the same physical dimension at the intersection. These days all around the globe efforts are being put forward to protect the environment to save earth. In this paper an attempt has been made to study the various intersections, so as to minimize the delays at these intersections and consequently improve the level service. Traffic signal can be synchronized so that a vehicle starting at one end of the Street and traveling at Preassigned speed can go to other end without stopping for red light. At each intersection the existing traffic has been estimated and then signal designed. Improve the level of service at intersections and to minimize delay, optimized signal has been synchronize and estimated the benefits.

I. INTRODUCTION

Transportation is involved with the movement of people and material from one place to other i.e. from origin to designation. Transportation creates place and time utility for goods for both finished and raw, but also ensuring that the right kinds of goods are available at the right time. Doing this efficiently, in other words at the least cost in the least time, also satisfies in the essence of transportation, the relative facilities. The increasing vehicular traffic on urban road in network demands effective measure of traffic control on road –network, especially at the intersection, where turning movement of vehicle and mixed traffic creates congestion, traffic jam. All the Metropolitan cities in India face this problem in acute form. The provision of signal at the intersection is one of the methods to control the traffic, signal permits the leg wise movement of the traffic and synchronization is the coordination between relative signals.

In congested parts of the cities, traffic control at road intersection in practical and economical only with the help of traffic signals under the prevailing conditions. A major objective of Traffic Signal Synchronization at intersection is to clear maximum number of vehicles through the intersection in a given length and time with least number of accidents, at maximum safe speed and with minimum delay. Indore city having many heavy traffic corridors like Agra bombay road, Mahatma gandhi road, Eastern ring road, MR-10, Western ring road. In which Eastern ring road is one of the most important roads having traffic 22716 PCU per day.

A. Need of Study

Due to mixed nature of traffic it becomes very difficult to accommodate the traffic on road particularly at intersection. The loss of time and fuel due to delay and traffic congestion on urban road is phenomenon. Traffic congestion is a severe problem at an intersection in urban, having create many critical problems like traffic jam, delay, pollution, accidents etc. It challenges in major and most populated cities around the world. Which can be solved by applying traffic signal management and engineering measures?

At the time of heavy traffic condition, traffic jam condition is developed on ring road. Due to more traffic jam the delay of vehicles is more. Excessive fuel is loss due to low running speed and delays. Excessive burned fuel creates excessive smoke in nature which creates air pollution. More traffic jam and delay is also reason of the noise pollution which is the reason of many health problems. Due to these traffic jams intersection traffic handling capacity and road capacity will reduce. The objectives of present study are to reduce the delay and time saving due to synchronization of signal in series, to reduce pollution produced by traffic and fuel loss due to low running speed.

II. MATHADOLOGY

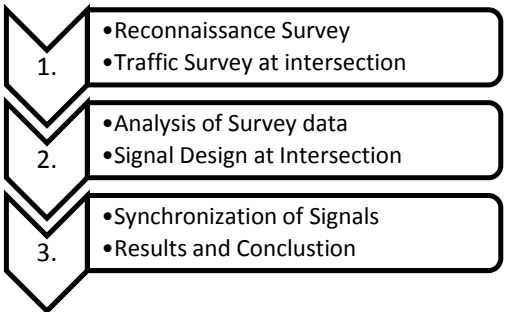

III. TRAFFIC SURVEY AND DATA COLLECTION

Eastern ring road corridor having eleven intersections between Devash naka to Rajeev gandhi intersection. The traffic growth on this road is day by day increase rapidly because new colony and town ship developing along corridor. Now day's problem facing at various intersections due to rapid growth in this section.

A. Detail Information of Road

[Devesh naka Intersection (N) to Rajeev Gandhi Intersection(S)]

Name of road : Eastern Ring Road Corridor.

Total Length of road: 14.6 km.

No of Intersection: 11No.

Rotary at Intersections: 08 No.

B. Geometry and Traffic at intersection survey

The detail measurements have taken for analysis of road. Line diagram of ring road at fig.1, Video survey have accuracy higher than the accuracy of manual data collectors methods, this method has been used to determine traffic survey at each intersection of road.

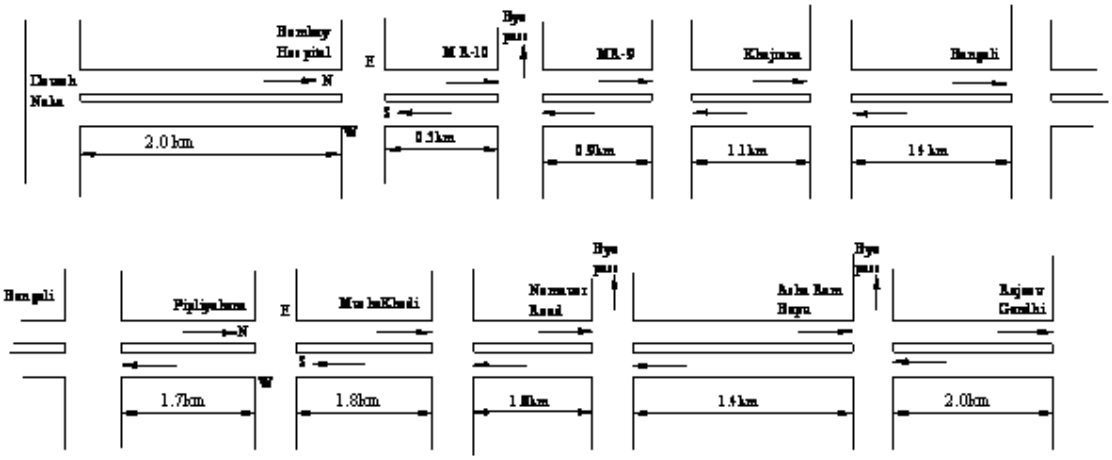

Fig. 1 : Line Diagram of Eastern Ring Road Devesh Naka to Rajeev Gandi intersection

Table 1 : Traffic Survey Data at Intersections of Eastern Ring Road (PCU)

Sr. No.	Name of Intersection	Distance (m.)	From		N			E			S			W	
			To	E	S	W	S	W	N	W	N	E	N	E	S
1	Devash naka Junction	800		-	-	-	225	146	-	621	-	195	-	89	612
2	Bombay Hospital Junction	2000		111	1135	191	192	229	70	409	757	296	228	370	378
3	M R -10 Junction	500		378	728	236	162	628	468	648	760	300	165	412	456
4	M R - 9 Junction	900		165	1462	232	114	107	63	357	1285	197	102	138	196

5	**Khajrana Junction**	1100		311	1231	327	113	474	136	123	663	46	401	608	169
6	**Bangali Junction**	1400		247	938	227	133	681	103	224	1086	195	193	717	221
7	**Pipliya Junction**	1700		152	927	549	52	103	49	299	867	68	582	112	161
8	**Musha khedi Junction**	1800		100	828	388	49	126	75	119	864	174	204	285	53
9	**Nemaver road Junction**	1800		267	1027	172	181	846	183	607	747	625	337	871	177
10	**Asharam Bapu Junction**	1400		382	845	242	208	651	265	92	901	143	346	466	57
11	**Rajeev Gandhi Junction**	2000		-	1109	-	-	-	-	-	1046	-	-	-	-

Chart-1 Avg. Vehicle Flow N to S (Veh/hr)

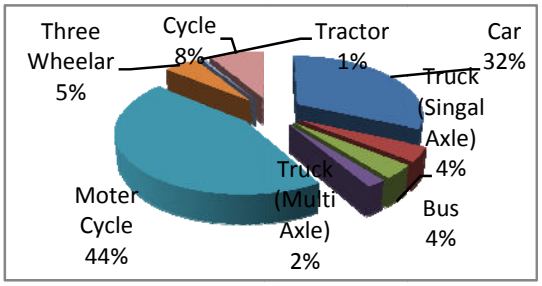

Chart-2 Avg. Vehicle Flow S to N (Veh/hr)

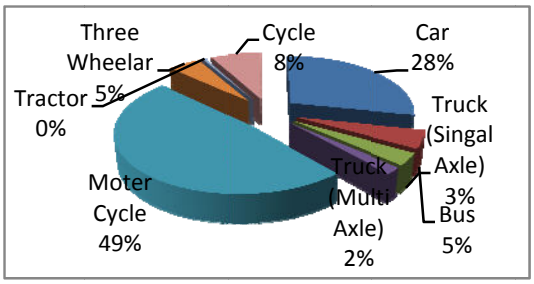

IV. RESULTS

All intersection Signal Design based on webster's signal design method. Detail design One of them is given below in table 2.

Table.2. Traffic Signal Design at Intersection of Eastern Ring Road

Approach	**N**	**E**	**S**	**W**		
Approach Width W	10.5	10.5	10.5	10.5	Optimum Cycle Time Co (sec.)	103
Flow V (PCU/hr.)	963	1096	1041	864	Effective Green Time G_E (sec.)	87
Green Phase (sec.)	25	28	27	23	Inter Section Capacity	4656
Green Time G (sec)	20	23	22	18	Determination of Critical lane group	0.72
Amber Time (sec.)	5	5	5	5	Critical V/C Ratio for Intersection Xc	0.85
Red Time (sec.)	78	75	76	80	Total Intersection Delay D_I (sec.)	34.37
Delay di (sec./veh.)	34.8	32.9	33.7	36.3	Intersection Level of Service	D
V/C Ratio (X)	0.89	0.89	0.89	0.90		

Fig. 2 : Timing Diagram of MR-10 Intersection

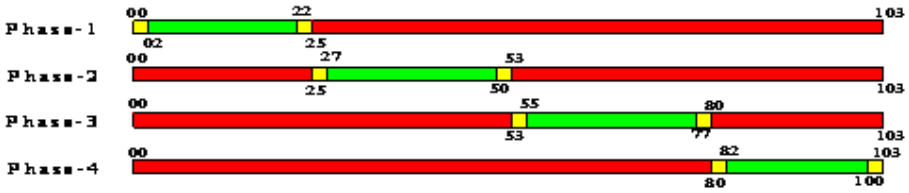

Table3. Signal Design Detail Intersections

Sr. No	Name of Intersection	Distance (m.)	Cycle Time Co	Green Phase (sec.)				Red Phase (sec.)			
				1	2	3	4	1	2	3	4
1	Bombay Hospital Intersection	-	102	33	14	27	28	69	88	75	74
2	M R -10 Intersection	500	103	25	28	27	23	79	76	77	81
3	M R - 9 Intersection	900	101	41	10	36	15	61	92	65	86
4	Khajrana Intersection	1100	136	47	29	24	36	89	107	112	100
5	Bangali Intersection	1400	182	46	43	50	43	137	139	132	139
6	Pipliyahana Intersection	1700	65	28	8	19	11	37	57	46	54
7	Musha khedi Intersection	1800	65	24	9	21	12	42	56	44	53
8	Nemaver road Intersection	1800	185	48	41	54	42	137	144	131	143
9	Asharam Bapu Intersection	1400	82	24	21	23	14	58	61	59	69

.

Table. 4 : Different parameters of Signal Design

Sr. No	Name of Intersection	Distance (m.)	Cycle Time	V/C Ratio	Delay Sec/Veh	LOS
1	Bombay Hospital	-	102	0.85	31.89	D
2	M R -10	500	103	0.85	34.37	D
3	M R - 9	900	101	0.85	27.59	D
4	Khajrana	1100	136	0.89	42.13	E
5	Bangali	1400	182	0.92	57.52	E
6	Pipliyahana	1700	65	0.73	19	C
7	Musha khedi	1800	65	0.74	20.26	C
8	Nemaver Road	1800	185	0.92	58.4	E
9	Asharam Bapu	1400	82	0.80	27.38	D

A. Synchronization of Signals

Traffic signal synchronization allows a series of lights along a street to turn green based on synchronized timers set and preassigned speed to current traffic patterns and congestion levels. It is a cost effective way to reduce overall stops and travel delays. Synchronization of traffic Signals has been done and it's detail is given in Figure 4 and Figure 5.

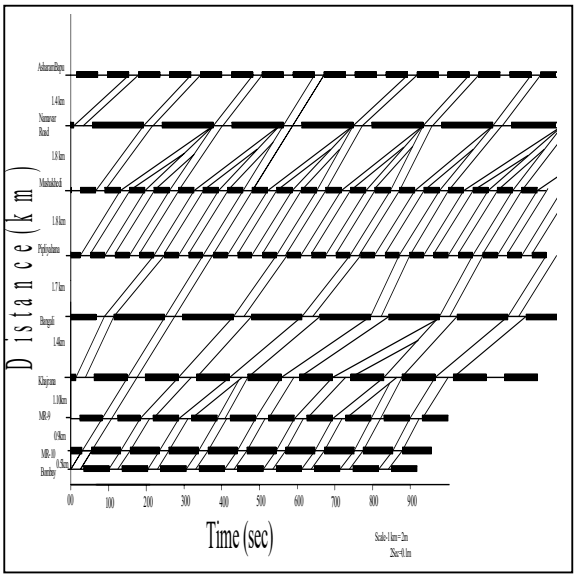

Fig. 4 : Time and Distance Diagram Bombay Hospital to Asharam Bapu Intersection (N to S)

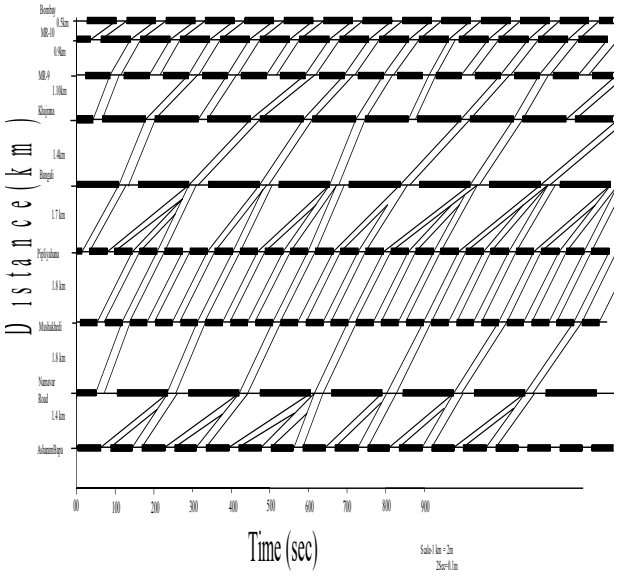

Fig. 5 : Time and Distance Diagram Asharam Bapu to Bombay Hospital Intersection (S to N)

B. Economic Analysis Details

After Applying Synchronization saving time per hour per passenger is 210 sec. and 151 sec. As per Avg. Traffic survey detail Converted into passenger per hour 3332 and 3211. By the report of Advance Estimation of National income 2010-11 estimates at current prices Per Capita income is Rs. 54,527, so per capita per sec. income is Rs 0.00519. Peak traffic hours of the day is 6 hour, then benefits in terms of money is Rs 21,725 per Day and Rs 15,052 per Day. Due to low running Speed of vehicle the extra fuel has been burn, synchronization of signal can save this loss from N-S & S-N, Petrol 627.02 Lit/Day and Diesel 911.44 Lit/Day. Cost of this fuel is Petrol Rs.42,870 and Diesel Rs.41,115. Due to Delay the vehicle burn extra fuel , this fuel loss is ideal fuel consumption of vehicles, it can save loss of fuel Petrol 34.32 Lit/Day and Diesel 20.90 Lit/Day, Cost of fuel Rs.2347 and Rs.949. Detail of this data given below in table 6 & table 7.

Table 6 : Results of Synchronization

	N to S Time Saving-		**S to N Time Saving-**	
	Before	**After**	**Before**	**After**
Journey time (sec)	986	776	995	844
Journey Speed (kmph)	38.70	49.14	38.352	45.19
Delay time (sec)	31	0	45	0
No of Passengers per hr	3332		3211	
Time Saving Sec/hr/pass.	210		151	

Table 7:Benefits of peak hours traffic in terms of Money

Direction	**Bombay Hospital To Asharam Bapu (N-S)**		**Asharam Bapu To Bombay Hospital (S-N)**		**Total**
Save Time (Sec./Day)	4188382		2901843		
Time Saving in Rs. (Per Day)	21725		15052		36777
Low Running Fuel Loss(Lit/Day)	343.73 P	491.53 D	283.29 P	419.91D	
Loss of fuel in Rs. (Per Day)	45821		38436		84257
Delay Fuel Loss (Lit./ Day)	15.01 P	9.37 D	19.31 P	11.53 D	
Loss of Fuel in RS. (Per Day)	1452	1844	3296		
Total Rs. (Per Day)	68997	55332	124392		
Total Rs. (Per Annum)	25184070	20196251	45380320		

C. Carbon Dioxide (CO_2) Emission

Now days Global Warming is very big problem in front of us. One of the important cause of the global

warming is Emission of CO_2. After applying Synchronization fuel save up to 241 kl petrol and 340 kl diesel per annum, so emission of CO_2 may be reduce 1.50 Million kg per Annum.

Fuel (Per Liter)	CO2 Emission (kg.)
Petrol	2.3
Diesel	2.7

V. CONCLUSIONS

Based on analysis of data collated from Eastern ring road, conclusions are signal design and synchronization has been done for nine intersections of eastern ring road to minimize delay. Journey time 241Sec. N to S and 151sec. S to N are reduced by synchronization. 241 kl petrol and 340 kl diesel per annum have been saved. The loss occurred of Rs.1.20 million/annum, 30.15 million/annum and 13.42 million/annum due to vehicle delay, low running speed of vehicle and loss of people's time of respectively. CO_2 emission is estimated to reduce by 1.50 million Kg. per annum through

REFRENCES

[1] Hu Qionghong and Zhou Zhiyun, "Study on the urban road traffic safety management" Eastern Asia Socitey for Transportation Studies-05, 2005, pp 2062-2074,.

[2] Dr. Parida, Dr. Gangopadhay and Goel, "Transport measure to reduce fuel loss on chelmsforad road, New Delhi" Institute of Urban Transportation, 07 (01), 2006, pp 42-51.

[3] Kiran Sandhu and Gurodh Dhillon, "Roads or death traps? impacts and quality of life outcome of road traffic accidents" Highway Research journal, special issue-2008, pp.65-72.

[4] C.T. Wannige and D.U.J. Sonnadara, "Adaptive neuro-fuzzy traffic signal control for multiple junctions", International Conference on Industrial and Information Systems, 2009, 28-31.

[5] Stefan Lammer and Dirk Helbing "Self-stabilizing decentralized signal control of realistic, saturated network traffic" Journal of Transportation Engineering (ASCE), 2009, pp.01-17.

[6] Lin Dong and Wushan Chen, "Real-time traffic signal timing for urban road multi-intersection" Intelligent Information Management, 02, 2010, pp.483-486.

[7] HaiBo Mu, JianNing Yu and LinZhong Liu (). "Traffic Signals Ccontrol of Urban Traffic Intersections Group Based on Fuzzy Control" Seventh international Conference on fuzzy Syatems and knowledge discovery, 2010, pp. 763-767.

[8] Liang-Tay Lin, Li-Wei Chris Tung and Hsin-Chuan Ku. "Synchronized signal control model for maximizing progression along an arterial" Journal of Transportation Engineering (ASCE), 136 (08), 2010, pp.727-735.

[9] Government of India Central Statistics office report on "Advance Estimation of National Income 2010-11".

◈◈◈

Formulation of Equivalent Steel Section for Partially Encased Composite Column under Concentric Gravity Loading

Debaroti Ghosh & Mahbuba Begum

Dept. of Civil Engineering, Bangladesh University of Engineering and Technology, Dhaka, Bangladesh

Abstract **-** Partially encased composite column (PEC) consists of thin walled welded H- shaped steel section with transverse links provided at regular intervals between the flanges to inhibit the occurrence of local buckling in the thin flange plates. The space between the flanges and the web plate are filled up with concrete. Extensive experimental investigations have been conducted by several research groups to understand the behavior of this relatively new composite column under both concentric and eccentric loading conditions along with sophisticated non-linear finite element analysis. But the separation between concrete and steel initiates the unstable condition in the finite element analysis near the ultimate point when flange plate buckles. To avoid the expensive and cumbersome modeling of the behavior at the interface of two dissimilar materials, an attempt has been made in this study to replace the composite section of PEC column with an equivalent steel section which can easily be incorporated in commercially available finite element softwares.

Key words - *column: composite; concrete: encased: equivalent; steel.*

I. INTRODUCTION

Steel-concrete composite columns can substantially improve the behavior and cost efficiency of steel-only columns used in the construction of mid-rise and high-rise buildings. A welded H–shaped steel section figures the partially encased composite (PEC) section with concrete infill between the flanges (Fig. 1). In Europe, in the early 1980s, PEC columns and beams were introduced using standard-sized rolled steel sections. In 1996, the Canam Group in North America proposed a PEC column section constructed from a thin–walled built–up steel shape with transverse links provided at regular intervals to restrain local buckling as shown in Fig.1. Extensive experimental research has been performed in Ecole Polytechnique de Montréal [1-3] on small-scale and large-scale PEC column specimens under various conditions of loading. The influences of high performance materials on the behavior of these columns have also been investigated experimental by Prickett and Driver [4] at the University of Alberta. The results of these experimental investigations indicated that the behavior of this composite column is significantly affected by the local instability of the thin steel flanges. Begum et al. [5] were able to overcome these challenges in the finite element model through the implementation of a dynamic explicit formulation along with a damage plasticity model for concrete and a contact pair algorithm at the steel-concrete interface. The developed model was applied successfully to reproduce the behavior of 34 PEC columns from five experimental programs. However, despite of the accuracy, the composite finite element model developed by Begum et al. [5] is very sophisticated due to the presence of two dissimilar materials. Moreover, modeling of the interfacial behavior between steel and concrete requires extensive calculations as well as skilled and experienced users. Due to these complexities most of the structural analysis and design software do not handle such composite members. In this paper an attempt has been made to develop a fictitious steel section of the partially encased composite steel section. This equivalent steel section has added a new dimension to the analysis of partially encased composite column renovating the numerical procedure.

II. OBJECTIVES AND SCOPES

The main objective of this study is to formulate the methodology for the development of fictitious steel section for partially encased composite column built up with thin steel plates. The methodology is then used to simulate ten test PEC test columns from the published literature with variety of geometric properties subjected to concentric gravity loading only. The formulation of the fictitious steel section is based on the equivalence criteria of the basic geometric properties of the composite column. Linear elastic material behavior is assumed for steel as well as for concrete in the composite section.

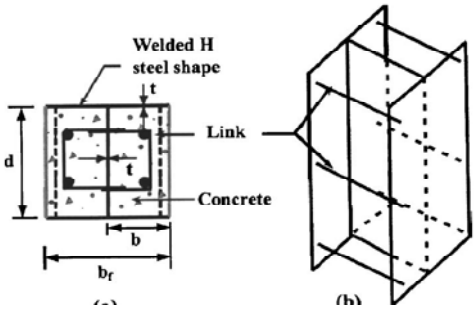

Fig. 1 : Partially Encased Composite Column with Thin-Walled Built-Up Steel Section, (a) Column Cross-Section and (b) 3D view of the Steel Configuration

III. REFERENCE TEST COLUMNS

Ten test PEC columns from the published literature are selected for current study. The lists of these specimens, along with their properties, are given in Table 1. Fig. 2 shows the cross-section and elevation of a typical test column. Specimens C-2 to C-7 were tested during the initial phase of the research program by Tremblay et al. [1] to study the behavior under concentric gravity loading which had square cross-sections of 300 mm × 300 mm and 450 mm × 450 mm, and a length equal to 5d, where d is the depth of the cross-section. Specimens C-8 to C-11, tested by Chicoine et al. [2] under axial compression, were larger in their cross–sectional dimensions (600 mm×600 mm) as compared to the previous test specimens.

All the test columns were fabricated from CSA-G40.21-350W grade steel plate. Normal strength concrete (nominally 30 MPa) was used in the test region of these columns. To strengthen the end regions of these test specimens, high strength concrete of 60 MPa nominal strength was used along with the closer link spacing provided in these zones.

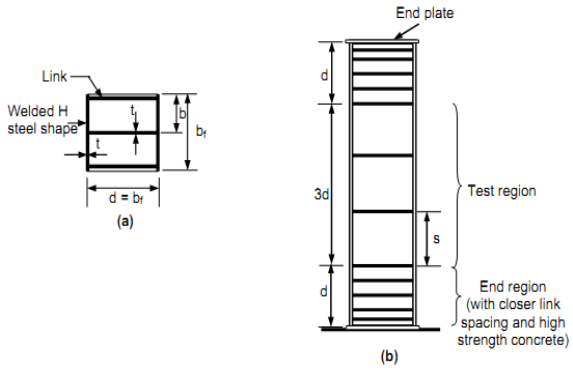

Fig. 2 : Typical PEC Test Column, (a) Cross-section, (b) Elevation

IV. FORMULATION OF EQUIVALENT STEEL SECTION

The fictitious steel cross-section consists of the actual steel cross-section and two additional pairs of plates, one perpendicular to the web at mid-height and one perpendicular to the flanges at mid-width as shown in Fig.3. The cross-sections of the fictitious and the actual column are equivalent in that they have the same:

1. Resistance in compression, and
2. Bending stiffness about the two principal centroidal axes.

In order to produce the equivalent fictitious steel section, the dimensions of the two pairs of steel plates added to the initial cross-section is to be determined from the algebraic expressions of the three equivalence criteria: compression resistance and bending stiffness about the two principal axes.

TABLE I : PROPERTIES OF REFERENCE TEST SPECIMENS

Reference	***Specimen***	***Plate size b_f x d x t***	***Link spacing s***	***Link diameter Φ***	***Length L***	***Compressive Strength of concrete f'_c***	***Yield strength of plates F_y***
		(mm)	(mm)	(mm)	(mm)	(MPa)	(MPa)
Tremblay et al. (1998	C-2	450x450x9.70	225	12. 7	2250	32. 7	370
	C-3	450x450x9.70	337.5	12. 7	2250	32. 4	370
	C-4	450x450x9.70	450	12. 7	2250	31. 9	370
	C-5	450x450x9.70	225	22. 2	2250	34. 3	370
	C-6	450x450x6.35	337.5	12. 7	2250	33. 1	374
	C-7	300x300x6.35	300	12. 7	1500	31. 9	374

Chicoine et al. (2002	C-8	600x600x12.88	600	15. 9	3000	34. 2	360
	C-9	600x600x12.91	600	15. 9	3000	34. 2	360
	C-10	600x600x12.81	300	15. 9	3000	34. 2	360
	C-11	600x600x9.70	600	15. 9	3000	34. 2	345

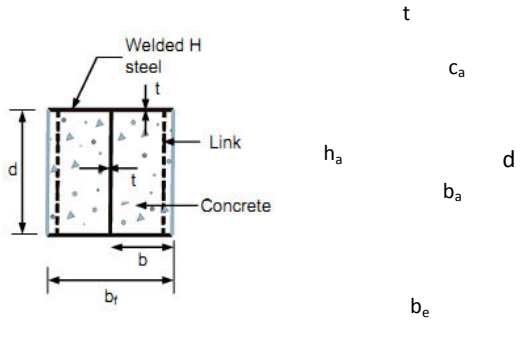

(a) (b)

Fig. 3 : Equivalent steel section for PEC column, (a) Actual cross-section, (b) Equivalent steel section

A. Equivalence in compression resistance

The compression resistance of a composite steel-concrete cross section comprises of the plastic resistance of the steel cross-section, steel links and the concrete. The total area of the fictitious cross-section represents the area combining area of the initial steel cross-section and the additional plates.

$$P_{actual} = A_{se} f_s + A_c f_c$$
$$P_{fictit} = (A_{se} + A_a) f_s \qquad (1)$$

Here, A_{se} = effective area of the steel shape including the I section and the links

A_a = total steel area of the additional steel plates in fictitious section

f_s= design stress of steel= f_y

f_c= design stress of concrete

The effective area of a non-compact steel section can be defined as,

$$A_{se} = (d - 2t + 2b_e)t \qquad (2)$$

Here, d = overall depth of the cross section

t = Thickness of the steel plates

b_e = Total effective width of the flange

Now, $b_e = \frac{b_f}{(1+\lambda_p^{2n})^{1/n}} \leq b_f$

$$\lambda_p = \frac{b}{t}\sqrt{\frac{12(1-\nu_s^2)F_y}{\pi^2 E_s k}}$$

$$k = 0.9/(s/b_f) + .2(s/b_f)2 + .75 \quad (.5 \leq s/b_f \leq 1)$$

Here, b_f = full width of a flange plate

λ_p = Slenderness parameter

E_s = Elastic modulus of steel

ν_s = Poisson's ratio of steel

n = 1.5 as proposed by Chicoine et al. [3]

Considering the condition of equivalence in compression resistance and the relation in (1), it is obtained

$$A_a = A_c \frac{f_c}{f_s} = A_c m_{cd} \qquad (3)$$

Here, m_{cd} = design-stress ratio for concrete-to-steel

The total area of the composite cross-section comprises the equivalent steel cross section A_{se} and concrete section Ac.

$$b_f d \equiv A_{se} + A_c \qquad (4)$$

Dividing Eq. (2) by $b_f d$ and introducing the non dimensional parameters ρ_{se}, and a positive constant q_x [2],

$$A_a / b_f d = m_{cd} \rho_{se}^{"} = q_x^2 \qquad (5)$$

The total cross-secional area of the four additional plates in the fictitious section as shown in Fig.3 is,

$$A_a = 2b_a \times h_a + 2c_a \times t \qquad (6)$$

Which after normalization by $b_f d$ and introduction of normalized plate dimensions β, η, χ and γ becomes:

$$A_a / b_f d = (2\beta)\eta + (2\chi)\gamma \qquad (7)$$

Since equation (4) and (6) are identical in left hand sides, the outcome is:

$$q_x^2 = (2\beta)\eta + (2\chi)\gamma \qquad (8)$$

Here the unknowns are β, η and χ on the left side and the combined geometric and material attributes of the actual cross-section enter through the constants γ and q_x^2.

B. Equivalence in stiffness about the major axis

The flexural stiffness about the major axis y-y of the actual composite steel-concrete cross-section and its fictitious purely steel counterpart are given by:

$$(EI)_{y,actual} = E_{se}I_{se,y} + E_{ce}I_{c,y}$$
$$(EI)_{y,fictit} = E_{se}I_{se,y} + E_{se}I_{a,y} \qquad (9)$$

Here, E_{se} and E_{ce} are the effective elastic modulous of steel and concrete respectively. $I_{se,y}, I_{c,y}$ and $I_{a,y}$ are the moment of inertia about minor axis for actual steel section, concrete and additional steel plates respectively.

To enforce the condition of equivalence in major-axis stiffness, solving for $I_{a,y}$ and introducing the concrete-to-steel ratio of elasticity moduli,

$$I_{a,y} = \left({}^{E_{ce}}/_{E_{se}}\right) \times I_{c,y} = m_e I_{c,y} \qquad (10)$$

In reference to Fig.1(a)

$${}^{b_f d^3}/_{12} \equiv I_{se,y} + I_{c,y}$$

$$I_{se,y} \equiv A_{se} r_{se,y}^2$$

Equation (9) may be written as:

$$I_{a,y} = m_e \left({}^{b_f d^3}/_{12} - A_{se} r_{se,y}^2 \right) \qquad (11)$$

After normalization of (11) by dividing it with $b_f d^3/12$ and using q_y^2 as a positive constant to sum up the effects of the geometry and material properties of the actual cross section, the final equation is,

$$\left({}^{12I_a}/_{b_f d^3} \right) = m_e\left(1 - 3\rho_{se} \times \lambda_{se,y}^2\right) = q_y^2 \qquad (12)$$

Here, $\lambda_{se,y} = 2\, r_{ay}/d$

$$\rho_{se} = {}^{A_{se}}/_{b_f d}$$

The additional major-axis flexural stiffness of the fictitious cross-section as a function of the dimensions of the additional plates is given by:

$$I_a = \left(2\, {}^{b_a h_a^3}/_{12}\right) + \left({}^{t}/_{12}\right) \times \{(2c_a + d)^3 - d^3\}$$

This, after normalization with $(b_f d^3/12)$ and introduction of the non-dimensional geometric properties β, η, χ, and γ, yields:

$${}^{12I_{a,y}}/_{b_f d^3} = (2\beta)\eta^3 + \gamma\{(2\chi + 1)^3 - 1\} \qquad (13)$$

Since (12) and (13) have identical left-hand sides,

$$(2\beta)\eta^3 + \gamma\{(2\chi + 1)^3 - 1\} = q_y^2 \qquad (14)$$

Here the unknowns are β, χ on the left side and the combined geometric and material attributes of the actual cross-section enter through the constants γ and q_y^2.

C. Equivalence in stiffness about minor axis

The treatment of major axis stiffness equivalence presented in the previous subsection is repeated here in shorthand for the minor-axis case.

First, minor-axis counterpart of (11):

$$I_{a,z} = m_e \left({}^{b_f^3 d}/_{12} - I_{se,z} \right)$$
$$= m_e \left({}^{b_f^3 d}/_{12} - A_{se} r_{se,z}^2 \right) \qquad (15)$$

After normalization of (15) by dividing it with $b_f d^3/12$ and using q_z^2 as a positive constant the obtained equation is

$$\left({}^{12I_{a,z}}/_{b_f^3 d} \right) = m_e\left(1 - 3\rho_{se} \times \lambda_{se,z}^2\right) = q_z^2 \qquad (16)$$

Here, $\lambda_{se,z} = 2\, r_{az}/d$

$$\rho_{se} = {}^{A_{se}}/_{b_f d}$$

Similarly for the additional elements of the fictitious steel cross-section, one obtains the counterpart of (13),

$${}^{12I_{a,z}}/_{b_f^3 d} = \{\{(2\beta + \gamma)^3 - \gamma^3\}\eta + (2\chi)\gamma^3\} \qquad (17)$$

Since (16) and (17) have identical left-hand sides, the outcome is

$$\{(2\beta + \gamma)^3 - \gamma^3\}\eta + (2\chi)\gamma^3 = q_z^2 \qquad (18)$$

Here the unknowns are β, χ on the left side and the combined geometric and material attributes of the

actual cross-section enter through the constants γ and q_z^2.

In order to transform the actual section in to fictitious section, three non-linear (8), (14) and (18) were developed. Three non-dimensional parameters, q_x^2, q_y^2 and q_z^2 describe the additional compression resistance major-axis stiffness, and minor-axis stiffness, respectively, due to concrete and links. These equations must be solved for the three non-dimensional unknowns' β, χ and η to determine the dimensions of the additional steel plate's b_a, h_a, and c_a in the fictitious cross-section.

V. COMPARISION OF FICTITIOUS SECTION WITH ACTUAL SECTION

The methodology described in the previous section is implemented to compute the equivalent steel sections of the reference test PEC columns mentioned in Table I. The dimensions of the additional steel plates representing the concrete part of the composite section are provided in Table II. The geometric properties of the equivalent steel sections for columns C-2 to C-11 is calculated and compared to their actual composite cross-section. Table III presents the comparison between the cross-sectional area and moment of inertias of the composite and equivalent steel section of the column. The results show that the cross-sectional area and the moment of inertia about the major axis for equivalent steel section are in excellent agreement with the actual composite section. The moment of inertia about minor axis of the steel section is found to be around 4% lower than that of the composite section. This difference is within acceptable range.

Table II : Develpoment of Equivalent Steel Section for Partially Encased Composite Column

	Composite steel section					***Equivalent steel section***				
Specimen	***bf***	***d***	***t***	***s***	***φ***	***be***	***ba***	***ha***	***ca***	***t***
C-2	450	450	9.7	225	12.7	368.08	304.90	21.46	196.36	9.7
C-3	450	450	9.7	337.5	12.7	371.48	304.91	21.45	196.36	9.7
C-4	450	450	9.7	450	12.8	375.89	309.98	20.42	196.36	9.7
C-5	450	450	9.7	225	22.2	368.08	295.48	23.54	196.36	9.7
C-6	450	450	6.35	337.5	12.7	265.46	303.64	23.19	259.36	6.35
C-7	300	300	6.35	300	12.7	247.74	223.58	12.18	142.27	6.35
C-8	600	600	12.88	600	15.9	503.43	382.01	33.51	258.57	12.88
C-9	600	600	12.91	600	15.9	503.97	382.00	33.50	258.15	12.91
C-10	600	600	12.81	300	15.9	491.82	382.00	33.58	259.57	12.81
C-11	600	600	9.7	600	15.9	420.41	382.21	35.09	312.89	9.7

Table III. Comparison between the properties of composite and fictitious section

Specimens	***Area***			***Moment of inertia about of major axis***			***Moment of inertia about minor axis***		
	CPS *10³	***EQS *10³***	$\frac{A_{CPS}}{A_{EQS}}$	***CPS *10⁶***	***EQS *10⁶***	$\frac{I_{y,CPS}}{I_{y,EQS}}$	***CPS *10⁶***	***EQS *10⁶***	$\frac{I_{z,CPS}}{I_{z,EQS}}$
C-2	16.76	16.90	0.99	410.13	410.63	1.00	443.14	425.22	1.04
C-3	16.76	16.89	0.99	410.13	410.63	1.00	443.14	425.06	1.04
C-4	16.35	16.47	0.99	410.13	410.57	1.00	443.14	424.86	1.04
C-5	17.58	17.72	0.99	410.13	410.77	1.00	443.14	425.22	1.04
C-6	17.17	17.38	0.99	432.84	433.47	1.00	455.13	446.56	1.02
C-7	7.20	7.25	0.99	91.40	91.47	1.00	98.61	94.67	1.04
C-8	32.03	32.27	0.99	1264.62	1267.01	1.00	1365.96	1309.64	1.04

C-9	32.02	32.26	0.99	1264.15	1266.55	1.00	1365.71	1309.21	1.04
C-10	32.04	32.30	0.99	1265.69	1268.10	1.00	1366.54	1311.73	1.04
C-11	32.56	32.89	0.99	1314.18	1316.93	1.00	1392.22	1356.36	1.03
MEAN	1.04		0.99			1.00			
SD	0.01		0.00			0.00			

.

VI. CONCLUSIONS

The composite cross-section of thin walled partially encased composite column was replaced by an equivalent steel section. The formulation of the fictitious steel plates replacing the concrete part of the composite cross-section was presented in the paper. Linear elastic material behavior was considered during the formulation. The local buckling of the thin flange plates were incorporated by considering the effective width of the flange plates. The proposed methodology was used to calculate the equivalent steel section of ten PEC columns with a variety of geometric properties under concentric gravity loading only. The geometric properties of the actual composite section and the equivalent section were compared. The cross-setional area and moment of inertias for the equivalent steel section were found to be very close to properties of the actual composite section. The proposed methodology can reliably replace the composite section with an equivalent steel section.

VII. ACKNOWLEDGMENT

All assistance including laboratory, computing and financial supports from Bangladesh University of Engineering and Technology (BUET), Dhaka, Bangladesh are gratefully acknowledged

REFERRENCES

[1] Tremblay, R., Massicotte, B., Filion, I., and Maranda, R. “Experimental study on the behaviour of partially encased composite columns made with light welded H steel shapes under compressive axial loads.” Proc., Structural Stability Research Council Annual Technical Session and Meeting, Atlanta, 195–204, 1998.

[2] Chicoine, T., Tremblay,R., Massicotte, B., Ricles, J., and Lu, L.-W. “Behavior and strength of partially-encased composite columns with built up shapes.” J. Struct. Eng., 128(3), 279–287, 2002.

[3] Bouchereau, R., and Toupin, J.-D.. “Étude du comportement en compression-flexion des poteaux mixtes partiellement enrobés.” Rep.No. EPM/GCS-2003-03, Dept. of Civil, Geological, and Mining Engineering, cole Poly Technique, Montréal, 2003.

[4] Prickett, B. S. and Driver, R. G.: Behaviour of Partially Encased Composite Columns Made with High Performance Concrete.” Structural Engineering Report No 262, Dept. of Civil and Environmental Engineering, University of Alberta, AB, Canada, 2006.

[5] Begum, M., Elwi, A. E., and Driver, R. G. .” Finite-Element Modeling of Partially Encased Composite Columns Using the Dynamic Explicit Method.” Journal of Structural Engineering, ASCE, 133 (3), 326-334, 2007.

◈◈◈

Recommendations to Develop all-in-one ERP System for Construction Industry

Sheetal Gogoi & S. S. Pimplikar

Civil Dept., MIT, Pune, India

Abstract - Because of involvement of uncertainty and high risk, it is challenging to complete the project in given time and budget. Also, there are many channels of communication in a typical organization for the flow of information. It is necessary to properly channelize and screen the information before it is passed to the respective authority, particularly when the information is to be passed to higher level management for decision making. Because of inter-dependencies between various departments and business units, (internal and external relationships) there are many chances of miss communication leading to failure of task. It is therefore necessary to synchronize the flows of information for better productivity and to overcome the miss communication.

Enterprise Resource Planning software is one of the tools that can handle this problem effectively. It is software that encompasses all functional departments of enterprise. It helps management for better analysis of data and acts as decision support systems (DSS) and data retrieving, reducing the paperwork and errors.

The objective of this paper is to recommend strongly, the need of developing an all-in-one ERP software for construction industry as a total quality management tool. The methodology employed is a mix of literature review & market studies in the form of questionnaire survey, based on which analysis is done before making the recommendation as stated above.

Key Words - *ERP, TQM, DSS, EC&O*

I. INTRODUCTION

Enterprise resource planning (ERP) system is a business management system that comprises integrated sets of comprehensive software, which can be used, when successfully implemented, to manage and integrate all the business functions within an organisation. These sets usually include a set of mature business applications and tools for financial and cost accounting, sales and distribution, materials management, human resource, production planning and computer integrated manufacturing, supply chain, and customer information (Boykin, 2001; Chen, 2001; Yen et al., 2002). These packages have the ability to facilitate the flow of information between all supply chain processes (internal and external) in an organisation.

ERP packages touch many aspects of a company's internal and external operations. Consequently, successful deployment and use of ERP systems are critical to organizational performance and survival (Markus et al., 2000b). Potential benefits include drastic declines in inventory, breakthrough reductions in working capital, abundant information about customer wants and needs, along with the ability to view and manage the extended enterprise of suppliers, alliances and customers as an integrated whole (Chen, 2001). In the manufacturing sector, ERP implementation has reduced inventories anywhere from 15 to 35 per cent (Gupta, 2000).

An overview of ERP systems including some of the most popular functions within each module is shown in fig. no. 1

II. NEED OF ERP IN CONSTRUCTION INDUSTRY

ERP systems are being used by construction companies to improve responsiveness in relations to customers, strengthen supply chain partnerships, enhance organizational flexibility, improve decision making capabilities, and reduce project completion time and lower costs. The goal of ERP is to support one time entry of information at the point where it is created and to make it available to all the participants within the organization. The aim of this study is to investigate the suitability and the importance of the ERP systems in construction industry to improve the efficiency and productivity.

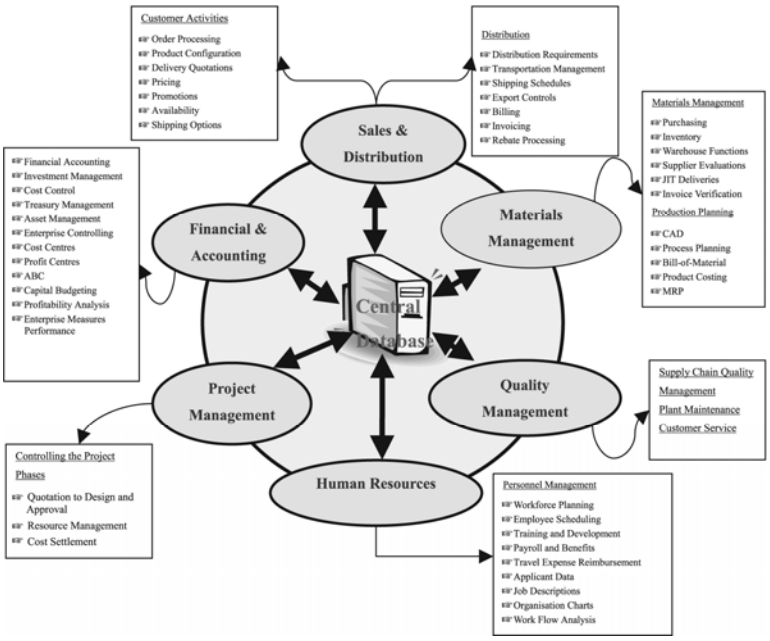

Fig1 ERP System modules

III. NECESSITY OF INTEGRATED APPROACH

Because the construction industry is capital-intensive, construction companies need to be able to manage all resources accurately in order to increase profit while encouraging quality and business model improvement. Companies from the construction industry can take advantage of software solutions such as enterprise resource planning (ERP) systems that specialize in service delivery to support specific construction project portfolio management (PPM) and back-office operations, among other operations. Integrated approach is the key to successful implementation of ERP. Figure 2 explains the typical relationship and connections between various major processes / departments in a company.

Fig.2 ERP- Integrated approach

Although computers are widely used in the construction projects, they are not generally used in an integrative manner, and if so are specific to a single company on projects comprised of many players. The importance of managing projects in lesser funds and time is immerging. This will require optimal utilization of available resources. One cannot now allow heap of material lying on site, spending money on non-productive marketing exercises, allotting extra funds than required, get into cash flow problems, so on and so forth. As the construction industry is a highly fragmented industry, it needs to communicate on a large scale with other related businesses such as material and equipment suppliers, vendors, sub-contractors and clients.

ERP is available in various forms. On the basis of its application, ERPs are basically categorized in to customized package and readymade packages.

IV. MARKET SURVEY

Based on the suggestions received from the software developers, some of the best clients were selected those who are using ERP software for min. 2 to 3 years of time period. The impact of the use of software was found out from the change in the turnover of the company and the feedback from the users. Departmental processes, organizational and departmental structure play a vital role in the success of the ERP. In the

survey, various departments are visited and ongoing processes are observed to find out the mismatch between requirement/ capabilities of ERP and the processes/needs. Roles and responsibilities of major posts are noted and software authorities are also cross checked. Following feedback is received by two of the companies viz. M/s Goel Ganga and M/s Amit Enterprises that use readymade software – Highrise. Readymade software has got its limitation based on the development of the software. Following feedback is received from the users of the software from various departments-

V. PROBLEMS FACED BY USERS-

1) Documentation is found difficult.
2) Data analyzing is tedious and time consuming.
3) Training of site staff is a very tedious Job.
4) To assign computer on every site is a very expensive job.

.

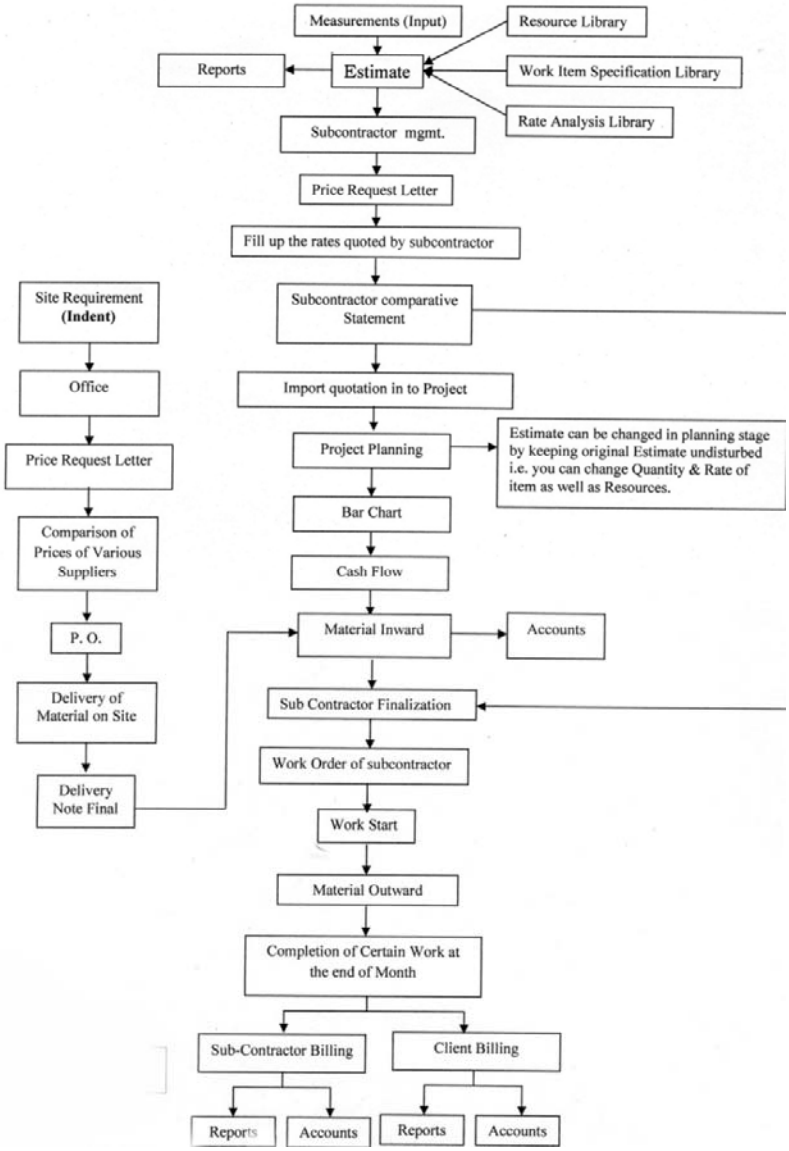

Figure 3 : Work process for readymade software

5. Connectivity of internet connection is the major problem on site due to which whatever the data entries have to be done on site are kept pending. Due to this problem whatever work is left requires more time & this becomes a tedious job.
6. Estimate differs from actual expenditure.
7. Delays due to changes in the work at site in planned activities.
8. Lack of technical staff at site and hence incapability of solving technical problems while using software

VI. FEEDBACK BY USERS:

1) Easy on screen process is required to be fulfilled by software.
2) Continuous good quality internet is required so an alternative system is required to be given by company to fulfill the same work of internet connection.
3) Direct detailed estimation by drawings is possible and found to be useful.

Application of software in construction industry

Information Technology plays a vital role in Construction industry. Any project starts with site surveying and goes through various stages such as Estimation, Tendering, Bidding, Planning, Contracting, Billing, etc. At every stage in the project, there is a need of appropriate software to compile the available data, process it and give output in desired manner. Various software are developed by IT that has made various jobs easy. Figure 4 explains the process of a typical construction project.

Typical construction project undergoes various phases from conceptual phase to close out and maintenance. In absence of software, integrating functions of all these phases is a challenging and tedious job. But, every individual software has got its own functional limitations. Because of which while developing ERP system, one has to understand all project phases, respective project processes, organizational structure, interlinking between departments, as-is and to-be reports, and the most appropriate modules to be interlinked in ERP to assure best coordination and communication of information amongst the organization. In the context of TQM, no single software is available. Also, within the individual software, many important functions are not really catered for.

Applications of individual software available in market are –

- Financial software,
- Project Management Software,
- Personal Communication Software
- Client Communication Software
- Customer Relations Management Software
- Construction Project Management Tools
- Project Portfolio Management Software
- Integrated Construction Estimating Software
- Online Construction Management

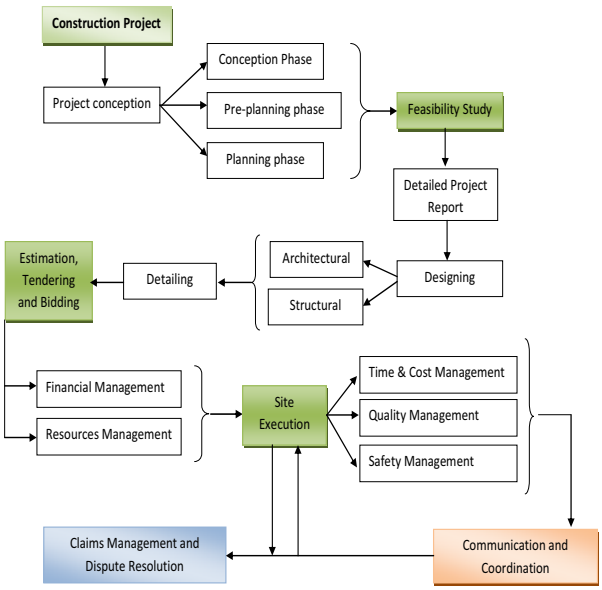

Fig. 4 Process flow chart of a typical construction project

Existing ERP systems: Table 1 summarizes the application some of the existing ERP systems.

.

Table no. 1 : Applications of the ERP systems

Sr. No.	Name and Manufacturer of ERP Software	Cost of Software	Survival in Market (Yrs.)	Software applications
1	HIGHRISE Make: Kanix Infotec. Pvt. Ltd., Pune	15 Lakhs/ Professional Module	14	Engineering, Materials, Management, Contract Management, Marketing & Sales Management, Accounts & Finance Management, Lease & Mall Management, Land & Legal, Human Resource Management
2	HITOFFICE Make: EDSS Pune	1.50 Lakhs/ Per User	25	Quotation, Planning, Master data, Purchase, ISO, Safety, Staff-management, Correspondence, Trade, Builder, Address-management, Accountancy, Equipment
3	Oracle 11i Make: Oracle	Not available	33	Financials, Projects, Product Development, Lease Management, Maintenance Management, Manufacturing, Order Management, Procurement, Supply Chain Planning, Payroll
4	ebuild Make: IMT, MUMBAI	Not available	11	Engineering, Purchase, Sales, Maintenance, Payroll, Architecture, Finance, Administration, Legal, Accounting
5	Qudra suite Make: Quadra Software Solutions Pvt. Ltd., Bangalore	Not available	20	Land Management, Legal Management, Liaison Management, Tender Bid Management, Estimation, Material Management, Contractors Billing, Labour Management, Plant & Machinery, Fixed Asset Management, Enquiry Management, Client Management, Marketing Financials, Financial Accounts, Salary & Payroll, Employee Portal, Project Scheduling, Vendor Portal, Contractor Portal, MIS, Lease & Rental, After Sales

All-in-one ERP

In general or other readymade ERP systems, company either has to adopt the practices in the ERP system (which is not as per company's current practice) or has to customize the solution to its specific needs. An attempt has been made to address all the project management, financial and operational requirements of executing construction and infrastructure projects. It should help one to manage and control the construction projects by giving complete and instant access to its progress with full analysis of costs, revenues, liabilities and subcontractor performance by easily entering the data and getting the relevant reports.

A lot of construction companies use a variety of software in their business, with different programs being used for different tasks. The problem here is that these different programs are usually not well integrated. This can lead to inaccurate records as data entered by one department is not reflected in the records kept by other departments. The answer to these potential nightmares in a construction company office is a fully integrated suite of software which addresses the needs of construction companies Information Technology plays a vital role in Construction industry.

In project execution, bulk of time is taken up by managing an enormous amount of data – site specs, project plans, estimates, contracts, schedules and more. Analysis by various construction software engineers revealed that project managers in the construction industry need software which can help them to manage this data efficiently in order to streamline operations for maximum efficiency and exceeding client expectations. All in one construction software can give company the edge it needs to stay ahead in this fast paced, severely competitive industry.

Like most midsize engineering, construction, and operations (EC&O) companies today, the organization faces many challenges that characterize a volatile and maturing market. These include increased competition, client pressure to provide greater cost and project transparency, slim margins, and demand for flawless project execution. While one search for practical and

affordable ways to meet these challenges, he is constantly looking for new ways to improve the operations and profitability.

To succeed, one must coordinate suppliers, manage a diversified project portfolio, and deal with a project value chain that may be poorly integrated and fraught with manual business process. Plus, one needs to satisfy customer demands for on-time completion, competitive pricing, and innovative solutions.

Recommendations for all-in-one ERP software:

Following are the modules recommended for development of all-in-one ERP system to overcome the lacunas in existing ERP software:

- **Module of Conceptual Planning:** To carry out pre planning of project at conceptual stage to take care of project risks – financial, market, technological, business and other projected by client based on the type of project.
- **Module of Feasibility study and Surveying:** To carry out detailed site survey, soil exploration etc. needed to prepare Techno-economical feasibility report to generate detailed project to minimize errors at later stage in the successful completion of project. Also it should cover various techno-legal requirements and approval checks covering all legal, environmental and other issues in the module.
- **Module of Designing and engineering** – Develop and launch quality, innovative projects faster and more cost-effectively including various functions such as cost estimation, rate analysis from detailed drawings to incorporate changes made in designing at various stages of project. It will save time required to do manual corrections in estimation and tendering documents because of change taken place in drawing and design.
- **Module of Project management with cost and profit control** – Plan and schedule projects and compare project progress to contract cost-effectively. Improve efficiency with a solution that has the functionality to support your business processes. Use of value engineering and reengineering.
- **Module of Safety Management**: ERP needs to take care of safety issues of site, training, punishment and rewards, accident prevention, safety tools, records, to aim at zero accident culture.
- **Module of Machinery Management**: For right selection of equipment for the project activity, best match of equipment, routine and periodical maintenance, life cycle assessment, rent/buy/lease decision etc.
- **Module of Quality Management:** Available ERP systems only include quality checks for various tasks in a project but fail to continual improvement and assessment aiming at total quality management. This module should support all standards such as IS 1200 in Indian context for estimation, IS 456 for RCC design, IS 800 for steel design etc.
- **Module of Supply chain management and Logistic:** to coordinate and integrate resource flow both within and among stake holders, to reduce project inventory (with the assumption that resources are available when needed) in the pipeline.
- **Module of Project Maintenance:** It is one of the important but ignored areas in existing ERP systems. Various processes such as project performance after handover, recording of delays, NRCs, penalties, project maintenance, follow ups, etc. should be taken care of.
- **Module of Claims management & Dispute resolution:** Claims raising and recording, dispute resolution and arbitration in context with tender document needs to be covered in ERP system that is missing from existing ERP modules. It will help save time in dispute handling and claims settlement.
- **Module of Project close out:** For close out planning, customer handover, demobilization of resources and project learnings.
- **Module of Multi project at multi locations:** The system should provide the facility for handling multiple projects from various locations for projects spread over a vast geographic area to easily tract the project status and to optimize the resources.

VII.CONCLUSION

Though ERP has many advantages, there are few disadvantages such as late return on investment, high cost and skilled workforce requirement. Success or failure depends on top management support, planning, training, team contribution, right software selection to suite the organizational structure and needs, and ERP consultant support. Failures were not because the ERP software were coded incorrectly, rather companies failed to match the true organizational needs and systems required to solve the business problems.

It is understood that individual software as well as available ERP software- whether tailor made or readymade has got its own functional limitations. Because of which while developing ERP system, one has to understand all project phases, respective project processes, organizational structure, interlinking between departments and the most appropriate modules to be interlinked in ERP to assure best coordination and communication of information amongst the organization. In the context of TQM, no single software is available. Also, within the individual software, many important functions such as project cost and time control, project inception and closure etc. are not really catered for.

ERP software was found useful as an effective TQM tool subjected to availability of right information such as estimation, quality checks etc. with minimal changes in the due course of commencement of project. Authorities and securities given in ERP help observe better control on successful project progress.

There are lacunas in the existing ERP modules studied, and recommendations were made to develop all-in-one ERP software to best suite the construction processes. It is suggested to develop all-in-one ERP system to accommodate modules such as –Conceptual planning, Feasibility and surveying, Designing, Estimation and Rate analysis, Safety and Quality management, Project maintenance, Claims and Dispute resolution, cost and time control, Machinery management, Multi project multi locations, Supply chain as well as Project closer module.

REFERENCE :

[1] Alan R. Peslak, Enterprise resource planning success An exploratory study of the financial executive perspective, journal of Industrial Management & Data Systems Vol. 106 No. 9, 2006, pp. 1288-1303

[2] Amarolinda Zanela Saccol, Cristiane Drebes Pedron, Silvio Cesar Cazella, Marie Anne Macadar, Guilherme Liberali Neto, University of Vale do Rio Sinos, Sao Leopoldo, Rio Grande do sul: "The impact of ERP systems on organizational strategic variables in Brazilian companies", pp. 1-10

[3] Boo Young Chung, "An Analysis of success & Failure Factors ERP Systems in Engineering & Construction Firms, pp. 1-218

[4] Boo Young Chung, Miroslaw J. Skibniewski & Young Hoon Kwak "Developing ERP Systems Success Model for the Construction Industry" Journal of Construction Engineering & Management, ACSE, March 2009, pp. 207-216

[5] Boo Young Chung, Miroslaw J. Skibniewski, Henry C. Lucas Jr. & Young Hoon Kwak: "Analyzing Enterprise Resource Planning System Implementation Success Factors in the Engineering-Construction Industry", Journal of Computing in Civil Engineering, ASCE, Nov/Dec 2008, pp. 373-282

[6] Carl Marnewick & Lessing Labuschange, "A conceptual model for enterprise resource planning (ERP)", Information Management & Computer Security

[7] Elbanna, Amany, "The Construction of the relationship between ERP and the organization through negotiation", pp. 1-13

[8] Ike C. Ehie, Mogens Madsen: "Identifying critical issues in enterprise resource planning (ERP) implementation", Science direct, pp. 545-557

[9] Ike C. Ehie, Mogens Madsen: "Identifying Critical issues in enterprise resource planning (ERP) implementation", Computers in Industry 56 (2005), pp. 545-557

[10] Jha V S and Joshi H. "Relevance of TQM or Business Excellence Strategy Implementation for ERP – A Conceptual Study", pp. 1 to 11

Transit Scheduling: "A Case Study of Eastern Ring Road Corridor of BRTS Indore"

H. S. Goliya[1] & Vikram Singh Patel[2]

[1]CE-AMD, SGSITS Indore , MP, India
[2]ME Transportation Engineering, CE-AMD, SGSITS Indore, MP, India

Abstract - Indore is a fast growing industrial city of Madhya Pradesh. To meet the large demand and improve the capacity and productivity of buses, ICTSL has proposed to plan, to develop and operate Bus Rapid Transit System (BRTS) in Indore. Bus Rapid Transit System is a new form of public transportation which is an emerging approach to using buses as an improved high-speed transit system. Bus Rapid Transit involves coordinated improvements in a transit system's infrastructure, equipment, operations, and technology that give preferential treatment to buses on urban roadways. We are selecting eastern ring road corridor for our case study of transit scheduling now a day's eastern area of Indore is developing rapidly. To provide faster and effective transit services, I make schedule for transit units going to be run on that route. The schedule is made for 14 hours in a day (7:00 AM To 09 PM). For finding out schedule of transit units, traffic data are collected at different road sections along the route. The traffic data is then analyzed and traffic flow and passenger flow along the route is taken out. Transit units are provided on the basis of passenger flow at different sections and at different time within a day.

Key words *- BRTS, Scheduling, Transit Scheduling, Dwell Time.*

I. INTRODUCTION

Indore is a fast growing industrial city of Madhya Pradesh. It is the only metropolitan city in the state, with a growth rate of 32.7% in the last decade. Its population size was 1.6 million in 2001, 2.2 million in 2011 and is projected to be 4.2 million by 2025. Planning, development, operation and management of the transport system of Indore to meet the increasing travel demands of the city in an efficient, convenient, safe and economical manner is important to sustain the economic viability, productivity and competitiveness of Indore City. To meet the large demand and improve the capacity and productivity of buses, ICTSL has proposed to plan, to develop and operate Bus Rapid Transit System (BRTS) in Indore.

In the context of rapid growth of the city, increasing mobility, high travel demand, increasing congestion, delays, accidents, need for conservation of energy, growing community consciousness towards environmental quality and to address a host of such other problems and objectives, public mass transport system of the city stands out as the most critical element. It needs to be rationally planned, efficiently operated and diligently managed to be effective and productive by itself and in turn enable the city to be productive and competitive.

A. Concept of Bus Rapid Transit System

Bus Rapid Transit System is a new form of public transportation which is an emerging approach to using buses as an improved high-speed transit system. Bus Rapid Transit involves coordinated improvements in a transit system's infrastructure, equipment, operations, and technology that give preferential treatment to buses on urban roadways

B. Need for Present Study

In the context of rapid growth of the Indore city, increasing mobility, high travel demand, increasing congestion, delays, accidents, need for conservation of energy, growing community consciousness towards environmental quality and to address a host of such other problems and objectives, public mass transport system of the city stands out as the most critical element. It needs to be rationally planned, efficiently operated and diligently managed to be effective and productive by itself and in turn enable the city to be productive and competitive.

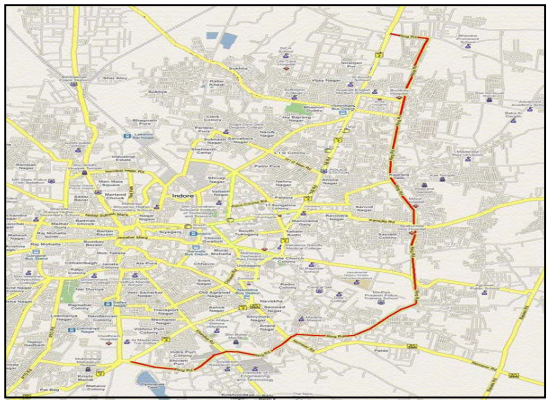

Fig. 1 : Eastern Ring Road Corridor of BRTS Indore

II. OBJECTIVES OF THE STUDY

- To find out the traffic volume of selected route.
- To find out number of buses.
- To schedule the arrival and departure time of buses at stops.
- To reduce the traffic congestion.
- To improve the traffic management in the city .
- To popularize public transport and reduce the dependability over private vehicles.

III. METHODOLOGY

The case study is carried out on a predefined route, eastern ring road corridor of BRTS Indore. In this case, traffic data are collected from the field and then analysis is done to find out passenger flow in between the sections on the basis of which number of transit units are taken out and scheduling is done for them for 14 hours. (07 AM TO 09 PM).

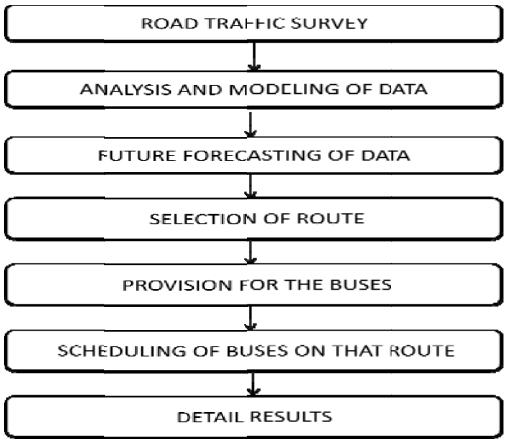

IV. EASTERN RING ROAD CORRIDOR OF BRTS INDORE

Eastern ring road corridor of BRTS offers a fast and non-interrupted transportation facility to the road users. Eastern ring road lies in between the A.B. road and By Pass road of Indore. Starting from Rajiv Gandhi Square to Dewas naka Square (Niranjanpur). It carries a major part of traffic of eastern part of Indore. And the traffic is likely to be increased in future. The growth rate of the area near it is very high, and so many development schemes are going on.

DETAIL INFORMATION OF ROAD

Name of road : Eastern Ring Road Corridor.

Total Length of road: 15.40 km.

Four arm intersection of road: 10 No.

Rotary at road intersection: 09 No.

V. TRAFFIC SURVEY AND DATA COLLECTION

Data collection comprises of primary data and secondary data. Primary data was collected from primary surveys and secondary data is collected from various sources such as libraries, internet websites, and from some of the organizations concerned with BRTS such as CEPT Ahmadabad, CRRI, TRB, HCM etc

The Data collection comprises of selection of the case study BRT corridor, basic details of the corridor, locations of the major intersections on the corridor, primary survey locations on the corridor route map, list of primary surveys conducted, inferences drawn from the primary surveys and impact parameters identified for the case study. Primary data has been collected from primary surveys carried out on the pilot BRTS corridor for three days at each section for pre BRT and post BRT situations. Secondary data such as literatures, maps, previous studies, various BRT studies carried out worldwide, from various literatures and international case studies from journals and internet are collected.

VI. DATA ANALYSIS

Data analysis is a process of gathering, modelling, and transforming data with the goal of highlighting useful information, suggesting conclusions, and supporting decision making.

Primary data was collected from various traffic and travel surveys along the proposed BRTS corridor and analyzed with traffic engineering parameters.

Traffic impact parameters were identified in broad such as traffic characteristics, speed, travel characteristics, etc and analyzed as per traffic engineering techniques and compared at different sections of the corridor with the present and past study.

VII. TRAFFIC FLOW STUDY

Here, traffic flow study was carried out for at ten mid sections, located between all major intersections of the corridor. The surveys were conducted during morning; noon and evening hours between 9:00am to 11:00am, 01pm to 03pm and 05pm to 08pm and finally the numbers in peak hours are represented. Manual Count and Video Graphic technique was applied, using video cameras focusing the running traffic on the corridor from the appropriate level. Analysis is carried out for the traffic flow characteristics, vehicular traffic composition of all modes types, peak hour and off-peak hours traffic, PCUs, etc. Traffic Data, traffic composition, hourly traffic volume, hourly variation of traffic flow, traffic comparison chart, and hourly variation of passenger flow on BRTS etc. are shown on below tables, charts and graphs of the Rajiv Gandhi Square to Khandawa Naka Square section of eastern ring road corridor of BRTS.

.

RAJIV GANDHI SQUARE:

Table 1 : Showing Traffic Flow From Rajiv Gandhi Square To Khandawa Naka Square

Date : Average Traffic 02-04 May

Location : Rajiv Gandhi Square TO Khandwa Naka Square

Survey Carried By : Rajiv Gandhi Square TO Khandwa

Type of vehicle	08 to 09 AM	09 To 10 AM	10 To 11 AM	01 To 02 PM	02 To 03 PM	05 To 06 PM	06 To 07 PM	07 To 08 PM	Total
Truck (multi axel)	11	23	32	48	35	64	75	52	340
Truck	24	57	73	70	58	70	82	83	517
Tractor	2	8	6	4	2	2	4	3	31
Loading Rikshaw/Pickup	52	88	75	63	51	52	64	37	482
Bus	10	14	9	15	12	21	27	17	125
Omni/Magic (Public Trans.)	12	19	14	11	7	9	7	10	89
Auto/Taxi	9	17	21	19	13	17	15	24	135
Four Wheeler (Car/Jeep)	139	195	181	161	143	142	157	167	1285
Two Wheeler	657	853	777	590	545	588	645	540	5195
Total No .of Vehicles	916	1274	1188	961	866	965	1076	933	

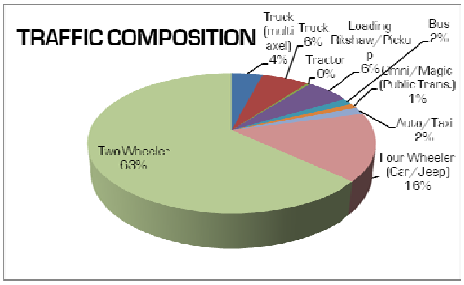

Fig. 2 : Showing Traffic Composition

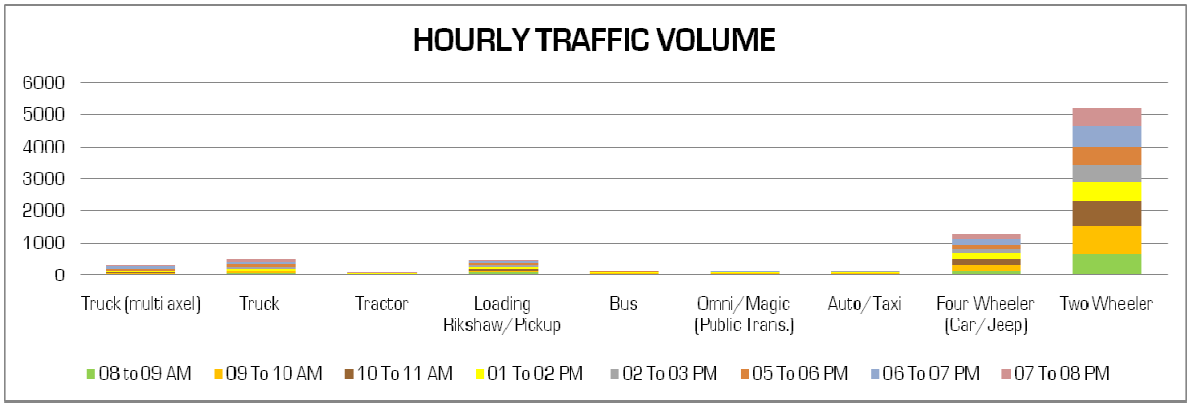

Fig. 3 : Showing Hourly Traffic Volume

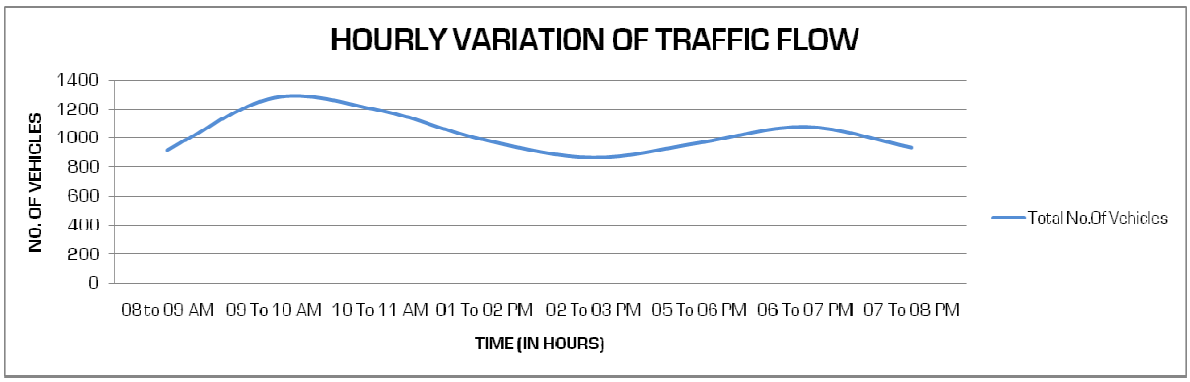

Fig. 4 : Showing Hourly Variation of Traffic Flow

Total Goods Transportation	99	190	195	200	158	209	252	192	1495
Total Public Transport	817	1084	993	781	708	756	824	741	6704

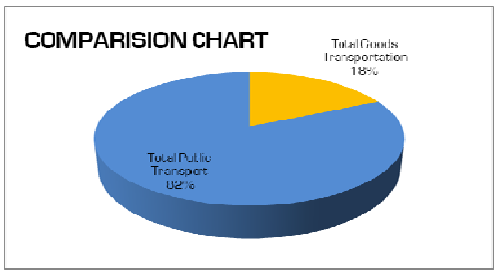

Fig. 5 : Comparison Chart

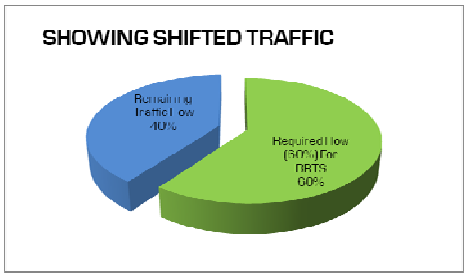

Fig. 6 : Showing Shifted Traffic

Provision for Public Transportation									
Required Flow (60%) For BRTS	490.2	650.4	595.8	468.6	424.8	453.6	494.4	444.6	4022.4
Remaining Traffic Flow	326.8	433.6	397.2	312.4	283.2	302.4	329.6	296.4	2681.6

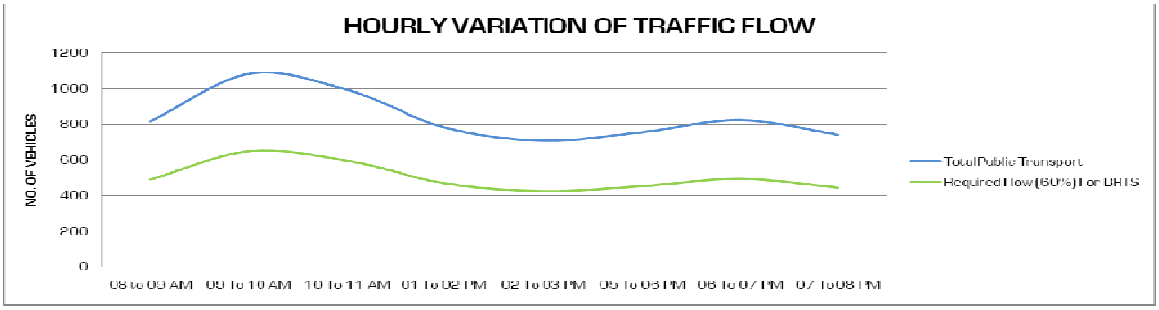

Fig. 7 : Showing Hourly Variation of Traffic Flow

Table 2. Showing Passenger Flow From Rajiv Gandhi Square To Khandawa Naka Square

Passenger Flow									
No. of Passenger	08 to 09 AM	09 To 10 AM	10 To 11 AM	01 To 02 PM	02 To 03 PM	05 To 06 PM	06 To 07 PM	07 To 08 PM	Total
Omni/ Magic (Public Trans.)	48	76	56	44	28	36	28	40	356
Auto/ Taxi	22.5	42.5	52.5	47.5	32.5	42.5	37.5	60	337.5
Four Wheeler (Car/ Jeep)	417	585	543	483	429	426	471	501	3855
Two Wheeler	985.5	1279.5	1165.5	885	817.5	882	967.5	810	7792.5
Total No. Of Passenger	1473	1983	1817	1459.5	1307	1386.5	1504	1411	
Passenger Flow on BRTS (60%)	883.8	1189.8	1090.2	875.7	784.2	831.9	902.4	846.6	7404.6

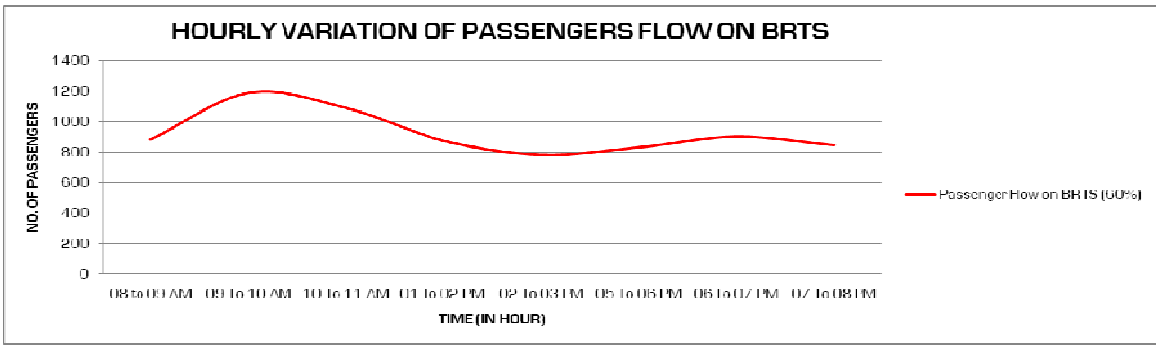

Fig. 8 : Showing Hourly Variation of Passenger Flow on BRTS

The traffic data shown here is of one intersection only. In the same manner, traffic flow and passenger flow is taken out at each intersection. The above traffic data, traffic composition, hourly traffic volume, hourly variation of traffic flow, traffic comparison chart, and hourly variation of passenger flow on BRTS etc. shown on tables, charts and graphs of the different road sections of eastern ring road corridor of BRTS, gives us the peak hour passenger flow at different intersections, which is required by us for deciding the number of buses to be run at different time on the eastern ring road corridor of BRTS.

With the help of this graph we get the traffic composition at different sections, hourly variation of traffic flow at road section in between the different intersections, at different time period of day. From the above data we get the hourly variation of traffic flow and passenger flow in between the sections of different nodes on the BRTS corridor.

A. Peak Hour and Off-Peak Graphs

The peak hour and off-peak hour passenger flow graph (Figure 09 and 10) shows the flow of passenger at the particular intersection at the specified time and at the specified time interval within a day. With the help of this we can find out number of buses required for the transportation on the BRTS corridor.

Peak Hour Passenger Flow

- Between 10am – 11 am
- Between 06 pm – 07 pm

Off-Peak hour Passenger Flow

- Between 02 pm – 03 pm

Table 3 : Showing Peak and Off peak Hour Traffic Flow

Location	Rajiv Gandhi To Dewas Naka		
Name Of Intersection	10 To 11 AM	02 TO03 PM	06 To 07 PM
Rajiv Gandhi Square	1090	784	902
Khandawa Naka Square	1712	1303	1455
Teenimli Square	1374	835	1267
Musakhedi Square	1061	850	1347
Pipliyapala Square	1471	942	1251
Bengali Square	2082	1525	1792
Khazarana Square	2822	1899	2348
MR-9 Square	2766	1746	1388
Bombay Hospital Square	1017	702	600
Dewas naka Square	679	538	443
Niranjanpur Square			

Table 4 : Showing Peak and Off peak Hour Traffic Flow

Location	Rajiv Gandhi To Dewas Naka		
Name Of Intersection	10 To 11 AM	02 TO03 PM	06 To 07 PM
Rajiv Gandhi Square	1090	784	902
Khandawa Naka Square	1712	1303	1455
Teenimli Square	1374	835	1267
Musakhedi Square	1061	850	1347
Pipliyapala Square	1471	942	1251
Bengali Square	2082	1525	1792
Khazarana Square	2822	1899	2348
MR-9 Square	2766	1746	1388
Bombay Hospital Square	1017	702	600
Dewas naka Square	679	538	443
Niranjanpur Square			

VIII. THE SCHEDULING

Scheduling a set of processes consists of sequencing them on one or more processors such that the utilization of resources optimizes some scheduling criterion. Scheduling is traditionally performed statically, off-line, while in an operating system, the information from which scheduling decisions must be made is dynamic, suggesting that the best scheduling decisions should be made dynamically.

Transit system run on specified routes and schedules. A schedule is a statement of times at which transit unit arrives at particular stop over a period of time. It is also the statement of time at which a single transit unit of a given route arrives at different stops on its route. The later information can always be derived once the schedule of arrivals and departures of all the stops are known.

A. Scheduling Policies

For a practical real-time operating system, it is necessary to provide a mechanism to express the application-defined scheduling policies needed to implement our scheduling model; the system should be able to modify these policies at runtime in order to take advantage of the flexibility of the model.

B. The Transit Scheduling

Another optimization problem related to the transit system design is the scheduling of transit units (say buses). The problem here is that given a set of routes, one needs to develop schedules for bus arrivals and departures at all the stops of the network. A good or efficient schedule is one which minimizes the waiting time of passengers while operating within a set of resource and service related constraints.

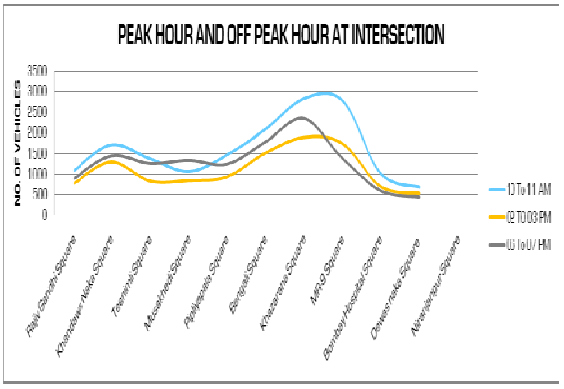

Fig. 9 : Showing Peak Hour and Off Peak Hour Passenger Flow at Intersection

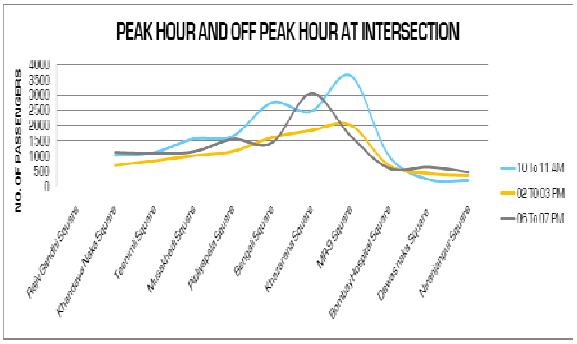

Fig. 10 : Showing Peak Hour and Off Peak Hour Passenger Flow At Intersection

IX. DWELL TIME

Dwell time is the single most important factor affecting vehicle capacity. It is the time required to serve passengers at the busiest door, plus the time required to open and close the doors.

Dwell times may be governed by boarding demand and the alighting demand or by total interchanging passenger demand (e.g., at a major transfer point on the system). In all cases, dwell time is proportional to the boarding and/or alighting volumes times the service time per passenger.

X. SCHEDULE DETERMINATION OF EASTERN RING ROAD CORRIDOR FOR BUS TRANSIT RAPID SYSTEM:

Table 5. For Schedule Determination

Sr. No	Name Of Stop	Distance (km)	Dwell Time	Travel Time Required
1	Rajiv Gandhi Square	–	2 min	-
2	Bholaram Ustad Marg Square	0.6	2 min	0 min 40 sec
3	Khandawa Naka Square	1.4	2 min	1 min 40 sec
4	Teenimli Square	1.8	2 min	1 min 40 sec
5	Musakhedi Square	1.8	2 min	2 min 10 sec
6	Pipliyapala Square	1.7	2 min	2 min 10 sec
7	Bengali Square	1.4	3 min	2 min 00 sec
8	Khazarana Square	1.1	3 min	1 min 40 sec
9	MR-9 Square	0.9	3 min	1 min 20 sec
10	MR-10 Square	2	2 min	1 min 00 sec
11	Bombay Hospital Square	0.5	2 min	0 min 40 sec
12	Dewas naka Square	2	2 min	2 min 20 sec
13	Niranjanpur Square	0.9	2 min	1 min 00 sec

- Total Length Of The Route 15.5 km
- Round Trip Time Of Transit Unit 90 minute
- Running Speed Of Transit Unit 50 km/hr
- Journey Speed Of Transit Unit 35km/hr
- The Peak hour headway between the buses is 4 minute
- Off Peak hour headway between the buses is 6 minute

The Schedule of off- peak hour and -peak hour is given below in the tables for the buses travelling from Rajiv Gandhi Square to Niranjanpur Square. The schedule is developed from 07 am to 09 pm along the route.

Some buses are introduced into the route from other routes at the time of peak hours, to accommodate the passenger traffic at the stop and to maintain the BRTS facility.

XI. CONCLUSION:

- The route is analyzed and transit units are provided on the basis of passenger traffic flow along sections on the route.
- Schedule is developed on the bases of their departure time.
- 16 transit units are required to run along the route, continuously throughout the day.
- Additional 34 transit units are required to accommodate the peak hour traffic at some specified sections of the route.
- 60 % of passenger traffic is travelling through the BRTS.
- Traffic congestion is reduced on the route, as two wheeler and four wheeler traffic is getting shifted on BRTS.
- Well managed traffic system has been designed along the route.
- Public transport get popularize and reduce the dependability over private vehicles.

REFERENCES:

[1] E. Douglas Jensen, C. Douglass Locke, Hideyuki Tokuda (1985): "A Time-Driven Scheduling Model for Real-Time Operating Systems", CH2220-2/85/OOOO/011, 1985 (IEEE)

[2] Liping Fu, Qing Liu, and Paul Calamai (2003): "Real-Time Optimization Model for Dynamic Scheduling of Transit Operations", Transportation Research Record 1857, *Paper No. 03-3697*

[3] Michael G. H. Bell (2004): "Games, Heuristics, and Risk Averseness in Vehicle Routing Problems", Vol. 130, No. 1, March 1, 2004 J. URBAN PLANNING & DEVELOPMENT, ASCE

[4] Liqun Xu (2005): "A Decision Support Model Based on GIs for Vehicle Routing", 0-7803-897 1 - 9/05, 2005 (IEEE)

[5] Qiang Meng, Der-Horng Lee and Ruey Long Cheu (2005): "Multiobjective Vehicle Routing and Scheduling Problem with Time Window Constraints in Hazardous Material Transportation", Vol. 131, No. 9, September 1, 2005. Journal of Transportation Engineering, ASCE,

[6] Jian Sun, Shikui Zhai, Shuying Wang (2010): "Research and Application of Solution of Vehicle Routing Problem Based on GIS", 2010 Sixth International Conference on Natural Computation (ICNC 2010), 978-1-4244-5961-2/10, 2010 IEEE

[7] Gong Yancheng (2010): "Vehicle Scheduling Problems of Military Logistics Distribution Based on Improved Genetic Algorithm", International Conference on Computer Application and System Modeling (ICCASM), 2010

[8] Ming Wei, Wenzhou Jin, Weiwei FU, HAO Xiao-ni (2010): "Improved Ant Colony Algorithm for Multi-depot Bus Scheduling Problem with Route Time Constraints", World Congress on Intelligent Control and Automation, 978-1-4244-6712-9/10, 2010 IEEE

[9] Transit cooperative Research Program "TCRP REPORT 90" Bus Rapid Transit V*olume 1: Case Studies In Bus Rapid Transit*

[10] Transit Cooperative Research Program "TCRP REPORT 90" Bus Rapid Transit V*olume 2: Implementation Guidelines*

[11] Parth Chakroborty and Animesh Das "Principles of Transportation Engineering"

[12] "Traffic Engineering and Transportation Planning" Dr. L.R. Kadiyali.

[13] Indore Muncipal Corporation, indore

[14] Indore city transport service limited, indore

[15] CEPT Ahamdabad.

Table 6 : Showing Schedule From 07 AM To 09 AM Travelling Direction from Rajiv Gandhi Square To Niranjanpur Square.

07 AM TO09 AM													
Sr. No.	1	2	3	4	5	6	7	8	9	10	11	12	13
Time Required		00:00:40	00:01:40	00:01:40	00:02:10	00:02:10	00:02:00	00:01:40	00:01:20	00:01:00	00:00:40	00:02:20	00:01:00
Dwell Time		00:02:00	00:02:00	00:02:00	00:02:00	00:02:00	00:03:00	00:03:00	00:03:00	00:02:00	00:02:00	00:02:00	00:02:00
Bus No. 01	07:00:00	07:02:40	07:06:20	07:10:00	07:14:10	07:18:20	07:23:20	07:28:00	07:32:20	07:35:20	07:38:00	07:42:20	07:45:20
Bus No. 02	07:06:00	07:08:40	07:12:20	07:16:00	07:20:10	07:24:20	07:29:20	07:34:00	07:38:20	07:41:20	07:44:00	07:48:20	07:51:20
Bus No. 03	07:12:00	07:14:40	07:18:20	07:22:00	07:26:10	07:30:20	07:35:20	07:40:00	07:44:20	07:47:20	07:50:00	07:54:20	07:57:20
Bus No. 04	07:18:00	07:20:40	07:24:20	07:28:00	07:32:10	07:36:20	07:41:20	07:46:00	07:50:20	07:53:20	07:56:00	08:00:20	08:03:20
Bus No. 05	07:24:00	07:26:40	07:30:20	07:34:00	07:38:10	07:42:20	07:47:20	07:52:00	07:56:20	07:59:20	08:02:00	08:06:20	08:09:20
Bus No. 06	07:30:00	07:32:40	07:36:20	07:40:00	07:44:10	07:48:20	07:53:20	07:58:00	08:02:20	08:05:20	08:08:00	08:12:20	08:15:20
Bus No. 07	07:36:00	07:38:40	07:42:20	07:46:00	07:50:10	07:54:20	07:59:20	08:04:00	08:08:20	08:11:20	08:14:00	08:18:20	08:21:20
Bus No. 08	07:42:00	07:44:40	07:48:20	07:52:00	07:56:10	08:00:20	08:05:20	08:10:00	08:14:20	08:17:20	08:20:00	08:24:20	08:27:20
Bus No. 09	07:48:00	07:50:40	07:54:20	07:58:00	08:02:10	08:06:20	08:11:20	08:16:00	08:20:20	08:23:20	08:26:00	08:30:20	08:33:20
Bus No. 10	07:54:00	07:56:40	08:00:20	08:04:00	08:08:10	08:12:20	08:17:20	08:22:00	08:26:20	08:29:20	08:32:00	08:36:20	08:39:20
Bus No. 11	08:00:00	08:02:40	08:06:20	08:10:00	08:14:10	08:18:20	08:23:20	08:28:00	08:32:20	08:35:20	08:38:00	08:42:20	08:45:20
Bus No. 12	08:06:00	08:08:40	08:12:20	08:16:00	08:20:10	08:24:20	08:29:20	08:34:00	08:38:20	08:41:20	08:44:00	08:48:20	08:51:20
Bus No. 13	08:12:00	08:14:40	08:18:20	08:22:00	08:26:10	08:30:20	08:35:20	08:40:00	08:44:20	08:47:20	08:50:00	08:54:20	08:57:20
Bus No. 14	08:18:00	08:20:40	08:24:20	08:28:00	08:32:10	08:36:20	08:41:20	08:46:00	08:50:20	08:53:20	08:56:00	09:00:20	09:03:20
Bus No. 15	08:24:00	08:26:40	08:30:20	08:34:00	08:38:10	08:42:20	08:47:20	08:52:00	08:56:20	08:59:20	09:02:00	09:06:20	09:09:20
Bus No. 16	08:30:00	08:32:40	08:36:20	08:40:00	08:44:10	08:48:20	08:53:20	08:58:00	09:02:20	09:05:20	09:08:00	09:12:20	09:15:20
Bus No. 01	08:36:00	08:38:40	08:42:20	08:46:00	08:50:10	08:54:20	08:59:20	09:04:00	09:08:20	09:11:20	09:14:00	09:18:20	09:21:20
Bus No. 02	08:42:00	08:44:40	08:48:20	08:52:00	08:56:10	09:00:20	09:05:20	09:10:00	09:14:20	09:17:20	09:20:00	09:24:20	09:27:20
Bus No. 03	08:48:00	08:50:40	08:54:20	08:58:00	09:02:10	09:06:20	09:11:20	09:16:00	09:20:20	09:23:20	09:26:00	09:30:20	09:33:20
Bus No. 04	08:54:00	08:56:40	09:00:20	09:04:00	09:08:10	09:12:20	09:17:20	09:22:00	09:26:20	09:29:20	09:32:00	09:36:20	09:39:20
Bus No. 05	09:00:00	09:02:40	09:06:20	09:10:00	09:14:10	09:18:20	09:23:20	09:28:00	09:32:20	09:35:20	09:38:00	09:42:20	09:45:20

Table 7 : Showing Schedule From 09 AM To 10 AM Travelling Direction from Rajiv Gandhi Square To Niranjanpur Square.

09 AM To 10 AM													
Stop No.	1	2	3	4	5	6	7	8	9	10	11	12	13
Transfer Time		00:00:40	00:01:40	00:01:40	00:02:10	00:02:10	00:02:00	00:01:40	00:01:20	00:01:00	00:00:40	00:02:20	00:01:00
Dwell Time		00:02:00	00:02:00	00:02:00	00:02:00	00:02:00	00:03:00	00:03:00	00:03:00	00:02:00	00:02:00	00:02:00	00:02:00
Bus No. 831								09:18:00	09:22:20	09:25:20			
Bus No. 731							09:15:20	09:20:00	09:24:20				
Bus No. 631						09:14:20	09:19:20	09:24:00					
Bus No. 05	09:00:00	09:02:40	09:06:20	09:10:00	09:14:10	09:18:20	09:23:20	09:28:00	09:32:20	09:35:20	09:38:00	09:42:20	09:45:20
Bus No. 832								09:30:00	09:34:20	09:37:20			
Bus No. 06	09:04:00	09:06:40	09:10:20	09:14:00	09:18:10	09:22:20	09:27:20	09:32:00	09:36:20	09:39:20	09:42:00	09:46:20	09:49:20
Bus No. 07	09:08:00	09:10:40	09:14:20	09:18:00	09:22:10	09:26:20	09:31:20	09:36:00	09:40:20	09:43:20	09:46:00	09:50:20	09:53:20
Bus No. 131			09:16:20	09:20:00	09:24:10	09:28:20	09:33:20	09:38:00	09:42:20	09:45:20			
Bus No. 08	09:12:00	09:14:40	09:18:20	09:22:00	09:26:10	09:30:20	09:35:20	09:40:00	09:44:20	09:47:20	09:50:00	09:54:20	09:57:20
Bus No. 732							09:37:20	09:42:00	09:46:20	09:49:20			
Bus No. 09	09:16:00	09:18:40	09:22:20	09:26:00	09:30:10	09:34:20	09:39:20	09:44:00	09:48:20	09:51:20	09:54:00	09:58:20	10:01:20
Bus No. 632						09:36:20	09:41:20	09:46:00	09:50:20	09:53:20			
Bus No. 10	09:20:00	09:22:40	09:26:20	09:30:00	09:34:10	09:38:20	09:43:20	09:48:00	09:52:20	09:55:20	09:58:00	10:02:20	10:05:20
Bus No. 833								09:50:00	09:54:20	957:20:00			
Bus No. 12	09:24:00	09:26:40	09:30:20	09:34:00	09:38:10	09:42:20	09:47:20	09:52:00	09:56:20	09:59:20	10:02:00	10:06:20	10:09:20
Bus No. 132			09:32:20	09:36:00	09:40:10	09:44:20	09:49:20	09:54:00	09:58:20	10:01:20			
Bus No. 13	09:28:00	09:30:40	09:34:20	09:38:00	09:42:10	09:46:20	09:51:20	09:56:00	10:00:20	10:03:20	10:06:00	10:10:20	10:13:20
Bus No. 14	09:32:00	09:34:40	09:38:20	09:42:00	09:46:10	09:50:20	09:55:20	10:00:00	10:04:20	10:07:20	10:10:00	10:14:20	10:17:20
Bus No. 834								10:02:00	10:06:20	10:09:20			
Bus No. 15	09:36:00	09:38:40	09:42:20	09:46:00	09:50:10	09:54:20	09:59:20	10:04:00	10:08:20	10:11:20	10:14:00	10:18:20	10:21:20
Bus No. 733							10:01:20	10:06:00	10:10:20	10:13:20			
Bus No. 16	09:40:00	09:42:40	09:46:20	09:50:00	09:54:10	09:58:20	10:03:20	10:08:00	10:12:20	10:15:20	10:18:00	10:22:20	10:25:20
Bus No. 835								10:10:00	10:14:20				
Bus No. 01	09:44:00	09:46:40	09:50:20	09:54:00	09:58:10	10:02:20	10:07:20	10:12:00	10:16:20	10:19:20	10:22:00	10:26:20	10:29:20
Bus No. 133			09:52:20	09:56:00	10:00:10	10:04:20	10:09:20	10:14:00	10:18:20				
Bus No. 02	09:48:00	09:50:40	09:54:20	09:58:00	10:02:10	10:06:20	10:11:20	10:16:00	10:20:20	10:23:20	10:26:00	10:30:20	10:33:20
Bus No. 836								10:18:00	10:22:20	10:25:20			
Bus No. 03	09:52:00	09:54:40	09:58:20	10:02:00	10:06:10	10:10:20	10:15:20	10:20:00	10:24:20	10:27:20	10:30:00	10:34:20	10:37:20
Bus No. 734							10:17:20	10:22:00	10:26:20				
Bus No. 04	09:56:00	09:58:40	10:02:20	10:06:00	10:10:10	10:14:20	10:19:20	10:24:00	10:28:20	10:31:20	10:34:00	10:38:20	10:41:20
Bus No. 837								10:25:00	10:29:20	10:32:20			
Bus No. 633						10:16:20	10:21:20	10:26:00	10:30:20	10:33:20			
Bus No. 05	10:00:00	10:02:40	10:06:20	10:10:00	10:14:10	10:18:20	10:23:20	10:28:00	10:32:20	10:35:20	10:38:00	10:42:20	10:45:20

Table 8 : Showing Schedule From 01 PM To 03 PM Travelling Direction from Rajiv Gandhi Square To Niranjanpur Square

01 PM TO 03 PM													
Sr. No.	1	2	3	4	5	6	7	8	9	10	11	12	13
Time Required		00:00:40	00:01:40	00:01:40	00:02:10	00:02:10	00:02:00	00:01:40	00:01:20	00:01:00	00:00:40	00:02:20	00:01:00
Dwell Time		00:02:00	00:02:00	00:02:00	00:02:00	00:02:00	00:03:00	00:03:00	00:03:00	00:02:00	00:02:00	00:02:00	00:02:00
Bus No. 09	01:00:00	01:02:40	01:06:20	01:10:00	01:14:10	01:18:20	01:23:20	01:28:00	01:32:20	01:35:20	01:38:00	01:42:20	01:45:20
Bus No. 10	01:06:00	01:08:40	01:12:20	01:16:00	01:20:10	01:24:20	01:29:20	01:34:00	01:38:20	01:41:20	01:44:00	01:48:20	01:51:20
Bus No. 11	01:12:00	01:14:40	01:18:20	01:22:00	01:26:10	01:30:20	01:35:20	01:40:00	01:44:20	01:47:20	01:50:00	01:54:20	01:57:20
Bus No. 12	01:18:00	01:20:40	01:24:20	01:28:00	01:32:10	01:36:20	01:41:20	01:46:00	01:50:20	01:53:20	01:56:00	02:00:20	02:03:20
Bus No. 13	01:24:00	01:26:40	01:30:20	01:34:00	01:38:10	01:42:20	01:47:20	01:52:00	01:56:20	01:59:20	02:02:00	02:06:20	02:09:20
Bus No. 14	01:30:00	01:32:40	01:36:20	01:40:00	01:44:10	01:48:20	01:53:20	01:58:00	02:02:20	02:05:20	02:08:00	02:12:20	02:15:20
Bus No. 15	01:36:00	01:38:40	01:42:20	01:46:00	01:50:10	01:54:20	01:59:20	02:04:00	02:08:20	02:11:20	02:14:00	02:18:20	02:21:20
Bus No. 16	01:42:00	01:44:40	01:48:20	01:52:00	01:56:10	02:00:20	02:05:20	02:10:00	02:14:20	02:17:20	02:20:00	02:24:20	02:27:20
Bus No. 01	01:48:00	01:50:40	01:54:20	01:58:00	02:02:10	02:06:20	02:11:20	02:16:00	02:20:20	02:23:20	02:26:00	02:30:20	02:33:20
Bus No. 02	01:54:00	01:56:40	02:00:20	02:04:00	02:08:10	02:12:20	02:17:20	02:22:00	02:26:20	02:29:20	02:32:00	02:36:20	02:39:20
Bus No. 03	02:00:00	02:02:40	02:06:20	02:10:00	02:14:10	02:18:20	02:23:20	02:28:00	02:32:20	02:35:20	02:38:00	02:42:20	02:45:20
Bus No. 04	02:06:00	02:08:40	02:12:20	02:16:00	02:20:10	02:24:20	02:29:20	02:34:00	02:38:20	02:41:20	02:44:00	02:48:20	02:51:20
Bus No. 05	02:12:00	02:14:40	02:18:20	02:22:00	02:26:10	02:30:20	02:35:20	02:40:00	02:44:20	02:47:20	02:50:00	02:54:20	02:57:20
Bus No. 06	02:18:00	02:20:40	02:24:20	02:28:00	02:32:10	02:36:20	02:41:20	02:46:00	02:50:20	02:53:20	02:56:00	03:00:20	03:03:20
Bus No. 07	02:24:00	02:26:40	02:30:20	02:34:00	02:38:10	02:42:20	02:47:20	02:52:00	02:56:20	02:59:20	03:02:00	03:06:20	03:09:20
Bus No. 08	02:30:00	02:32:40	02:36:20	02:40:00	02:44:10	02:48:20	02:53:20	02:58:00	03:02:20	03:05:20	03:08:00	03:12:20	03:15:20
Bus No. 09	02:36:00	02:38:40	02:42:20	02:46:00	02:50:10	02:54:20	02:59:20	03:04:00	03:08:20	03:11:20	03:14:00	03:18:20	03:21:20
Bus No. 10	02:42:00	02:44:40	02:48:20	02:52:00	02:56:10	03:00:20	03:05:20	03:10:00	03:14:20	03:17:20	03:20:00	03:24:20	03:27:20
Bus No. 11	02:48:00	02:50:40	02:54:20	02:58:00	03:02:10	03:06:20	03:11:20	03:16:00	03:20:20	03:23:20	03:26:00	03:30:20	03:33:20
Bus No. 12	02:54:00	02:56:40	03:00:20	03:04:00	03:08:10	03:12:20	03:17:20	03:22:00	03:26:20	03:29:20	03:32:00	03:36:20	03:39:20
Bus No. 13	03:00:00	03:02:40	03:06:20	03:10:00	03:14:10	03:18:20	03:23:20	03:28:00	03:32:20	03:35:20	03:38:00	03:42:20	03:45:20

◈◈◈

4D Modeling and Virtual Prototyping in Construction

Col. S. Gopikrishnan

Military Engineer Services, Commander Works Engineers (Army), Colaba, Mumbai, India

Abstract **-** 3D modeling has been in vogue for decades. Development in hardware and software continue to bring better and less expensive 3D computing capabilities to designers, architects and constructors. A fourth dimension is added to animate the construction sequence and produce 4D computer modeling. It integrates three dimensional CAD drawings with a fourth dimension, time to improve co ordination, communication and development of construction projects. This process enhances the capabilities of engineers to visualize the problem areas and iron out kinks. It also reduces the co ordination problems at ground level between the executive staff and the contractors. 4D modeling can be used for new construction projects as well as retrofitting/reconstruction.

Virtual Prototyping is a computer aided design process concerned with construction of digital project modules (virtual prototypes) and realistic graphic simulations that addresses the issues of physical layout, operational concepts, functional specifications and dynamic analysis under various operating environments. Virtual Prototyping technology is the latest and effective way of envisaging real circumstances that enhance effective communication of design and ideas. Whereas a large number of digital technologies have been developed to visualize innovative architectural design, very few have been developed to facilitate integral planning and visualization of construction plans of building projects. The construction virtual prototyping (CVP) system allows the project teams to check constructability, safety and to visualize 3D models for a facility before commencement of construction. Virtual prototyping makes a 4D model more complete by visualizing variables.

This paper analyzes 4D modeling and construction visual prototyping (CVP) system for their application in planning and execution of large scale and complex construction projects.

Key words - *4D Modeling, Virtual Prototyping, Building Information model.*

I. INTRODUCTION

During the formulation of a complete construction schedule, planners and site managers are required to simulate various construction processes, required to build the project. Computer-based decision support tools have provided the construction planner with the ability to plan construction tasks efficiently using techniques such as 3D- CAD, Prima Vera and MS Projects. The basis of these Project Management techniques is the construction activity, which concentrates mainly on the temporal aspect of construction planning. Emerging research efforts are currently focused in the provision of project planners and managers with computer-based advisory tools to visualize the construction plan in a 4-dimensional (3D computer model + time) environment. 4D CAD is a natural progression from 3D CAD models, as it adds a further dimension, time. Commercial 4D CAD applications are becoming more accessible and the use of this technology allows the construction planner to produce more efficient construction schedules.

II. CONSTRUCTION SCHEDULE GENERATION

a. Construction Schedule

A construction schedule is a sequencing document that defines when construction activities will occur and may also provide information on when resources, materials and previously completed work will be utilized. Schedule generation is an important part of the construction planning process. Scheduling is generally carried out several times during the life of a construction project from preliminary schedules at the project feasibility phase to detailed short interval schedules during field construction. Most planning efforts in construction use the schedule and the design documents as the primary planning tools supported by estimating packages and other aids.

b. Current Schedule Generation Processes

In current practice, construction schedules (baseline schedules) are usually generated during the pre-mobilization phase, (Figure 1). During this stage, and

based on an understanding of the design documents, including design drawings (2D) and/or CAD models (3D) of the facility, the scheduler determines a list of activities required to construct the project. Using common knowledge of construction methods and based on available resources, the scheduler creates sequential relationships among the activities and calculates activity and project duration to generate the schedule. Once construction starts, the person responsible for maintaining the schedule performs schedule updating and develops short interval schedules. In many cases, tasks involving schedule maintenance and/or detailed Short-Interval schedules generation are performed by project personnel other than the original scheduler. Schedule generation is mainly dependent on the scheduler's interpretation of the contract documents including 2D drawings and/or 3D CAD and manually translating such interpretation into a list of activities. These activities are manually linked together through knowledge of construction methods and crew availability. This process of translating the visual understanding of the project documents into a schedule is time consuming and may lead to schedule errors.

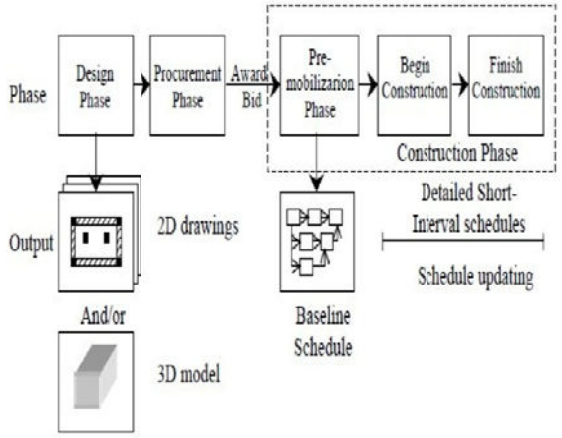

Fig. 1: Schedule generation during pre-construction phase

c. Disadvantages in the current schedule generation

Schedule generation is only thought of during the pre-construction phase as well as the construction phase with no serious consideration to its generation during the design phase. There is no information, in the schedule, on the method that the designer, estimator or construction planner envisaged would be used to perform the work. This results in the schedule being built with little consideration of construction and production issues. This problem has long been recognized by those involved in field construction. Computer-interpretable models and discrete event simulation was tried in the late 90s for the representation of construction methods and automated generation of schedules. But they were found inadequate and posed problems to the contractor's performance.

d. Activity Generation and Sequencing using Virtual Construction

The proposed scheduling process involves utilizing virtual construction for automatic generation of project activities and their sequential relationships. As depicted in Figure 2, using a preliminary 3D CAD model of the facility, the user can manually construct the project by re-assembling the 3D graphical elements in the virtual construction window in the perceived order of construction. The user can click and drag a graphical element, or a group of elements, from the 3D CAD model window and place it into the virtual window

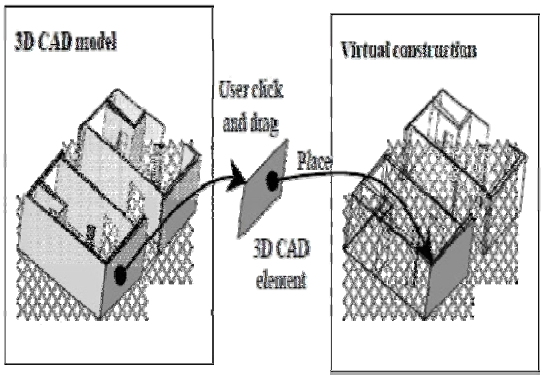

Fig. 2: The Virtual Construction Generation Process

To generate activities of the project, the user will select one or more graphical elements. Each graphical element or group of elements will represent an activity in the project activity list. The sequence of dragging the selected graphical elements will allow for creating the relationship among the activities. The relationship between the activities requires further specification. It will be possible for the user to specify concurrency, lags, and other relationships between activities in the virtual construction process.

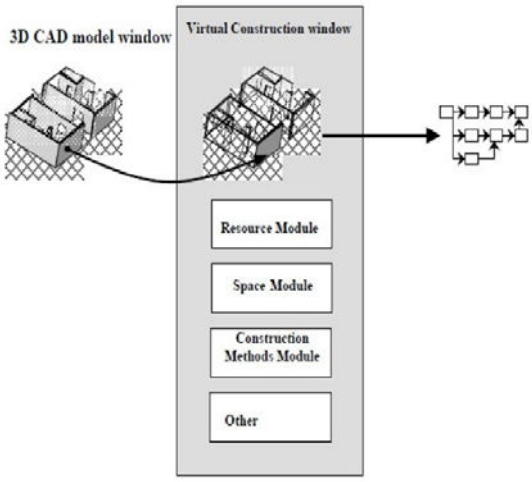

Fig. 3 : The proposed VCE model

As depicted in Figure 3, modules defining knowledge about resources, space and construction methods will help guide the user in constructing the schedule during the virtual construction session. The virtual construction system will utilize a Petri Net based tool (Wakefield and Sears 1997) to record information developed during the virtual session. Information recorded will include construction methods selected, resource utilization, and space decisions made. This will allow for carrying further checks on resources, space and construction methods following the virtual session.

III. 4D MODELING

a. 4D Modeling

4D modeling uses the virtual construction environment to integrate a 3D model and the corresponding construction schedule in order to create a "virtual" construction simulation. 4D simulation is a 3D interface to the construction process model, with an ability to visualize progress of the construction phase, by linking units of work to the work tasks on the construction schedule.

A 3D model of a construction project is generated using the existing commercial software like 3D Max etc. Construction schedules are generated for these projects using the existing commercial software like prima vera and MS Project. These two are then linked with the interface software that has been developed to integrate the 3D model with the schedules. The available software for integration of 3D models with the construction schedules are as under. [2]

(a) Bentley Schedule Simulator
(b) Common Point 4D
(c) Smart Plant Review
(d) Project Navigator
(e) Four Dviz
(f) Visual Project Scheduler
(g) Synchro project constructor

b. Advantages of 4D modeling

Major advantages of 4D modeling[3] are

Schedule creation - 4D models help visualize schedule constraints and opportunities for schedule improvements through re sequencing of activities or reallocation of workspace.

Schedule analysis - 4D models help analyze the schedule and visualize conflicts that are not apparent in the Gantt charts and CPM diagrams.

Communication – In a project team, many members join the team in midstream of the project. 4D modeling is a very useful tool to bring the new members abreast with the latest state on the project.

Team building - 4D modeling is an effective team building tool that also facilitates creation of a conducive team atmosphere where the planning, design, executive and contract staff solves problems together.

Certain significant advantages of 4D modeling during various stages in construction of a project are as under.

Planning phase - 4D modeling allows the construction teams to focus on the planning aspects instead of the traditional focus in constructability. It helps in optimizing the project scope/schedule and will validate the planning for the project by assessing its feasibility.

Design phase - It will enable the designers and constructors to co ordinate activities where they can visualize the construction in the virtual environment and improve upon their design.

Contract phase - 4D modeling facilitates contract with realistic timeframe for construction of the project by visualizing and linking it with the scheduling. It will immensely help the contractor to plan his execution in a more practicable manner which will improve on site performance, enhance productivity and better utilization of resources.

Construction phase - The field engineers can visualize the schedule, the sequence of erection, and the equipment logistics and look for potential interference in

the construction plan. They can rehearse the construction plan in the virtual environment to ensure the construction plan is most cost-efficient. Problems associated with logistics and layout such as work execution space can be solved. It will also help in resolving safety issues during construction.

Post construction phase – It will enable flawless documentation of the project, visualize post construction operation and maintenance and also dispute resolution and litigation.

Reduction in time - Rehearsals of construction process using 4D modeling will result in most effective scheduling of the project reducing the duration of the project as a whole.

Reduction in cost - Effective planning of project, proper scheduling, effective utilization of resources results in minimization of errors, wastage etc and culminates in reduction of costs.

Quality of construction – 4D modeling enables optimization of design suiting the project requirements. It provides various alternatives without investment. Choice of most appropriate design accommodating project scope, user aspirations and most suitable aesthetics will result in improved quality of construction.

User satisfaction – It will be beneficial to the user if he is involved during planning stage to visualize the end product during interaction with project team. It enables any midcourse corrections to be effected to suit user requirement.

Trg - 4D simulation is a useful training tool for inexperienced planners.

c. Case Study - Use of 4D CAD on Renovation of a Hospital[4]

The project involved demolition, renovation, remodeling, and new construction on an existing old hospital. The hospital had to be functional at all times and the disruptions to hospital operations had to be minimized. This motivated the project manager of the project to accept the assistance from the researchers to develop a 4D model for construction planning.

The project team created 3D AutoCAD models from the 2D AutoCAD drawings obtained from the architect of the project. The entire site and all the buildings, including 27,000 sq. meters of old, new, and soon-to-be-remodeled buildings ranging in size from 1,800 sq. meters to over 10,000 sq. meters were modeled in 3D. The model contained over 25,000 objects. The Primavera schedule obtained from the project manager was used to generate the 4D model. A detailed 4D model was then generated by linking the 3D model to the schedule using Jacobus Technology's Construction Simulation Toolkit software. The 4D model of this $10 million central utility plant incorporated 100 design drawings and 600 schedule activities totaling 14 months. The 4D models animated the schedule in different colors to highlight objects under construction during that time frame. For example, red was used when critical path activities were under construction and green was used when non-critical path activities were under construction. The time frame can be viewed on the screen and is illustrated in weekly or monthly intervals, or any other interval the viewer selects. A video of the animation of the construction schedule was also generated. Everyone involved in the project was able to view these videos at the same time without being in front of a computer. The audiences included subcontractors, suppliers, owner representatives, neighborhood groups, and donors. The hospital management, doctors, nurses, and the technical staff were one of the most important groups that viewed the videos. The hospital personnel were able to understand the impact of the planned construction on their department, office, and daily operations.

4D models resulted in reducing coordination problems between on-going operations and construction, improve subcontractor coordination and improve the acceptance of the construction project by concerned individuals.

d. Challenges Encountered while Building 4D Models

Inconsistencies: Often, the geometry is defined in ways that conflict with the schedule. For example, the architect defined the geometry by building elements, but the constructor places concrete and steel not by element, but rather according to steel sequence. The geometry had to be broken down and recombined a great deal to get a geometrical configuration to match the schedule.

Other Data: Cranes, laydown and staging areas, scaffolding, etc. are not part of the architect's design model, but these elements play a large role on the construction site. These geometries need to be added in the 3D model.

e. Representation of activities with no geometry:

A 4D modeler has to be sensitive as to the best way to communicate any activity. e.g. Ductwork, by perhaps attaching the activity to a floor slab or ceiling framing

f. Lacunae in 4D Modeling

The current 4D models do not convey all the information required to evaluate the schedule. For example, building components and construction equipment are usually modeled in the 3D images and linked with schedule. These 4D CAD systems lack

construction-specific components such as scaffolding and other temporary works integrated in the 3D model. Such 4D models do not show the space needs and corresponding potential congestion of temporary works. However, temporary works are a critical element of the overall construction plan. Failure in planning appropriate temporary structures affects safety, quality, and productivity adversely. Virtual prototyping obviates the above problems.

IV. CONSTRUCTION VIRTUAL PROTOTYPING

a. Virtual Prototyping (VP)

Virtual Prototyping is a computer aided design process concerned with construction of digital project modules (virtual prototypes) and realistic graphic simulations that addresses the issues of physical layout, operational concepts, functional specifications and dynamic analysis under various operating environments. Virtual Prototyping technology is the latest and effective way of envisaging real circumstances that enhance effective communication of design and ideas. Large number of digital technologies has been developed to visualize innovative architectural design; very few have been developed to facilitate integral planning and visualization of construction plans of building projects. Virtual prototyping makes a 4D model more complete by adding environment and site factors as also temporary works. It aids the planners to review construction process planning and analyze the work-space layout more effectively. Some of course rightly call it Building Information Modeling (BIM)

b. Construction Virtual Prototyping[5]

Though the VP system is being effectively used in manufacturing of various products, it is in its stage of infancy in construction Industry. The construction virtual prototyping (CVP) system is one of the virtual prototyping systems which is developed for modeling, simulation, analysis and virtual prototyping of construction processes from digital design. It allows the project teams to check constructability, safety and to visualize 3D models for a facility before commencement of construction.

DELMIA of Dassault Systemes (DS) has developed software for CVP. The system can easily generate, reuse and modify 3D models of building components, construction equipment, temporary works as well as labour force. The proposed system will make 4D models more complete by adding temporary works and their activities to set them and dismantle them. It will aid planners to review the construction process planning and analyze the work space layout more efficiently. CVP helps to provide rapid prototyping of projects and present the feasibility of construction methods. The CVP system can also assist in developing a detailed or improved construction programme during the construction phase. Both constructability and safety can be evaluated in the virtual experiment.

V. BIM

Building Information Modeling (BIM)[6] is the process of generating and managing building data during its life cycle. Typically it uses three-dimensional, real-time, dynamic building modeling software to increase productivity in building design and construction. It encompasses building geometry, spatial relationships, geographic information, and quantities and properties of building components. BIM can be used to demonstrate the entire building life cycle including the processes of construction and facility operation. Quantities and shared properties of materials can easily be extracted. Scopes of work can be isolated and defined. Systems, assemblies, and sequences are able to be shown in a relative scale with the entire facility or group of facilities.

The interoperability requirements of construction documents include the drawings, procurement details, environmental conditions, submittal processes and other specifications for building quality. It is anticipated by proponents that BIM can be utilized to bridge the information loss associated with handing a project from design team, to construction team and to building owner/operator, by allowing each group to add to and reference back to all information they acquire during their period of contribution the BIM model. For example, a building owner may find evidence of a leak in his building. Rather than exploring the physical building, he may turn to his BIM and see that a water valve is located in the suspect location. He could also have in the model the specific valve size, manufacturer, part number, and any other information ever researched in the past, pending adequate computing power.

a. Advantages of CVP[5]

(a) The CVP system can convert 2D engineering design to a 3D construction model, and finally to a model with erection sequences.

(b) The CVP system produces a precise and detailed planning and scheduling prior to the execution of real construction work giving the ability to observe potential risks and foresee possible problems.

(c) CVP system provides the planner an opportunity to improve the resource utilization.

(d) In the visualization module, users can view the construction activities at a particular time, and their interrelationship with other activities.

(e) CVP increases the accuracy of the project schedule and their ability to predict and plan construction tasks.

(f) The most important benefits of virtual prototyping in tendering process are its ability to impress client and well define the project scope.

(g) Use of CVP in construction stage will help to reduce rework and change orders, and improve coordination and communication effectiveness

VI. CONCLUSION

The use of 4D modeling has significant potential for the construction industry. 4D simulations can have a positive impact on both pre-construction and the construction phases, whilst having the power to assist planners in producing improved planned projects, allowing them to see how their plan will unfold. In addition, 4D technology enables planners to predict potential problems at the construction stage, 4D simulations results in considerable savings in construction projects by identifying problems prior to construction and avoiding re-work during the project. The fundamental attributes required by 4D models vary depending on construction project planning practice. Whilst the use and application of this technology is increasing, further research will be required to incorporate GIS, cost estimation and safety.

Construction Virtual Prototyping (CVP) enables the users to rehearse and simulate construction process virtually prior to the commencement of a real construction project. It enables visualization of the constructability of the proposed construction approach. The CVP system also assists the project team to design a precise construction schedule so as to remove any potential unproductive activities. The rapid prototyping of the CVP system can be enhanced by improving the existing process and resource optimization, constructability and safety evaluation.

Both technologies put together with BIM added during the currency of the project have the potential to revolutionize the way we visualize, plan, manage, operate and maintain and ultimately demolish building projects. In fact these can be rightly described as Womb to Tomb solutions.

REFERENCES

[1] Virtual construction for automated schedule generation by W.Y. THABET, R.R. WAKEFIELD, and A.F. WALY, Department of Building Construction, 122 Burruss Hall, Virginia Tech, Blacksburg, VA 24061-0156, USA.

[2] Trends of 4D CAD applications for construction planning by DAVID EESOM(1) and LAMINE MAHDJOUBI(2) - (1) School of Engineering and the Built Environment, University of Wolverhampton, Wulfruna Street, Wolverhampton, WV1 1SB, UK and (2)Faculty of the Built Environment, University of the West of England, Bristol, UK

[3] Using 4 D CAD and Immersive Virtual Environments to Improve Construction Planning by Sai Yerrapathruni, © 2003 Sai Yerrapathruni

[4] A virtual environment for building construction by Norman Murray (1) , Terrence Fernand (1) , Ghassan Aouad (2)

(1) Centre for Virtual Environments, Business House, University of Salford, Salford, M5 4WT, U.K. n.murray@salford.ac.uk (2). School of Construction and Property Management, Bridgewater Building, University of Salford, Salford, M7 9NU, U.K.

[5] A virtual prototyping system for simulating construction processes by Ting Huang a, C.W. Kong a, H.L. Guo a, Andrew Baldwin b, Heng Li a (a) Department of Building and Real Estate, The Hong Kong Polytechnic University, Hong Kong, (b)

[6] Faculty of Construction and Land Use, The Hong Kong Polytechnic University, Hong Kong, September 2006

[7] Journal of Building Information Model (BIM) - www.wbdg.org

Analysis And Design of Flat Slab And Grid Slab And Their Cost Comparison

Amit A. Sathawane & R.S. Deotale

Department of Civil Engineering, Yeshwantrao Chavhan College of Engineering Nagpur, India

Abstract - The FLAT slab system of construction is one in which the beam is used in the conventional methods of construction done away with the directly rests on column and the load from the slabs is directly transferred to the columns and then to the foundation. Drops or columns are generally provided with column heads or capitals. Grid floor systems consisting of beams spaced at regular intervals in perpendicular directions, monolithic with slab. They are generally employed for architectural reasons for large rooms such as auditoriums, vestibules, theatre halls, show rooms of shops where column free space is often the main requirement. The aim of the project is to determine the most economical slab between flat slab with drop, Flat slab without drop and grid slab. The proposed construction site is Nexus point apposite to Vidhan Bhavan and beside NMC office, Nagpur. The total length of slab is 31.38 m and width is 27.22 m. total area of slab is 854.16 sqm. It is designed by using M_{35} Grade concrete and Fe_{415} steel. Analysis of the flat slab and grid slab has been done both manually by IS 456-2000 and by using software also. Flat slab and Grid slab has been analyzed by STAAD PRO. Rates have been taken according to N.M.C. C.S.R

It is observed that the FLAT slab with drop is more economical than Flat slab without drop and Grid slabs.

Keywords- *Flat slab with drop, Flat slab without drop, grid slab, drop, column capital.*

I. INTRODUCTION

A. FLAT SLAB

A reinforced concrete flat slab, also called as beamless slab, is a slab supported directly by columns without beams. A part of the slab bounded on each of the four sides by centre line of column is called panel. The flat slab is often thickened closed to supporting columns to provide adequate strength in shear and to reduce the amount of negative reinforcement in the support regions. The thickened portion i.e. the projection below the slab is called drop or drop panel. In some cases, the section of column at top, as it meets the floor slab or a drop panel, is enlarged so as to increase primarily the perimeter of the critical section, for shear and hence, increasing the capacity of the slab for resisting two-way shear and to reduce negative bending moment at the support. Such enlarged or flared portion of and a capital. Slabs of constant thickness which do not have drop panels or column capitals are referred to as flat plates. The strength of the flat plate structure is often limited due to punching shear action around columns, and consequently they are used for light loads and relatively small spans.

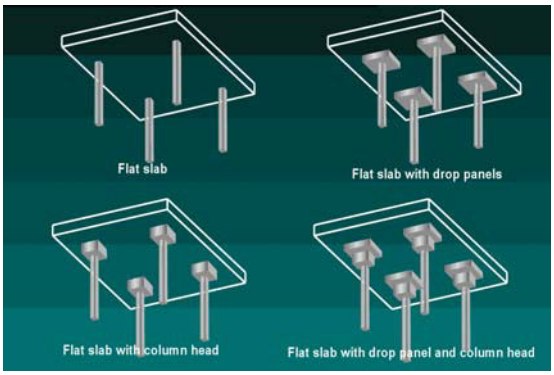

METHODS

DESIGN OF FLAT SLAB

Methods of Design:

Two approximate method methods are adopted by the codes for the design of flat slab or flat plate .These method can be used provided the limitations specified therein are *satisfied. The two design methods are a) The direct design method. (b) The equivalent frame method*

1.2 **GRID SLAB**

Grid floor systems consisting of beams spaced at regular intervals in perpendicular directions, monolithic with slab. They are generally employed for architectural reasons for large rooms such as auditoriums, vestibules, theatre halls, show rooms of shops where column free space is often the main requirement.The rectangular or square void formed in the ceiling is advantageously utilized for concealed architectural lighting. The sizes of the beams running in perpendicular directions are generally kept the same. Instead of rectangular beam grid, a diagonal.

ANALYSIS OF GRID SLAB

1) Approximate Methods
2) Analysis of grid Floor by Plate Theory

II. DESIGN OF FLAT SLAB WITH DROP INTERIOR PANEL OF SIZE 10.6 × 8.86 M

Size of columns = $L_1/16$ or H/8=500mm

Estimate size of column capital= D = L_2 /5=1772

Length of drop=1/3 span = 3.5 x 3.0 m

slab thickness= $L_n = L_1$-b=300 mm.

thickness of drop H=1.25 to 1.5 h=450mm

Size of external column =500 mm square

Size of edge beam= 300 × 600 mm

fck = 35 ; f_y = 415 ;

Load Calculations:

(a) Dead Load: bDγ = 1×0.3×25 = 7.5 KN/m
(b) Floor Finish = 1 kN/m
(c) Live Load = 4 kN/m

Total Design Load = 18.75 KN/m

Analyze the Interior X frame:

$M_0=wL_2L_n^2 / 8$ = 1618.34 kNm

DISTRIBUTION FACTORS:

longitudinal distribution Inter span

Support (-ve) = 0.65, Span (+ve) = 0.35

End spans: Interior –ve = 0.75-0.1R= 0.69

Span +ve =.63-0.28R = 0.45; Exterior –ve = 0.65

R= 0.42

Transverse distribution

Interior –ve : 75% to column strip;25% to mid

Span +ve : 60% to column strip;40%to mid-strip

Exterior –ve : 100% to column strip

Table-1

Item	**X**	**Y**
c to c span	10.6	8.86
Clear span(L_n)	10.6-1.772= 8.828	7.088
Width of span(L_2)	8.86	10.6
Width of column strip (BS)	4.43	4.43
Width of mid strip	4.43	6.17
L_2/L_1	0.836	1.20

Table-2

Type of moments	**Longitudinal Direction**		**Factors**	**Transverse Direction**	
	Factor	**Moment**		**CS**	**MS**
Negative	0.65	1051.92	0.75 0.25	788.9	262.98
Positive	0.35	566.41	0.6 0.4	339.8	226.5
End span analysis (IS 456)					
Interior (-ve)	0.685	1108.77	0.75 0.25	831.5	277.19
Span(+ve)	0.448	725.62	0.6 0.4	435.3	290.24
Exterior	0.422	682.34	1	682.3	

Check for shear:

Effective depth of slab = 270 mm,

Effective depth of slab = 270 mm,

Weight of drop projection below slab=25 × (0.3 – 0.24)×1.5 = 2.25 kN/m^2

Design shear at critical section around capital

V_{ud} =16.125(10.6 ×8.8 6 - (π ×(2.26 ^{2}/4))+2.25 (3.6 × 3 - π ×(2.26 ^{2}/4))

= 1450.0 + 15.0 = 1936.5 KN.

Design Shear strength of concrete:

$\tau c = k.\ \tau_c$ where, $\tau_c = 0.25\sqrt{f_{ck}}$

$\tau_{c=} 0.25\sqrt{35}$ = 1.48 N/ m^2

$k = (0.5+\beta)\,\tau_c$ but ≤ 1.0

$k = 1.0$; $\tau_{uc} = 1.48$ N/mm^2

Shear resistance of concrete

$v_{uc} = \tau_{uc} \times p \times d = 1.48 \times (\pi \times 2260) \times 0.260$
$= 4723.42$ KN $> v_{ud}$ (= 1936)

check for shear around the drop: The critical section is at a distance d/2 = 270/2 = 135 mm from the periphery of the drop

Design shear at critical section:

$v_{ud} = 18.125 \{(10.6 \times 8.8\ 6) - (3.6+0.20) \times (3.6 + 0.270)\} = 1480.4$ KN.

Shear resistance of concrete,

$v_{uc} = 1.48 \times 2(3800+3800) \times (270/1000)$

$= 6185$ KN $> v_{ud}$

LOCATION	MOMENTS (per m width)			AREA OF STEEL (mm^2)			DIAMETER OF BARS			Spacing (mm c/c)		
	Longitudinal direction	Transverse direction		Longitudinal	Transverse		Longi-tudinal	Transverse		Longi-tudinal	Transverse	
		Column	Middle		Column	Middle		Column	Middle		Column	Middle
Interior support												
-ve support	237.453	178.09	59.363	2775.30	2004.19	626.50	20	20	16	110	175	175
+ve support	127.85	76.72	51.143	1398.10	816.643	537.59	20	16	12	220	150	125
End span ACI METHOD												
Interior (-ve)	255.71	191.79	63.929	3026.87	2176.40	676.21	20	20	16	100	140	165
Span + ve	182.656	109.59	73.062	2061.24	1186.63	776.33	20	16	16	150	260	145
Exterior (-ve)	109.594	82.195	27.398	1186.63	877.40	284.75	20	16	12	260	355	395
End span IS 456												
Interior (-ve)	250.28	187.72	62.572	2951.28	2124.86	661.40	20	20	16	105	145	170
Span + ve	163.797	98.278	65.518	1827.81	1057.79	693.56	20	16	16	170	295	160
Exterior -ve	154.028	154.03		1709.10	1709.10		20	20	12	180	180	

Table-III

III. COMPARISION

3.1 Comparison of Maximum Moments obtained Manually and by Software for Flab Slab

Maximum Moments	Manually	Software
Column strip positive kNm	76.72	73
Column strip negative kNm	178.1	177
Middle strip positive kNm	51.14	54.06
Middle strip negative kNm	59.36	61.66

3.2 Comparison of Maximum Moments obtained Manually and by Software of Grid Slab

	MANUALLY	SOFTWARE
MAXIMUM MOMENT kNm	1020	1163
MAXIMUM SHEAR FORCE kN	625	618

3.3 Flat Slab With Drop:

SPAN (m)	7 ×6	8 × 7	9 × 8	10 × 9	10.6 × 8.86
CONCRETE (m^3)	88.2	137.52	190.696	270.1	293.01
AMOUNT (Rs)	853360	1348540	2052690	2972681	3009600

3.4 Rate Comparison:

	FLAT SLAB WITH DROP	FLAT SLAB WITHOUT DROP	GRID SLAB
CONCRETE (m^3)	293.01	281.87	314.63
STEEL (KG)	29800	38125	36500
TOTAL AMOUNT (Rs)	3009660	3292650	3420780
RATE PER Sqm	3524	3855	4005
RATE PER Sqft	327	358	372

4. **GRAPHS:**

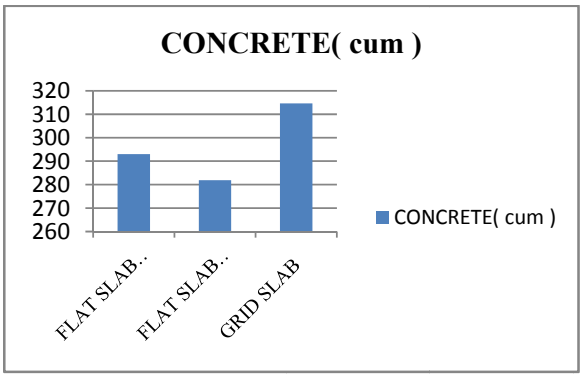

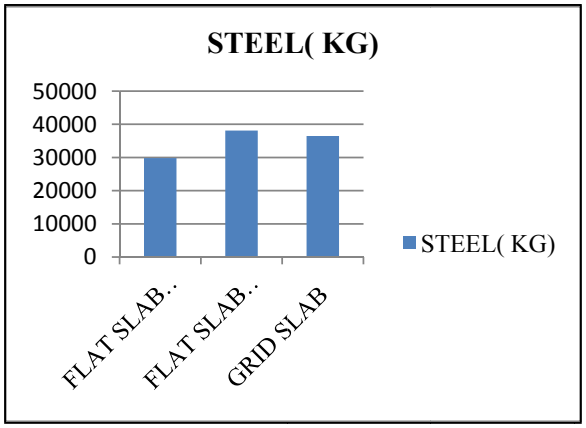

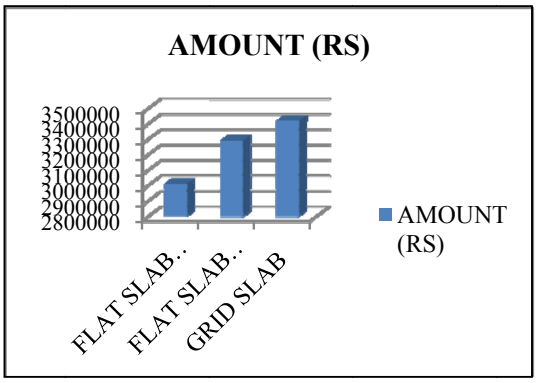

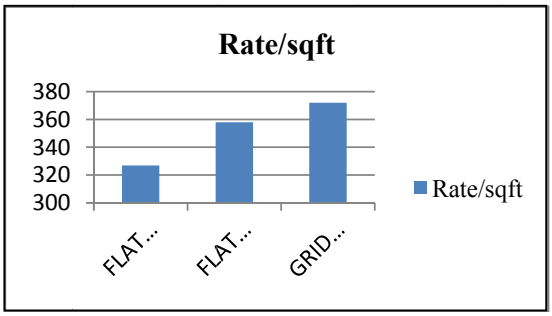

CONCLUSION :

1) Drops are important criteria in increasing the shear strength of the slab.
2) Enhance resistance to punching failure at the junction of concrete slab & column.
3) By incorporating heads in slab, we are increasing rigidity of slab.
4) The negative moment's section shall be designed to resist the larger of the two interior negative design moments for the span framing into common supports.
5) Concrete required in Grid slab is more as compared to Flat slab with Drop and Flat slab without Drop.
6) Steel required in Flat slab without Drop is more as compared to Flat slab with Drop and Grid slab.
7) Flat slab with drop is more economical than Flat slab without Drop and Grid slab.
8) Rate per square meter of flat slab with drop (3524) was found to be more economical than flat slab without drop (3855) and grid slab (4005).
9) Rate per square feet of flat slab with drop (327) was found to be more economical than flat slab without drop (358) and grid slab (372).

REFERENCES

Papers:

[1] Vemuri Venkata Rangarao, Naraparaju, Venkata Ramanarao FLAT STRIP SLAB SYSTEM, International Classes: E04B1/16; (03-04-2010)

[2] Gowda N Bharath; Gowda S. B. Ravishankar; A.V Chandrashekar; Review and Design of Flat Plate/Slabs Construction in India .

[3] Ahmed Ibrahim' ', Hani Salim and Hamdy Shehab El-Din; Moment coefficients for design of Flat slabs with and without openings. (11-06-2011)

[4] Dario Coronelli; 'Grid Model for For Flat Slab Structures

[5] Lawson,Patrick D; *STRUCTURAL GRID FOR SLAB FACING MATERIALS; (03-28-1972)*

P. C Books:

P. C. Varghese- Advanced Reinforced Concrete Design Ramachandra , vijay Gehlot –Limit state of Design concrete structure S. N. Sinha - Reinforced Concrete Design IS: 456 – 2000 – Plain and Reinforced Concrete – Code of Practice S.Ramamrutham - Design of Reinforced concrete structure Dr.V.L. Shah , Late Dr. S.r. kurve - Limit state theory & Design of Reinforced concrete

◈◈◈

Slope Stability Analysis for High Embankment with Metacomputing Technique "A Case Study of NATRAX High Speed Track"

H. S. Goliya & Priyesh Gour

Department of Civil Engineering, SGSITS Indore, MP, India

Abstract - In the present study an attempt has been made for find out the reason of slope failure on the basis of site investigations, experimental and design analysis to provide the standard geotechnical properties of materials with the suitable side slope. Some geotechnical characteristics of soil as Grain size, Optimum moisture content and Cohesive strength has been taken in consideration to design and construct the high embankment up to 20m. The optimization of side slope with required factor of safety as per IRC guideline has been also attempted in the present study. Treatment of embankment slopes for erosion control is considered to prevent from damage due erosion from rain and wind.

Key words - *Stability analysis, Geotechnical property improvement, Advance methods.*

I. INTRODUCTION

The evolution of slope stability analysis in geotechnical engineering has followed closely the developments in soil and rock mechanics as a whole. Slopes either occur naturally or are constructed by humans. Slope stability problems have been faced throughout history when men or nature has disrupted the delicate balance of natural soil slopes. Furthermore, the increasing demand for engineered cut and fill slopes on construction projects has only increased the need to understand analytical methods, investigative tools, and stabilization methods to solve slope stability problems. A case study carried out for NATRAX High Speed Track, Pithampur in Dhar District, about 45km from Indore, MP India. The proposed embankment will be the oval High Speed Track for vehicle testing purpose, at which the vehicle with speed up to 350 km/hr will be tested.

About the site

NATRAX (National Automotive Test Track) is a up leading test centre of NATRIP (National Automotive Testing and R&D Infrastructure Project). NATRAX will be the world class automotive proving ground set up on 4123 acres with digital testing infrastructure capable of sensing fine nuance of an automobile. The proving ground will have all verities of structure types to test vehicles against varying terrains and stringencies. The heart of the proving ground will be oval High Speed Track which is 13.28 km in length where vehicle with natural speed up to 350 kmph would be tested. A large part of test load relating to speed, noise, vibration, handling, stability etc. is expected to shift to India from abroad once this infrastructure is complete. Once ready, it will be world's largest providing ground.

NATRAX will be the CoE for vehicle dynamic. NATRiP has planned an expenditure of Rs 900 carores to create world-class facilities at NATRAX

Need for present study

The project has to recognize a need for consistent understanding and application of slope stability analysis for construction and remediation projects across the India and abroad. These analysis are generally carried out at the beginning, and sometimes throughout the life, of projects during planning, design, construction, improvement, rehabilitation, and maintenance. Planners, engineers, geologists, contractors, technicians, and maintenance workers become involved in this process. This body of information encompasses general slope stability concepts, engineering geology principles, groundwater conditions, geologic site explorations, soil and rock testing and interpretation, slope stability concepts, stabilization methods, instrumentation and monitoring, design documents, and construction inspection.

Objective of the study

- Identification of significant parameter those affect the system.
- To establish a simplified method of monitoring the performance of system to avoid the practical complexity.

- To improve the cohesion of soil with respective angle of internal friction (Ø) as required condition.
- To develop an appropriate system by using advance method with enhancing accuracy.

Scope of the study

With the present study it is possible to remove the geotechnical deficiencies in the existing ground set-up. High embankment (up to 20m) has been design with proper and safe side slope, optimization of slope with necessary safety factor has been kept in mind to enhance the proper land use. Safety provisions are considered for road users. Treatment of embankment slopes for erosion control is considered to prevent from damage due erosion from rain and wind. Drainage from road and side slopes is also considered to prevent damage in rainy seasons.

II. COMPUTER PROGRAMS

For more sophisticated analysis and complex slope, soil, and loading conditions, computer programs are generally used to perform the computations. Computer programs are available that can handle a wide variety of slope geometries, soil stratigraphies, soil shear strength, pore water pressure conditions, external loads, and internal soil reinforcement. Most programs also have capabilities for automatically searching for the most critical slip surface with the lowest factor of safety and can handle slip surfaces of both circular and noncircular shapes. Most programs also have graphics capabilities for displaying the input data and the results of the slope stability computations.

Types of computer programs

Two types of computer programs are available for slope stability analysis: The first type of computer program allows the user to specify as input data the slope geometry, soil properties, pore water pressure conditions, external loads, and soil reinforcement, and computes a factor of safety for the prescribed set of conditions. These programs are referred to as *analysis programs*. They represent the more general type of slope stability computer program and are almost always based on one or more of the procedures of slices.

The second type of computer program is the *design program*. These programs are intended to determine what slope conditions are required to provide one or more factors of safety that the user specifies. Many of the computer programs used for reinforced slopes and other types of reinforced soil structures such as soil nailed walls are of this type. These programs allow the user to specify as input data general information about the slope geometry, such as slope height and external loads, along with the soil properties.

Different methods for computing factor of safety

Different methods of stability analysis indicating equilibrium conditions, forces and factor of safety considered. Almost all computer programs employ one or more schemes for searching for a critical slip surface with the minimum factor of safety

S. No	Methods	Moment Equilibrium	Force Equilibrium	Inter Slice Normal ces	Inter Slice Shear Forces	Moment Factor of safety	Force Factor Of Safety	Inter Slice Force Function
1	Fellenius, Swedish circle or ordinary Method (1936)	Yes	No	No	No	Yes	No	No
2	Bishop Simplified method (1955)	Yes	No	Yes	No	Yes	No	No
3	Janbu Simplified method (1954)	No	Yes	Yes	No	No	Yes	No
4	Morgenstern -Price method (1965)	Yes	Yes	Yes	Yes	Yes	Yes	Constant Half -Sine

III. METHODOLOGY

The study has been carried out by collecting information of project site from Rites Ltd. and study the re-usability of the excavated material. Laboratory investigation of sub surface material and embankment fill materials have been collected from site. The conventional Limit Equilibrium method is used to analyze the high embankment slope stability. Program Geo-Studio (SLOPE/W) is formulated in terms of moment and force equilibrium factor of safety equations. Analysis provides a factor of safety, defined as a ratio of available shear resistance (capacity) to that required for equilibrium.

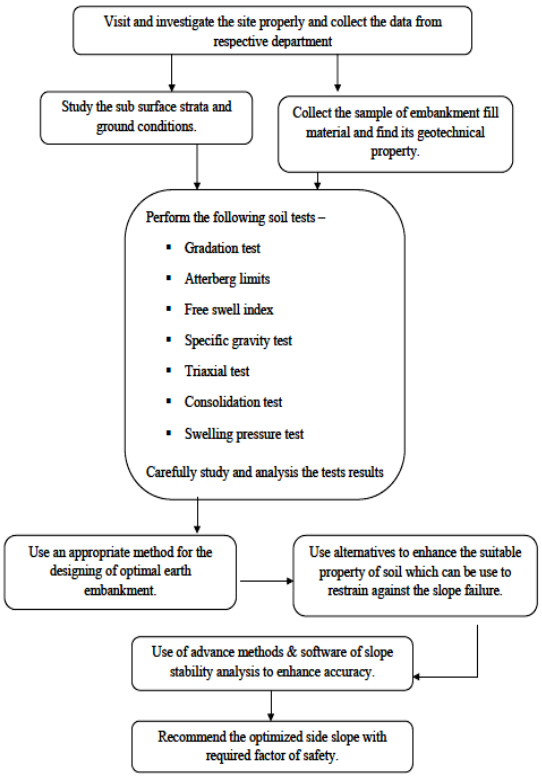

IV.TESTS AND SIMULATION RESULTS

4.1 Test results of Excavated Fill Materials collected from site.

Sr. No.	Sample	Proctor Compaction Test		Grain Size Analysis				Triaxial Compaction Quick Test	
		OMC %	MDD gm/cc	Gravel %	Sand %	Silt %	Clay %	C kg/cm^2	Ø^0
1	Fill material I	6	1.82	23.21	24.51	41.82	10.46	0.07	15
2	Fill material II	16	1.8	18.64	17.96	42.48	20.92	0.7	7
3	Fill material III	22	1.87	34.81	39.59	21.76	3.84	0.7	10
4	Fill material IV	9	1.94	69.71	12.53	16.33	1.42		
5	Fill material V	22	1.27	32.43	60.79	5.36	1.42		
6	Fill material VI	10	1.79	61.86	32.2	5.69	0.24		
7	Fill material VII	21	1.83	46.84	26.23	16.56	10.37	0.82	13

The tests mentioned above has been done for different types of material to enhance the check the geotechnical suitability of the material for high embankment side slope with required factor of safety. The excavated material has been collected from site perform the tests to ensure that whether this material is suitable for embankment fill or not, the test results are shown in table 4.1. The results of Borrowed Fill Materials collected from local area near site are shown in table 4.2.

Gravel and sand contain of some material is much higher that so that the triaxial test not possible for that kind of materials, to overcome from this problem it is possible to processing the soil in terms of altering its grain size distribution.

Some modifications have been done with the materials by mechanical blending to perform the triaxial test and can find out the cohesive strength of material. The test results of the altered grain size distribution of the soil samples are shown in table 4.3.

4.2 Test results of Borrowed Fill Materials collected from site

Sr. No.	Sample	Proctor Compaction Test		Grain Size Analysis				Triaxial Compaction Quick Test	
		OMC %	MDD gm/cc	Gravel %	Sand %	Silt %	Clay %	C kg/cm^2	Ø^0
8	Yeloowish Murrum	17	1.66	9	40	30	21	0.26	20
9	Brownish Murrum	14	1.9	40	41	19		0.21	32
10	SM	20	1.76	3	58	29		0.13	36
11	Silt Clay CH	26	1.62	1	11	48	40	0.69	10
12	Silt Clay CH	25	1.62	6	9	41	44	0.66	10
13	Silty Sand SP	8	1.81	0	98	2			
14	Sandy Gravel GP	7	2.2	95	1	4			

The materials with some grain size alteration (table 4.3) have been denoted by the coding as Fill material V with Gravel 20% (FV g20%) is denoted by M1, Fill Material V with Gravel 30% (FV g30%) is denoted by M2, Fill Material V with Gravel 40% (FV g40%) is denoted by M3, Fill Material V with Gravel 50% (FV g50%) is denoted by M4. Similarly some borrowed materials ware mixed together with some particular fixed percentage (as shown in Table 4.3) to check the change of geotechnical property of the materials, as the borrowed material 14 (Sandy Gravel GP) 60% and borrowed material 11 (Silt Clay CH) 40% is coded by M5, the same materials ware again altered with various percentage mix to verify the effect of gravel and silt quantity variations. The borrowed material 14 (Sandy Gravel GP) 40% and borrowed material 11 (Silt Clay CH) 60% is denoted by M6, again the borrowed material 13 (Sandy Gravel GP) and borrowed material 11 (Silt Clay CH) is added in same quantity (50% + 50%) which is coded by M7. Then the four borrowed materials 11, 12, 13, 14 were mixed together with same quantity i.e. 25% of all four materials, which is denoted by M8. All these materials test results is shown in Table 4.3.

4.3 Test results of Borrowed Fill Materials collected from site with some grain size alteration

Sr. No.	Sample	Proctor Compaction Test		Grain Size Analysis				Triaxial Compaction Quick Test	
		OMC %	MDD gm/cc	Gravel %	Sand %	Silt %	Clay %	C kg/cm^2	Ø^0
1	F V (g20%)	18	1.79	21.87	31.32	41.95	4.86	0.74	14
2	F V (g30%)	17	1.84	30.79	28.98	37.09	3.14	0.7	15
3	F V (g40%)	16	1.88	40.83	20.97	36.76	1.44	0.64	16
4	F V (g50%)	14	1.9	50.12	15.61	32.82	1.45	0.6	16
5	F14+F11 (60%+40%)	18	1.86	48.14	20.43	15.13	16.3	0.82	10
6	F14 + F11 (40%+60%)	19	1.88	38.23	6.13	31.14	24.5	0.84	8
7	F14 + F11 (50%+50%)	18	1.85	45.43	7.12	26.71	20.74	0.83	11
8	F11+F12+ F13+F14 (All 25%)	17	1.8	26.33	30.15	39.52	4	0.79	15

V. ANALYSIS AND FINDINGS

The analysis of collected data and test results will serve to identify the deficiencies in slope stability for high embankment and suggest for overcoming the deficiencies.

The conventional limit equilibrium methods investigate the equilibrium of the soil mass tending to slide down under the influence of gravity. Transitional or rotational movement is considered on assumed or known potential slip surface below soil mass. All methods are based on comparison of forces (moments or stresses) resisting instability of the mass and those that causing instability (disturbing forces). Two-dimensional sections are analyzed assuming plain strain conditions. These methods assume that the shear strengths of the materials along the potential failure surface are governed by linear (*Mohr-Coulomb*) or non-linear relationships between shear strength and the normal stress on the failure surface. Analysis provides a factor of safety, defined as a ratio of available shear resistance (capacity) to that required for equilibrium.

Functional slope design considers calculation with the critical slip surface where is the lowest value of factor of safety. Locating failure surface can be made with the help of computer programs using search optimization techniques. Program **SLOPE/W** is formulated in terms of moment and force equilibrium factor of safety equations. Limit equilibrium methods include *Morgenstern-Price*, *Spencer*, *Bishop*, *Ordinary*, *Janbu* etc. This program allows integration with other applications.

Analysis modeling

Modeling of the continuum is suitable for the analysis of soil slopes, massive intact rock or heavily jointed rock masses. This approach includes the finite difference and finite element methods that discretize the whole mass to finite number of elements with the help of generated mesh. Various types of models ware analyse for different soil properties and heights of

embankment with their respective side slope. These models are analysed on axis symmetry geometry.

The typical cross sections of the embankment of 20m height with side slope of 1:2 without any berm is shown in figure 5.1.

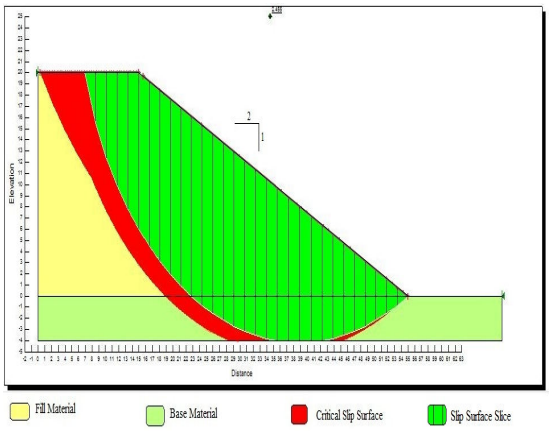

Fig. 5.1 : Typical cross sections of the embankment of 20m height with side slope of 1:2

The above cross section of the embankment defines different type of materials by different colours. Red colour shows the critical slip surfaces or the critical area. The hatched area shows the slice which divides the potential sliding soil mass into sections, the calculation of forces on slice will estimate the total sliding soil mass.

Table 5.3 : Stability Analysis by SLOPE/W for Excavated Fill Materials at side slope of 1:1.7

S no.	Embankment Height (m)	Side Slope	Material properties				Factor of Safety (calculated by different methods)			
			Material Index	Fill Material						
				γ kN/m³	C kN/m²	Ø⁰	Ordin-ary	Bisho-ps	Janbu	M. P.
1	20	1:1.75	F I	17	123	4	2.618	2.664	2.659	2.665
2	20	1:1.75	F II	15	68	7	2.121	2.141	2.066	2.418
3	20	1:1.75	F III	16	68	10	2.22	2.288	2.175	2.302
4	20	1:1.75	F VII	17	80	13	2.277	2.368	2.245	2.377
5	20	1:2	F I	17	123	4	2.605	2.679	2.627	2.674
6	20	1:2	F II	15	68	7	2.246	2.185	2.168	2.305
7	20	1:2	F III	16	68	10	2.304	2.334	2.263	2.405
8	20	1:2	F VII	17	80	13	2.303	2.428	2.259	2.237

Table 5.2: Stability Analysis by SLOPE/W for Excavated Fill Materials at side slope of 1:2

Table 5.3: Stability Analysis by SLOPE/W for Borrowed Fill Materials collected from site with some modifications

S no.	Embankment Height (m)	Side Slope	Material properties				Factor of Safety (calculated by different methods)			
			Material Index	Fill Material						
				γ kN/m³	C kN/m²	Ø⁰	Ordin-ary	Bisho-ps	Janbu	M. P.
1	20	1:1.75	M 1	14	72	14	2.003	2.074	2.02	2.074
2	20	1:1.75	M 2	15	68	15	1.883	1.963	1.886	1.96
3	20	1:1.75	M 3	15	62	16	1.838	1.925	1.837	1.922
4	20	1:1.75	M 4	16	58	16	1.723	1.815	1.714	1.81
5	20	1:1.75	M 5	15	80	10	1.929	1.984	1.952	1.958
6	20	1:1.75	M 6	15	82	8	1.92	1.969	1.946	1.971
7	20	1:1.75	M 7	15	81	11	1.954	2.011	1.986	2.012
8	20	1:1.75	M 8	14	77	15	2.07	2.141	2.098	2.14

Effect of Grain size on Cohesion

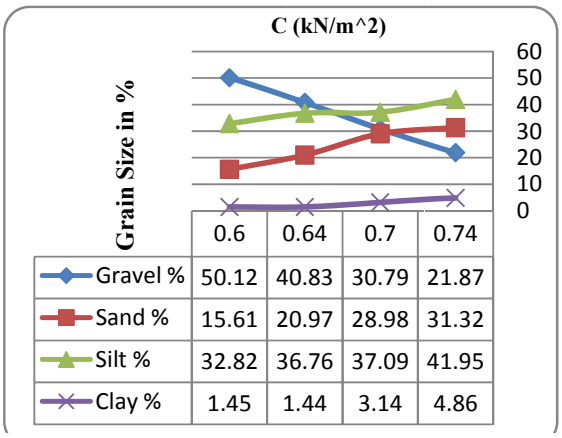

	0.6	0.64	0.7	0.74
Gravel %	50.12	40.83	30.79	21.87
Sand %	15.61	20.97	28.98	31.32
Silt %	32.82	36.76	37.09	41.95
Clay %	1.45	1.44	3.14	4.86

Factor of Safety V/s Cohesion of soil of side slope 1:1.75

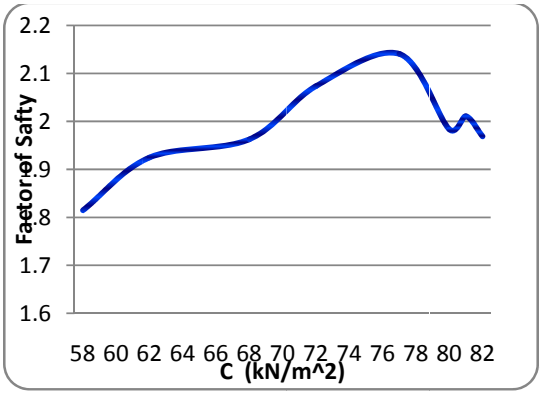

Factor of safety of modified material by different methods

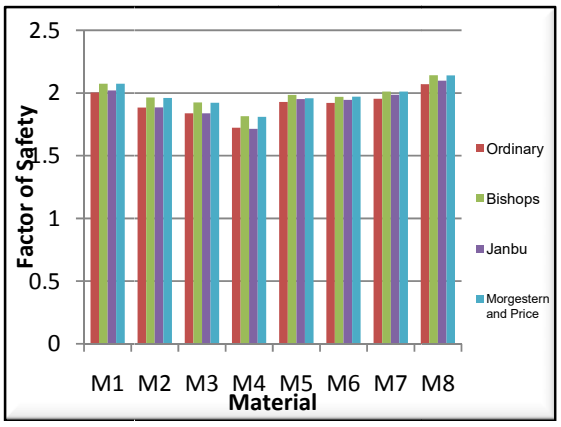

VI. CONCLUSION AND RECOMMENDATION

The selection of slope stability methods is critical since the accuracy of the analysis results depends on the mechanics of the failure. Based on the field observations, theoretical analysis and experimental study following points are concluded:

1. The Ordinary Swedish Circle Method always estimate lower factor of safety compared to other three methods like Bishop's Simplified Method, Janbu Method and Morgenstern and Price Method.
2. For embankment of height up-to 20m, the material should be homogeneous and well compacted, it should be ensure that the water content of the embankment material should be within the specific limit and that is uniformly distributed throughout the soil prior the rolling.
3. For safe embankment side slope the cohesion (C) of the soil or the fill material should be 72 – 80 kN/m^2 and the angle of internal friction (Ø) should be $15^0 – 20^0$.
4. Processing the soil in terms of altering its grain size distribution is rarely possible but in some critical cases mechanical blending procedure can be adopt to achieve the geotechnical property of the soil regarding withstanding the side slope.
5. Normally 40% – 45% of Gravel, 15% - 20% of Sand, 30% - 35% of Silt and 1% - 5% of Clay is suitable for fill material of 20m high embankment with the side slope of 1:1.75 to 1:2.
6. Treatment of embankment for erosion control shall be done by stone pitching from top of embankment.

REFERENCE

[1] Werneck, L. G. M., Lacerda A. W., and Ramalho-Ortigao J.A., (1983). "Embankment failure on clay near Rio de Janeiro." Journal of Geotechnical Engineering, vol.109(11),1460-1479.

[2] Wu, H.T., Randolph, W.B., and Huang C.S., (1993). "Stability of shale embankments." Journal of Geotechnical Engineering, vol. 119(1), 127-146.

[3] Manzari M.T., and Nour M.A., (2000). "Significance of soil dilatancy in slope stability analysis." Journal of Geotechnical and Geoenvironmental Engineering, vol. 126(1), 75-80.

[4] Zaretskii, Yu.k., (2001). "Provision for slope and embankment stability." Journal of soil

Mechanics and Foundation Engineering, vol. 38(6), 2-6.

[5] Ashford, S.A., and Sitar, N., (2002). "Simplified method for evaluating seismic stability of steep slopes." Journal of Geotechnical and Geoenvironmental Engineering, vol. 128(2), 119-128.

[6] Irsyam,M., Susila,E., and Himawan,A., (2006). "Slope failure of an embankment on clay shale at Km 97+500 of the Cipularang toll road and the selected solution." Int. Conf., on Geotechnical Engineering, Ground Improvement and Geosynthetics 2006, HSEP Bangkok, Thailand.

[7] Sinha, B.N. (2007). "Advance methods of Slope-Stability Analysis for Economical Design of Earth Embankment." IRC Journal, vol. 68(3), 201-222.

[8] Batog, A., and Stilger-Szydlo, E., (2009). "New Approach to Assessment of road embankment Stability." Studia Geotechnica et Mechanica, vol. 31(3) 27-46.

[9] Saha, S., (2009). "Control of landslide hazards through Slope Stability Analysis – Case Studies." IRC Journal, vol. 37(12), 23-31.

[10] Behera, J., (2009). "Slope SStabilization in hill roads using Bio-Engineering works: A case study of Mizoram state road projects." IRC Journal, vol. 37(10), 31-37.

[11] Zhang, J., Tang W.H., and Zhang, L.M., (2010) "Efficient probabilistic Back-Analysis of Slope Stability model parameters." Journal of Geotechnical and Geoenvironmental Engineering, vol.136(1), 99-109.

[12] Collins, B.D., and Sitar, N., (2011). "Stability of steep slopes in Cemented Sands." Journal of Geotechnical and Geoenvironmental Engineering, vol.137(1), 43-51.

◈◈◈